



Final Report

***TRANSPARENT COATINGS FOR
SOLAR CELLS RESEARCH***

Reporting Period: July 1, 2008 to December 31, 2012

Date of Report December 31, 2012

Award Number: DE-FG36-08GO88005

Sub-Contractors: NREL

Recipient Contacts: **Technical Contact** **Business Contact**

Paul Glatkowski

Joseph Piché

508-528-0300

508-528-0300

pflatkowski@eikos.com

jpiche@eikos.com

DOE Information: **Project Officer** **Project Monitor**

Leslie (Jim) Payne

Leon Fabick

Tel. 720-356-1744

Tel. 720-356-1537

jim.payne@go.doe.gov

Leon.Fabick@go.doe.gov



Table of Contents

| | |
|---|------------|
| Introduction..... | 7 |
| 2 Background..... | 7 |
| 1 Project Objectives..... | 8 |
| 3 Technical Approach..... | 10 |
| 4 Significant Accomplishments..... | 11 |
| 5 Results..... | 14 |
| 5.1 Task 1: TCC Material and Market Evaluation..... | 14 |
| 5.1.1 Survey of Thin Film PV Industry..... | 14 |
| 5.1.2 Development of Industrial Partnerships..... | 16 |
| 5.1.3 TCC Testing..... | 18 |
| 5.1.4 Commercial Nanoparticulate Inks/Dispersions..... | 22 |
| 5.1.5 CNT Comparison..... | 24 |
| 5.2 Task 2: Development of Novel Nanomaterials for TCC's..... | 26 |
| 5.2.1 Silver Nanowires..... | 26 |
| 5.3.2 Silver Nanowire/Carbon Nanotube Networks..... | 31 |
| 5.3.3 Gold Nanowires..... | 35 |
| 5.3.4 Synthesis of Gold Nanowires..... | 36 |
| 5.2.5 Characterization of Danubia SWCNT..... | 43 |
| 5.2.6 Purification of SWCNT via Heat Treatment..... | 44 |
| 5.3 Task 3: Inks and Dispersions from Novel Nanomaterials..... | 48 |
| 5.3.1 Ink Characterization..... | 50 |
| 5.3.2 Sonication study..... | 53 |
| 5.3.3 Ink Additives..... | 55 |
| 5.3.4 Curing to Remove Ink Additives..... | 56 |
| 5.4 Task 4: Coating/Deposition Development..... | 60 |
| 5.4.1 Ink-Jet printing..... | 60 |
| 5.4.2 Inkjet Deposition and Evaluation..... | 66 |
| 5.4.3 Inkjet Deposition in Practice..... | 66 |
| 5.4.4 PV Cell fabrication and Testing..... | 70 |
| 5.4.5 CNT Coatings for PV Applications..... | 72 |
| 5.4.6 Building PV Devices with NREL..... | 73 |
| 5.4.7 PV Test results..... | 76 |
| 5.4.8 Reducing Roughness..... | 82 |
| 5.4.9 Reducing Roughness Part II..... | 94 |
| 5.4.10 Particle Reduction..... | 97 |
| 5.4.11 Roll-to-Roll Coating..... | 100 |
| 5.4.12 Particle Reduction by Fractionalization..... | 101 |
| 5.4.3 Particle Reduction Via High-Speed Centrifugation..... | 104 |
| 5.4.4 Particle Reduction via Surfactant Centrifugation..... | 106 |
| 5.4.5 Particle Analysis Method..... | 108 |
| 5.5 Task 5: Binder Process Development/Formulation..... | 111 |
| 5.5.1 Binder Formulation and Deposition..... | 111 |
| 5.5.2 Binder Work Function and Roughness..... | 115 |

| | |
|---|-----|
| 5.5.3 Binder as AR Coating | 118 |
| 5.5.4 Binder Replacement of PEDOT/PSS..... | 119 |
| Task 6: Durability Testing | 120 |
| 6 Publications/Presentations/Travel/Meetings..... | 122 |
| 7 References Cited | 124 |

List of Figures & Tables

| | |
|---|----|
| Figure 1: Roll-to-roll printing is being used by many PV manufacturers as a way to reduce cost and increase production rates..... | 14 |
| Figure 2: Schematic of a transparent wide bandgap PV with an Invisicon [®] hole conducting back electrode..... | 17 |
| Figure 3: NovaCentrix PulseForge curing system. | 18 |
| Figure 4: Structure of thin film CdTe PV cell using ITO coated soda-lime glass..... | 19 |
| Figure 5: Transmission (A) and Absorption curves for ECI(Red) and ZC&R(Blue) ITO coatings compared with uncoated (Green), soda lime glass | 20 |
| Figure 6: Transmission for 7mil thick ITO coated PET specified to 300 Ω/\square (Red), 60 Ω/\square (Blue), and uncoated (green). | 21 |
| Figure 7: Comparison of spray coated CNT and thinly coated (A), and a thick coat (B) of Silver nanoparticulate ink. | 23 |
| Figure 8: Transmission though uncoated (blue), 255 Ω/\square ITO coated (green), and 400-500 Ω/\square CNT coated (red) glass (A) and PET(B). Resistivity of CNT coating is 489 Ω/\square on glass and 405 Ω/\square on PET. | 25 |
| Figure 9: A cluster of silver nanowires grown from the polyol process..... | 28 |
| Figure 10: AFM image of silver NW..... | 28 |
| Figure 11: Diameter determination of a AgNW from AFM imaging. Red arrows from the width bar on the image correspond to the high peek and trough on the graph. | 29 |
| Figure 12: Spliced AFM images of a >20 μm long AgNW. | 30 |
| Figure 13: Silver / CNT / Additives – One Hour After Silver Solution | 33 |
| Figure 14: AFM image of gold nanowires..... | 36 |
| Figure 15 Carbon disulfide synthesized NW heat treated to 300C to remove impurities. | 37 |
| Figure 16: AFM image of AuNW and other nanoparticulate coating on glass substrate at 35 x 35 μm (top), 8.5 x 8.5 μm (middle) and 3.5 x 3.5 μm (bottom) image size. | 39 |
| Figure 17: A series of consecutive AFM images taken from the same region of a coated slide showing long bundles of AuNW. Each square is 20 μm x 20 μm | 40 |
| Figure 18: Comparisson of a spray coated sample (right) and two samples that were prepared by smearing gold nanowire filter cake onto glass slides..... | 41 |
| Figure 19: Spectrophotometer transmission curves for uncoated PET (red) and SANTE film after 500 hours humidity testing with haze (blue) and with haze factored out (green). | 42 |
| Figure 20: TGA curves for Sineurop (Red) and commercially scaled Danubia (Blue) SWCNT..... | 44 |
| Figure 21: Raman Spectrum for annealed Carbon Solutions SWCNT using a 785nm laser. | 45 |



Figure 22: TGA curves for air oxidized and inert atmosphere annealed Carbon Solutions SWCNT..... 46

Figure 23: AFM Image of PEO Test #3, CNT & PEO WSR-N750 on Glass Slide..... 51

Figure 24: 3D View of AFM Image of PEO Test #3, CNT & PEO WSR-N750 on Glass Slide 52

Figure 25: CNT data normalized to 500 Ohms/Square. The same CNT ink was sprayed on the preparation day and then four days later. Ice was used during the higher sonication times. 54

Figure 26: Particles present in the final CNT coating. From the data there was not a general trend for particles present due to sonication time. 55

Figure 27: Resistance change using DI water, Ammonia water, and HCL water wash for 10 and 30 seconds 56

Figure 28: Photonic curing as a result of strobes of high powered flash lamps. 57

Figure 29: Dimatix Spectra SE-128AA industrial piezo jetting head assembly for inkjet printing..... 62

Figure 30: RFID tag used to print CNT pattern..... 64

Figure 31: Leaching of polymeric additives from printed CNT coating. 65

Figure 32: Complex CNT circuits deposited on transparent PET using ink-jet printing. 66

Figure 33: Printed Four Layer Field Effect Transistor Consisting of First CNT Layer then PVDF Polymer Layer Followed by a Top CNT Electrode which is then Over Coated with PVDF. 67

Figure 34: Printing process involves coating PET substrate with leveling agent before CNT..... 68

Figure 35: First layer of fingered electrodes printed using CNT ink..... 68

Figure 36: Example of a completed four layer device made with CNT. Note- the polymer layers are transparent. 69

Figure 37: Dimatix DMP-2800 Series Printer and complex CNT pattern printed with this instrument. 70

Figure 38: Comparison of performance between OPV cells made with ITO versus CNT electrodes. 72

Figure 39 - CNT Transfer Experiment Substrate Materials..... 76

Figure 40: Comparison of performance between OPV cells made with ITO versus CNT electrodes. 77

Figure 41: Optical profilometry images depicting surface roughness of CNT coatings with (L) and without (R) Asperities..... 78

Figure 42: Power output from OPV cells made with ‘flattened’ CNT coatings on PETG (top) and ‘rough’ CNT coatings on PET..... 79

Figure 43: Schematic diagram of CdTe devices made with NREL..... 80

Figure 44: I-V Curves for Best CdTe Devices with Various Back Contacts..... 81

Figure 45: Removal of surface asperities by blade leveling 84

Figure 46: Surface roughness of CNT/binder topcoat for one dip of sol-gel binder 3 dip (left) versus three dips of Binder 3 (right) 86

Figure 47: Diagram for silicon wafer polishing, via CMP, used in the microchip industry 87



| | |
|--|-----|
| Figure 48: Visual Progression of Press-Polishing Procedure | 89 |
| Figure 49: CNT on PETG Before (Left) and After (Right) Press Polishing | 90 |
| Figure 50: AFM Image of Blanket-Coated, Press-Polished PETG Sample | 90 |
| Figure 51: Optical Profilometry image of press polished CNT coating imbedded on the surface of PETG at 2.5X magnification (top) and 50X magnification (bottom) | 92 |
| Figure 52: Optical Profilometry of CNT coatings with (L) and without (R) Asperities .. | 93 |
| Figure 53: Glass Slides Coated with CNT to 50 Ω/\square in a 'Racetrack' Pattern | 96 |
| Figure 54 Euclid three roll offset Gravure Lab Coater with parts marked | 98 |
| Figure 55 - Iodixanol/CNT Experimental Setup..... | 102 |
| Figure 56 - Centrifuge Tubes Before (Top) and After (Bottom) Centrifugation..... | 103 |
| Figure 57: AFM and Optical Image Comparison | 110 |
| Figure 59: Transmission versus wavelength of glass and silica AR coating on glass. The glass was coated on both sides, reducing first and second surface reflectance. | 113 |
| Figure 60: Schematic of dip coating for a sol-gel coating..... | 114 |
| Figure 61: Work function for Eikos' AR binders. | 116 |
| Figure 62: Optical profilometry image depicting surface roughness for A) A1 binder/CNT coating; and B) CNT coating without binder top coat..... | 118 |
| Figure 63: Glass Slides 'Racetrack' patterned with CNT to 50 Ohm/sq..... | 120 |

Tables

| | |
|---|-----------|
| Table 1: Thin film PV companies and their technology..... | 15 |
| Table 2 TCC companies operating in the PV industry. | 16 |
| Table 3: Sheet resistance and transparency of AgNW coatings | 31 |
| Table 4: Additives and Weights Along With Copper Metal Data..... | 32 |
| Table 5: Summary of Normalized Results for Silver/CNT testing..... | 33 |
| Table 6: RT performance of NW-CNT dispersion as coated on glass. | 34 |
| Table 7: Strengths and weaknesses of commercial TCC materials for PV requirements | 43 |
| Table 8: Raman and TGA data for heat treated Carbon Solutions SWCNT | 47 |
| Table 9: Yield for heat treatment of Carbon Solutions SWCNT..... | 47 |
| Table 10 RT performance of polymer additive/CNT inks | 50 |
| Table 11: Particle reduction via centrifugation for four manufactures of carbon nanotubes. | 52 |
| Table 12: Solutions used to remove trace surfactants and Leveling agents | 55 |
| Table 13: High boiler and polymer additives to be tested for formulation of CNT ink. .. | 58 |
| Table 14: Summary of Solvent/Water (1:1) Mixtures on PET 453 at 60°C..... | 61 |
| Table 15: Classifications and Components of Printing Ink. | 63 |
| Table 16: Summary of Applied BathWorks to Patterned Samples – Same Ink in Initial BathWorks Testing | 65 |
| Table 17: Surface roughness data at 2.5x for a high conductivity thicker layer of CNT and a thinner layer deposited from low particle CNT ink. | 71 |
| Table 18: Rs drift in CNT TCC on glass, without protective a top coating. | 71 |
| Table 19: R/T performance of 75-100 Ω/\square SWCNT film coated on borosilicate glass slides. | 73 |
| Table 20 - CNT Substrate Transfer Experimental Matrix | 75 |



| | |
|---|-----|
| Table 21: Summary of best device performances using different back contacts and ZnTe:Cu layer thickness. | 81 |
| Table 22 - CNT Substrate Transfer Experimental Matrix | 83 |
| Table 23: Effects of oxide binder topcoat on surface roughness | 85 |
| Table 24: Characterization of Blanket-Coated, Press-Polished PETG Sample (#113-91-2) | 91 |
| Table 25: Sample Batch #1 - Binder Coated Samples | 95 |
| Table 26: Sample Batch #2 - CNT & Binder Coated Samples | 96 |
| Table 27: Sample Batch #3 - Patterned CNT & Binder Coated Samples | 97 |
| Table 28 Resistance values and transmittance for Gravure CNT coated PET after washing with and without top coatings | 99 |
| Table 29: Length Data | 100 |
| Table 30: Overall Grid Data | 101 |
| Table 31- Raman Peak Ratios using 633nm Laser | 104 |
| Table 32 - Raman Peak Ratios using 785nm Laser | 104 |
| Table 33: Effect of High Speed Centrifugation on Particle Count | 105 |
| Table 34: Effect of DOC Treatment on Particle Count | 107 |
| Table 35: AFM Grain Count and Optical Particle Analysis Comparison | 109 |
| Table 37: Materials Eikos can formulate and deposit via sol-gel method to form AR binder. | 113 |
| Table 38: Surface roughness for CNT/binder coatings | 117 |
| Table 39: RT performance and environmental stability of CNT/binder 3 coatings on PET using a protective top coat | 121 |



Introduction

Today's solar cells are fabricated using metal oxide based transparent conductive coatings (TCC) or metal wires with optoelectronic performance exceeding that currently possible with Carbon Nanotube (CNT) based TCCs. The motivation for replacing current TCC is their inherent brittleness, high deposition cost, and high deposition temperatures; leading to reduced performance on thin substrates. With improved processing, application and characterization techniques Nanofiber (NF) and/or CNT based TCCs can overcome these shortcomings while offering the ability to be applied in atmospheric conditions using low cost coating processes

2 Background

At today's level of development, CNT based TCC are nearing commercial use in touch screens, some types of information displays (i.e. electronic paper), and certain military applications. However, the resistivity and transparency (RT) requirements for use in current commercial solar cells are more stringent than in many of these applications. Therefore, significant research on fundamental nanotube composition, dispersion and deposition are required to reach the required RT performance commanded by photovoltaic devices.

Theoretical calculations indicate that CNT TCC's are capable of meeting the RT performance needed for use in solar cells. However, a gap currently exists between the theoretical and current state of the art CNT TCC performance. To increase RT performance requires successful application of specialized analytical tools, unique chemistries, and processes only recently discovered. This grant was used to conduct the research and development needed to improve the RT performance of these materials systems.

This project originated back in 2005, with the U.S. Department of Energy awarding Eikos, Inc. a grant to investigate the feasibility of developing and utilizing TCC based on carbon nanotubes for solar cell applications.

Joint collaboration with National Renewable Energy Laboratory (NREL) and commercial solar cell manufacturers demonstrated successful integration of Eikos CNT TCC known as Invisicon[®] into certain solar cell structures with promising energy conversion efficiencies. Though recent advances excite the photovoltaic community, successful use of CNT in solar applications is contingent upon further improvement of electrical conductivity and optical transmittance of Invisicon[®] coatings. In addition to improving RT performance, CNT coatings are sensitive to surrounding environments causing instability in surface resistance (i.e. R_s -drift). Eikos continues to develop a better understanding of the underlying mechanisms responsible for R_s -drift as well as exploiting ways, such as through binder materials, to minimize or eliminate changes in Invisicon[®] R/T performance during its use.



Eikos has made significant progress in developing these materials through a close collaboration with NREL. Versions of this TCC technology have been used to fabricate award winning laboratory scale solar cells, and have yielded several groundbreaking peer reviewed papers. Early proof-of-concept solar cells served to demonstrate the advantages and weaknesses of using CNTs in a wide variety of solar cell types and in entirely new cell structures. Eikos continued to conduct research on the purification, dispersion, formulation, and coating of the NT TCC. Furthermore Eikos continued working with NREL, to build a variety of prototypes using the coatings developed at Eikos, and measure their performance. NREL provided consultation on the direction, specification, and utility of the resulting TCC materials. Consequently, at the onset of this project it was estimated the commercial release of this new TCC is only a few years away. To meet this goal, this project sought to advance the development of these materials to a point where the commercial market will finally have a replacement for the troublesome, costly, and scarce metal oxides used today.

After a 1 year hiatus in funding from the previous project, Eikos received this two year grant in June 2008. Performance enhancement venues include: CNT purification and metallic tube separation techniques, chemical doping, CNT patterning and alignment, advances in commercial and research materials and field effect schemes, as identified in the updated statement of objectives. In addition, Eikos continued to develop improved efficiency coating materials and transfer methods suitable for batch and continuous roll-to-roll fabrication requirements. Finally, Eikos continued its long running collaboration with NREL and the PV-community at large in fabricating and characterizing Invisicon[®] enabled solar cells.

1 Project Objectives

The objective of this project is to research and develop transparent conductive coatings (TCC) based on novel nanomaterial composite coatings, which comprise nanotubes (NT), nanofibers (NF), and other nanostructured materials along with binder materials. One objective is to show that these new nanomaterials perform at an electrical resistivity and optical transparency suitable for use in solar cells and other energy-related applications. A second objective is to generate new structures and chemistries with improved Resistivity and Transparency (RT) performance. The materials under development also include the binders and surface treatments that facilitate the utility of the electrically conductive portion of these composites in solar Photovoltaic (PV) devices. This project shows that these materials are capable of being deposited using low energy, low temperature processes under atmospheric conditions and at a cost that is competitive with the current state of the art in transparent conductors. Additionally, this project pursued basic studies on the coating deposition techniques and the coatings durability to assess these novel nanomaterial TCC's for use in various solar PV and other EERE applications.



In summary the objectives were:

- Synthesize and characterize novel nanomaterials for transparent conductive coatings for use in thin film photovoltaics and other energy applications.
- Formulate inks for printing high conductivity nanomaterial-based coatings.
- Demonstrate suitable environmental stability of coatings.
- Evaluate cost-performance-processing tradeoffs of nanomaterials TCCs versus other TCCs.

To accomplish these objectives our effort was dispersed into the tasks listed below:

- Task 1: TCC Material and Market Evaluation
- Task 2: Development of Novel Nanomaterials for TCC's
- Task 3: Inks and Dispersions from Novel Nanomaterials
- Task 4: Coating/Deposition Development
- Task 5: Binder Process Development/Formulation
- Task 6: Durability Testing



3 Technical Approach

This project researched and developed transparent conductive coatings based on novel nanomaterial composite coatings, which comprise nanotubes, nanofibers, and other nanostructured materials along with binder materials. One objective was to show that these new nanomaterials perform at an electrical resistivity and optical transparency suitable for use in solar cells and other energy-related applications. A second objective was to generate new structures and chemistries with improved RT performance. The materials under development also included the binders and surface treatments that facilitate the utility of the electrically conductive portion of these composites in solar Photovoltaic (PV) devices. This project seeks to show that these materials are capable of being deposited using low energy, low temperature processes under atmospheric conditions and at a cost that is competitive with the current state of the art in transparent conductors. Additionally, this project pursued basic studies on the coating deposition techniques and the coatings durability to assess these novel nanomaterial TCCs for use in various solar PV and other EERE applications.

Eikos pursued several technical approaches in this project. These include:

- Surveying commercial TCCs for energy applications,
- Synthesizing and purchasing novel nanomaterials,
- Formulating inks and dispersions of nanomaterials for printing,
- Printing inks on a variety of substrates, including glass, plastic, and directly onto devices,
- Developing binders and post-print processing for environmental and mechanical durability.

Eikos pursued this broad-based approach because each component used to make a coating can have an effect on the final performance, overall stability, and the cost of the coating. This complete approach reduces risk associated with relying on external suppliers of processed nanomaterials for creating coatings.

Eikos worked with NREL to build a variety of prototypes using the coatings developed at Eikos and measure their performance. NREL provided consultation on the direction, specification, and utility of the resulting TCC materials. NREL also provided Eikos with nanomaterials from their research labs for Eikos to formulate into inks and coatings.



4 Significant Accomplishments

Noteworthy accomplishments throughout the grant are listed below under each task:

Task 1: TCC Material and Market Evaluation

- Eikos generated a comprehensive list of thin film PV manufactures and TCC material suppliers. Each company on this list was vetted to determine a technology match with Eikos TCC technology. It was hoped our understanding of the technical abilities of TCCs and the companies that use them would lead to partnerships with PV companies. The goal of these partnerships was to develop and commercialize revolutionary thin film PVs.
- Eikos developed collaborations with Ascent Solar, a major thin film PV manufacturer, and NovaCentrix, an advanced materials and equipment processing company. In addition, materials and aerospace giants 3M and Northrop Grumman have initiated contracts with Eikos for exploratory research in the field of thin film conductive coatings. Lastly a development relationship was established with Konarka Inc, the details of which are proprietary.

Task 2: Development of Novel Nanomaterials for TCC's

- Silver nanowires (AgNW) were synthesized as is, and in the presence of dispersed CNTs in solvent. Inks were made from these materials to determine RT performance. By integrating AgNW with CNTs of roughly the same size, Eikos aimed to improve RT performance of our coatings.
- Syntheses of gold nanowires (AuNW) were confirmed using an Atomic Force Microscope (AFM). AFM imaging not only allowed characterization of long chains of bundled AuNW. In addition, but this characterization step was used to develop purification methods to separate desirable AuNW from other particulate resulting from synthesis.

Task 3: Inks and Dispersions from Novel Nanomaterials

- Polymeric additives were used to stabilize CNTs in solvent suspensions. These mixtures were processed into ink and tested for RT performance. Improving the stability increased concentration and improve pot life of CNT inks.
- CNT inks were formulated that allow for uniform and complex patterns to be ink-jet printed. These inks are stable up to 30 days and print for nearly a week with 40 – 50 passes without clogging the print head. In addition, a commercially available ink-jet printer was modified to reduce flocculation and clogging of CNT ink in the print head, thereby enabling printing of CNT ink.
- Eikos determined gravure/roll coating is a suitable method for CNT/binder deposition for PV applications. The ability to roll coat allows easier scale up of CNT/binder on



flexible substrate. This is important to bring CNT TCCs into commercial applications in thin film PV.

- A relatively reliable method to purify good quality metallic NW was found. This enables the benefit of NW conductivity to be utilized in future PV applications.
- Eikos developed CNT ink with excellent RT performance from two new suppliers. This provides Eikos with at least two additional material suppliers enabling us to meet current and future orders. One of these new companies is American, ensuring material supply for sensitive government applications.
- Developed CNT ink formulations that can be easily ink jet printed and/or roll-roll coated. These inks deposit evenly on multiple substrates. Post deposition washing of these coatings provides a uniform and highly conductive transparent network on the substrate surface.

Task 4: Coating/Deposition Development

- Eikos developed a novel and important method to characterize particulate within CNT dispersions. This method was used to track the success of particle reduction processing. The ability to accurately measure efforts to reduce particulate is important to producing commercial quality conductive coatings.
- Particle reduction was scaled up five fold for CNT ink. Uniform inks result in uniform coatings suitable for multi junction PV cells.
- NREL utilized Eikos CNT coatings as a back contact in a Cadmium Telluride (CdTe) multi junction device. Characterization, done by NREL, shows our CNT coating out performs ITO. Given the fact CdTe is the dominant thin film PV cell and ITO is, by far, the dominant TCC material, this result has shown the potential of CNT to replace ITO in commercial PV applications.
- Eikos adapted ink formulations and developed new printing protocols to enable a more reliable deposition of complex and conductive CNT patterns of variable sizes by ink-jet printing. The ability to print highly conductive and robust circuits benefit printed electronic applications such as OPV and antennas.
- NREL fabrication and testing of OPV cells using CNT TCC as an electrode. These cells outperformed cells constructed with ITO, the industry standard TCC electrode.
- Eikos designed, built and validated a pilot scale roll-to-roll coating system to apply thin film CNT on polymeric substrates. This equipment was used to produce 20 ft² samples CNT coated polymer film to a large aerospace company.
- The development of several methods to level the surface of CNT electrodes. Press polishing using ultra flat glass plates proved the most promising technique. Press polished CNT coatings are both uniformly rough to >32nm, and partially embedded in the surface of the substrate, yielding a more durable composite CNT-polymer layer.
- NREL performed initial modeling to determine the optimum coating resistivity for layer electrodes in OPV cells. Based on ITO, the theoretical curve generated by this model was used as benchmark for comparison of experimental data for both ITO and CNT.



- Eikos collaborated with NREL to identify, plan, and start work in, three separate paths to solve the problem of electrode roughness and subsequent integration of these electrodes within OPV cells.
- Worked with NREL toward eliminating the need for PEDOT:PSS within OPV cells. This effort has the potential of providing improved charge transfer within the cell resulting in cell efficiencies better than the current state of the art.

Task 5: Binder Process Development/Formulation

- Eikos successfully developed a CNT/triple binder coating capable of meeting RT specifications and weathering environmental conditions.
- Eikos developed a new Antireflective (AR) binder system that enables CNT based TCC to meet PV specifications. This new formulation also simplifies processing and may reduce costs. In addition, these binders have the ability to be deposited/processed at room temperature, thus eliminating the need for expensive sputtering equipment and lowering process steps.

5 Results

Work on this program initially focused on surveying commercial TCCs for their performance, processing, and costs. Eikos also established metrics for commercially viable replacements based on feedback from PV manufacturers who use TCs. Eikos focused on manufacturers who employ roll-to-roll processing techniques for their devices, since this method has the greatest technological synergy with Eikos's core competencies and the Invisicon[®] materials technology.

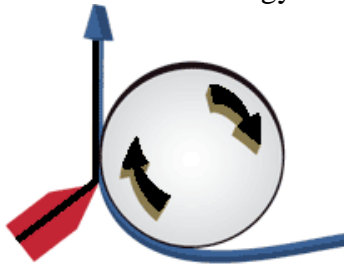


Figure 1: Roll-to-roll printing is being used by many PV manufacturers as a way to reduce cost and increase production rates.

Eikos also performed the synthesis of novel nanomaterials for TCCs. These nanomaterials included nanotubes, nanowires, and nanofibers. Eikos also purchased nanomaterials from commercial sources.

Our work on formulation leveraged almost a decade's knowledge on nanotube inks and dispersions for printing. Eikos formulated inks for compatibility with commercial printing equipment, including slot-die, gravure, inkjet, and screen printers.

This section of the report is divided into subsection, covering work performed on each task.

5.1 Task 1: TCC Material and Market Evaluation

The following sections cover efforts to: survey of the PV industry from the perspective of TCC, development of industrial partners; and comparisons of ITO and CNT performance.

5.1.1 Survey of Thin Film PV Industry

Eikos conducted a comprehensive technical survey of transparent conductive coatings. Eikos sought to find problems and opportunities with current materials in the PV market and establish mutually beneficial partnerships. Eikos has generated a comprehensive list of thin film PV manufactures (Table 1) and TCC material suppliers (Table 2).

Each company in Table 1 was vetted to determine a match with Eikos TCC technology. Criteria for selection included processing compatibility, material limitations, and

nationality. For instance, companies like Konarka have been excluded based on limited commercial potential of their PV polymer technology. In addition, Domestic companies are preferred. Q-cells and Schott have compatible technologies, but are German. For this reason they are not listed, though they have not been entirely excluded from consideration.

Table 1: Thin film PV companies and their technology.

| Company Name | Substrate | PV Material- Processing method | TCC- Deposition method |
|---------------|--------------------|--|-------------------------------|
| Innovalight | Silicon | a-Si ink jet printing | ZnO- Rapid Thermal Processing |
| Xunlight | Metal foil | a-Si plasma enhanced chemical vapor deposition (PECVD) | ZnO- sputtering |
| XsunX | Glass | a-Si sputtering | SnO ₂ - sputtering |
| Power films | Polymer | a-Si | Unspecified TCO |
| Uni-Solar | Metal foil | a-Si roll/roll vapor deposition | Unspecified TCO |
| AVA Solar | Glass | CdTe | ITO- sputtering |
| Bloo Solar | Glass | CdTe- catalysis of vertical nano bristles | Unspecified TCO |
| First Solar | Glass | CdTe | ITO or FTO- sputtering |
| Stion | Metal Foil | CIGS | ITO or ZnO- sputtering |
| Solyndra | Glass | CIGS | ZnO- Sputtering |
| DayStar Tech. | Glass | CIGS- sputtering | ZnO- sputtering |
| ISET | Glass/foil/polymer | CIGS- Ink printing | ZnO- selenization |
| Miasole | Metal foil | CIGS- roll/roll sputtering. | ZnO- sputtering |
| SoloPower | Metal foil | CIGS- roll/roll electro deposition | ZnO- Rapid Thermal Processing |
| Ascent Solar | Polymer | CIGS- evaporation | ZnO-evaporation |
| Heliovolt | Glass/foil/polymer | CIGS- FASST screen printing | ZnO- FASST |

Companies that produce nanoparticulate or nanoparticle based inks/coatings for the PV industry are listed in Table 2. Each companies coating technology and PV industrial customers are included. Eikos did order TCC material from these companies to test RT performance. Many of these companies provide products that are commercially available



to any customer, others prefer limited partnerships. Not all companies were willing to give out material. For instance, Cambrios is very secretive and Unidym is a direct competitor of Eikos.

Table 2 TCC companies operating in the PV industry.

| Company Name | Coating Technology | Customers/Partners |
|----------------------------------|--|---|
| Nanogram | Lasor reactive deposition of Silver, silicon, silicon nitride and nickel | OTB Group |
| Cambrios Technologies | Silver nanowire inks | Unspecified PV and display manufacturers |
| NanoMas Technologies | Printable Gold and Silver nanoparticulate ink. | Endicott Interconnect, Dimatix, Optomec, TFE. |
| Optomec | Aerosol jet printing of various materials. | Manz automation, NanoMas, and others. |
| All-Chemie | TCO coatings | Commercially available |
| International Advanced Materials | TCO coatings | Commercially available |
| Plasma Materials | Wide range of materials they can apply as thin film. | Commercially available |
| Cima Nanotech | Nanometal and metal alloy based inks and pastes. | Commercially available through Nanopowders |
| Five Star Technologies | Metal particulate based inks and pastes. | VC funding |
| Mitsubishi Materials | ITO and ATO powders for dispersions. | Commercially available |
| Sumitomo Metal | Metal particulate based inks and pastes. | Commercially available |
| Qioptiq Coatings | TCO coatings | Commercially available |
| Unidym | CNT based inks | Samsung, Battelle, MDA |
| Eikos | CNT based inks | Ascent solar |

5.1.2 Development of Industrial Partnerships

Eikos is actively seeking partners in the PV industry to incorporate our TCC technology. In addition, novel nanomaterials made by these and other companies were investigated. Materials were procured from these suppliers for side by side testing by Eikos.

A number of industrial partnerships were started based on Eikos' ability to provide CNT conductive coatings to a wide range of industries. Collaborations with Ascent Solar Technologies and NovaCentrix, along with seed contracts with Northrop Grumman and

3M Corporation seek to increase the industrial application of CNT conductive coatings and the market share for our industrial partners.

Ascent Solar

Eikos worked with Ascent Solar Technologies to integrate carbon nanotube-based electrodes into dual junction thin film PVs. Ascent Solar Technologies is a leader in thin film solar technology, from basic materials research to novel solar array designs. The efficiency, power density, and price needs of the DoD will be met by developing a new top cell design with significantly improved electronic compatibility of the device layers. Eikos sought to integrate Invisicon[®] into a dual junction thin film PV that is capable of specific power as high as 1,000 W/kg. By increasing TFPV efficiency to >20%, array area can be similar to SOA triple junction PVs (Figure 2).

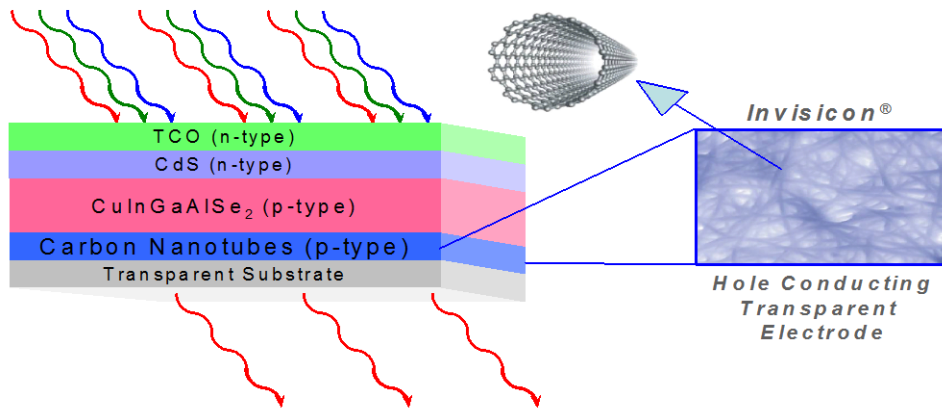


Figure 2: Schematic of a transparent wide bandgap PV with an Invisicon[®] hole conducting back electrode.

NovaCentrix

Founded in 1999 NovaCentrix originally specialized in silver and copper nanoparticulate inks. While they still obtain considerable formulation know how they have evolved into a supplier of PulseForge[®] curing tools for room temp light curing of conductive inks (Figure 3).



Figure 3: NovaCentrix PulseForge curing system.

It is claimed the PulseForge[®] produces conductivities 2-3 times higher than inks cured by conventional heat curing. NovaCentrix has accepted inks from many manufacturers who wanted to test their curing technology. All tested inks reportedly have better conductivity if cured via the PulseForge[®]. Eikos is including the PulseForge[®] in our future experiments to remove unwanted ink additives through curing. If successful, this could create a breakthrough in ink jet printing of CNT coatings and open a new market to both Eikos and NovaCentrix.

5.1.3 TCC Testing

The primary goal of this project is to research and develop transparent conductive coatings based on novel nanomaterials that compare favorably with existing TCC materials used in the PV industry. To that end, Eikos tested commercially available TCC materials in parallel with Eikos formulated nanoparticulate conductive coatings.

Evaluation of pre coated transparent conductive oxides (TCO) such as Indium tin oxide (ITO), Antimony doped tin oxide (ATO), and fluorine-doped tin oxide (FTO) is a focus for testing. In addition, conductive inks, pastes and nanoparticulate were investigated for use as suitable TCC for PV applications. Of particular are silver, gold and copper inks and dispersions that can be deposited using draw down casting, dip coating, spray coating and ink jet printing.

Testing the Baseline: ITO

Indium tin oxide is the industry standard transparent conductor due to its high conductivity, good transparency, and relative control of etching rate. Pre-coated ITO samples were obtained from several suppliers on glass, polycarbonate and PET substrate. Samples coated with, and without additive anti reflective properties to increase transparency, were also tested. Resistivity of each sample was tested by 4 point probe and 2 point hand held voltmeter, using leads 1 inch apart. Transparency and AR properties were tested using a UV/VIS spec across a broad spectrum wavelengths from 250-2,500nm. To date, the following pre-coated ITO samples have been tested:

- ZC&R supplied ITO coating specified to a resistivity of 200-300 Ω/\square on soda lime glass substrate.
- Evaporated Coatings inc. supplied ITO/AR coating on soda lime glass substrate.
- Evaporated Coatings inc. supplied ITO/AR coating on polycarbonate substrate.
- Sheldahl supplied ITO coating specified to 60 Ω/\square PET substrate.
- Sheldahl supplied ITO coating specified to 300 Ω/\square PET substrate.

Soda lime glass is the window layer of choice for thin film Cadmium telluride (CdTe) and copper indium gallium diselenide (CIGS) rigid solar cells. Cells are produced using thin-film technology in which a simple semiconductor film stack is deposited on a TCO (usually ITO) coated sheet of glass in conjunction with a back metal contact. An encapsulant layer binds the thin film-coated front glass with a tempered back glass creating an environmentally sealed module (Figure 4).

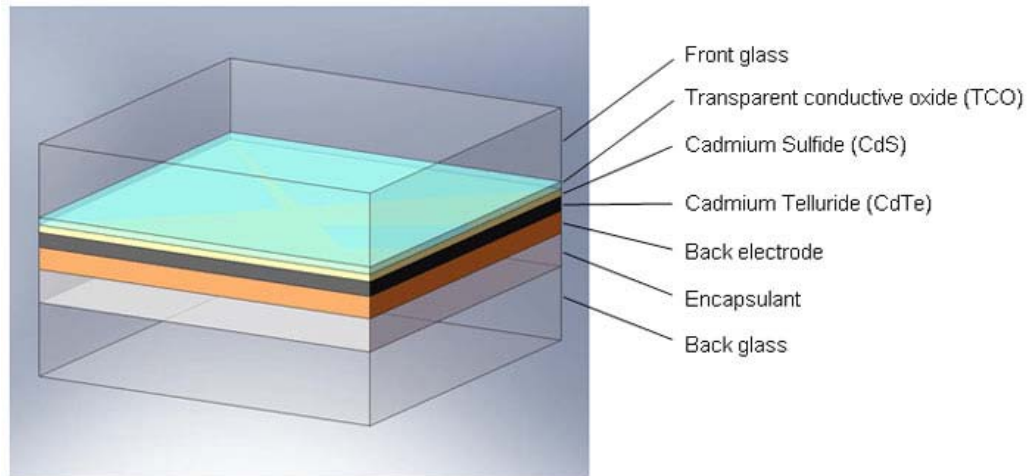


Figure 4: Structure of thin film CdTe PV cell using ITO coated soda-lime glass.

ITO coated samples were obtained on soda lime glass with AR properties (ECI) and without (ZC&R). Figure 5 shows the effect of anti reflective coatings added to the ECI ITO film vs. no such coating for the ZC&R sample. Transmission at 550nm is 94.5% for the ECI sample and 90.1% for the ZC&R sample. Four point probe measurements indicate ECI ITO coating is patchy and uneven. Average resistivity is 448 Ω/\square with a

standard deviation of $192 \Omega/\square$ after six tests. Many tests, not counted among the six used for calculation, gave out of range readings indicating a broken ITO network or patchy AR coating. ZC&R coating is much more uniform giving an average of $255 \Omega/\square$ with a standard deviation of $14 \Omega/\square$ after six tests

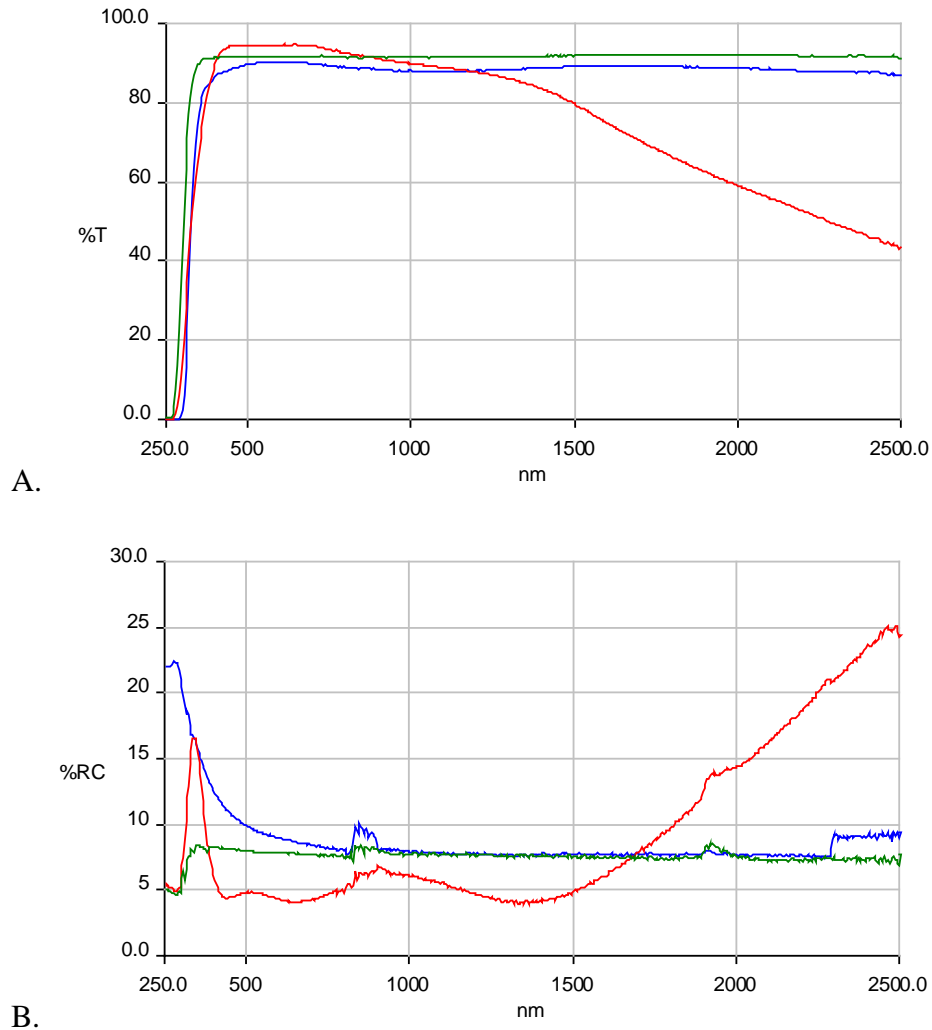


Figure 5: Transmission (A) and Absorption curves for ECI (Red) and ZC&R (Blue) ITO coatings compared with uncoated (Green), soda lime glass

Significant effort has been made in the PV industry to produce flexible thin film solar cells. Organic photovoltaics are a promising alternative to inorganic solar cells, offering an ideal combination of efficiency, light weight, flexibility and the capability to be produced easily and on a large scale¹.

TCO's such as ITO are unsuitable for this application. ITO coating is brittle and requires high deposition temperatures ($>200 \text{ C}$) to achieve the best performance. Furthermore, it is applied using a capital intensive vacuum sputtered deposition processes. When applied

at low temperature onto plastic substrates, ITO's optoelectric performance is compromised and it is susceptible to cracking.

In addition, ITO on plastic substrates can exhibit poor fatigue durability and is prone to cracking and de-lamination. During this quarter ITO coated PET film was tested in pristine condition (Figure 6), before durability tests are performed. The supplier of this material is Sheldahl, a commercial supplier of flexible materials for the electronics and PV industries. Sheldahl coatings are uniform along the surface of each sheet. Coatings specified to meet $60 \Omega/\square$ tolerance measured an average of $45 \Omega/\square$ with a standard deviation of $2 \Omega/\square$ derived from twelve four point probe tests spread evenly among the 5mil and 7mil ITO coated PET. More variation were seen for thinner coatings. For the $300 \Omega/\square$ tolerance an average of $259 \Omega/\square$ with a standard deviation of $17 \Omega/\square$ for the 5mil thick PET and $323 \Omega/\square$ with a standard deviation of $22 \Omega/\square$ for the 7mil coated PET resulted from six tests of each sample.

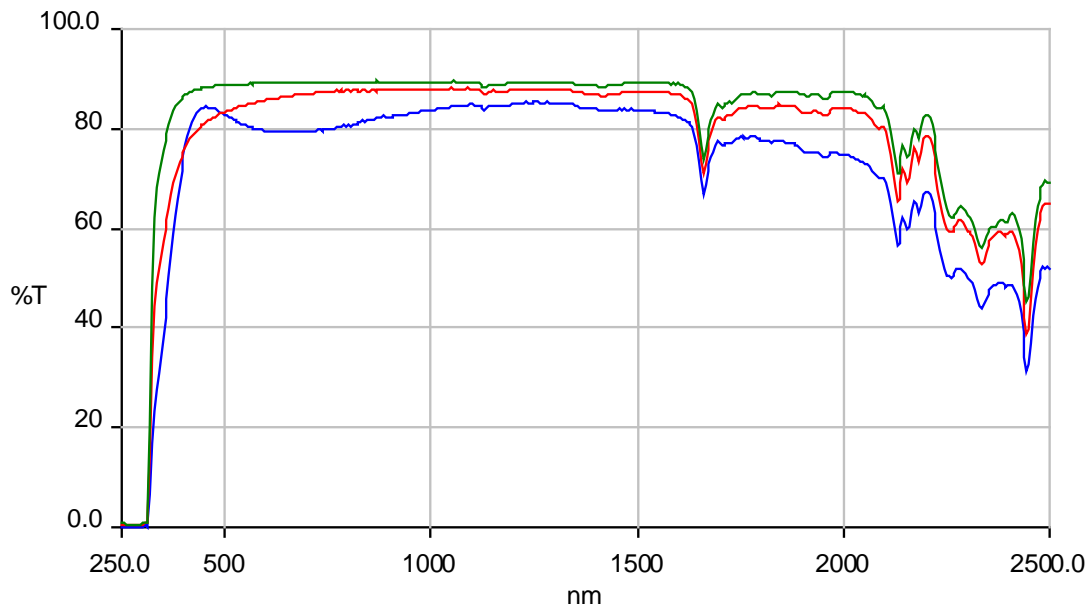


Figure 6: Transmission for 7mil thick ITO coated PET specified to $300 \Omega/\square$ (Red), $60 \Omega/\square$ (Blue), and uncoated (green).

Additional TCC Testing

Transparent conducting oxides are used as transparent electrical contacts in a wide variety of applications including flat panel displays, energy efficient windows, solid state lighting, and photovoltaics (PV). ZnO:Al (AZO), SnO₂:F (FTO), and In₂O₃:Sn (ITO) are the most commonly used TCOs for PV applications.² Soda lime glass is the window layer of choice for thin film cadmium telluride (CdTe) and copper indium gallium diselenide (CIGS) rigid solar cells. For this reason glass was the primary substrate used for environmental testing of TCC's. For this experiment ITO coated glass was obtained from ZC&R Glass, ITO coated PET from Evaporated Coatings, Inc., AZO coated glass



from NREL and FTO coated glass from Pilkington Glass. ITO coated PET was included in this experiment for its potential commercial applications.

Abrasion Testing

Abrasion testing was done according to the MIL-C-675C standard by rubbing a pencil eraser with 2 lb_f applied on the TCC on glass or by rubbing cheese cloth with 1 lb_f over the surface of ITO-coated PET. Samples were tested for 100 total cycles (one cycle equals a front and back stroke) with resistivity testing done using the four point probe method after 10, 20, 40, 60, 80 and 100 cycles.

AZO does not perform well following abrasion. It took only 60 cycles to remove AZO from the surface of glass. ITO on PET also performed poorly in abrasion testing. While the resistivities of ITO and FTO on glass were unchanged after 100 cycles, ITO on PET suffered a 6,680% decrease in electrical conductivity. This is not entirely surprising due to the differences in deposition conditions. FTO and ITO are coated on glass using high temperature vacuum sputtering. Though expensive, this technique results in a fully crystalline TCO layer that yields optimum performance for this material. High temperatures cannot be used to sputter on PET, or other polymers. Lower temperature sputtering deposits a partially crystalline TCO coating that is much less robust.

Humidity Testing

Samples of ITO, AZO, FTO and binder-free CNT coatings on glass were humidity tested for 500 hours at 85°C with 85% humidity (85/85). Each sample was tested for resistivity using the four point probe method before testing began and after 100, 200, 300, 400, and 500 hours at 85/85. In addition, each sample underwent a UV-Vis scan from 250-2,500nm before and after the 500 hours of testing.

ITO and FTO performed very well through the entire test. RT performance was unchanged for ITO and FTO. In addition to its poor performance in the abrasion test, AZO also failed humidity testing. After only 100 hours of exposure to 85/85, AZO lost 500% of its conductivity. After the full 500 hours this grew to a 2,600% loss.

5.1.4 Commercial Nanoparticulate Inks/Dispersions

Unlike TCO's which require expensive vacuum sputtering equipment to deposit conductive coatings conductive nanoparticulate offers the capability of being deposited using low energy, low temperature processes under atmospheric conditions and at a cost that is competitive with the current state of the art. During the second quarter of this project three separate commercially available silver nanoparticulate inks and dispersions were tested. These materials include:

- 1) NovaCentrix supplied 26% wt 35nm particle size silver ink and dry powder.
- 2) Cabot Corp. supplied 22% wt 50nm particle size silver ink.
- 3) Technic Inc. supplied 18% wt 80nm particle size silver powder suspension.

The commercial application of these inks and dispersion are for the printed electronics industry. Therefore, transparency is not a priority for these formulations. It became necessary to dilute these suspensions in order to produce a transparent coating. All three samples use either DI water or IPA as the solvent. Cabot and NovaCentrix inks also include up to 4% Ethylene Glycol for stability. Each suspension was diluted by 4/1, 20/1 and 100/1. Ethylene Glycol was added to each dilution to maintain the original concentration. 4% Ethylene glycol was also added to each Technic dilution to improve stability. Each diluted solution was then mixed at 7,000 RPM for 10 minutes in a high shear mixer. Mixed dilutions were deposited on glass slides using draw down casting before curing at 250°C for 2 hours. Dried castings were examined by eye to determine relative evenness of coatings.

Technic's silver dispersion deposited a very poor coating at all concentrations. All coating attempts with Technic silver resulted in a spotty 'coating' as particulate agglomerated together on the substrate. Cabot ink readily forms a uniform coating that cures into a mirror finish as a result of annealing of silver particulate. Any attempt at dilution hinders this ink from forming a uniform coating. Several solvent formulations were tried, using DMF and 1,4-Butanediol additives. All dispersions pooled into spots of concentrated ink as a result of heating.

Only the NovaCentrix ink produced even coatings at concentrations below 5%wt solids (4/1 dilution) NovaCentrix 100/1 dilution was then spray coated at various thickness for curing and subsequent RT characterization. Conductivity of silver ink coating could only be obtained by a thick film. Increased thickness caused silver coating to become uneven and virtually non-transparent. By comparison, Eikos CNT coatings enable conductivity with excellent transparency (Figure 7).

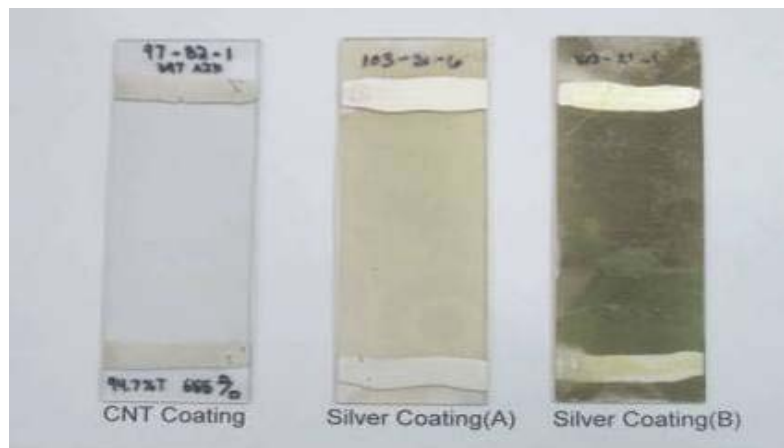
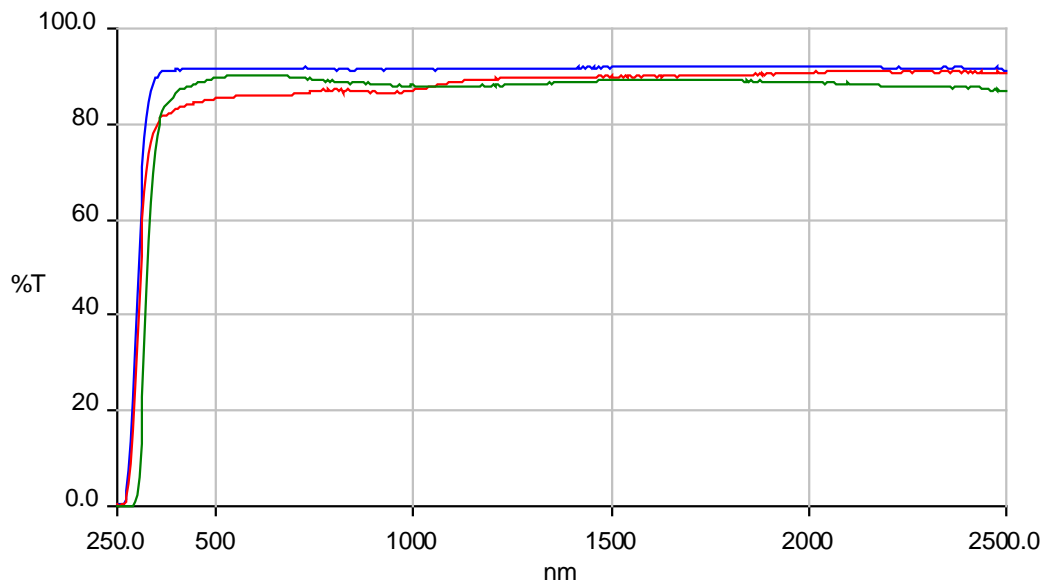


Figure 7: Comparison of spray coated CNT and thinly coated (A), and a thick coat (B) of Silver nanoparticulate ink.

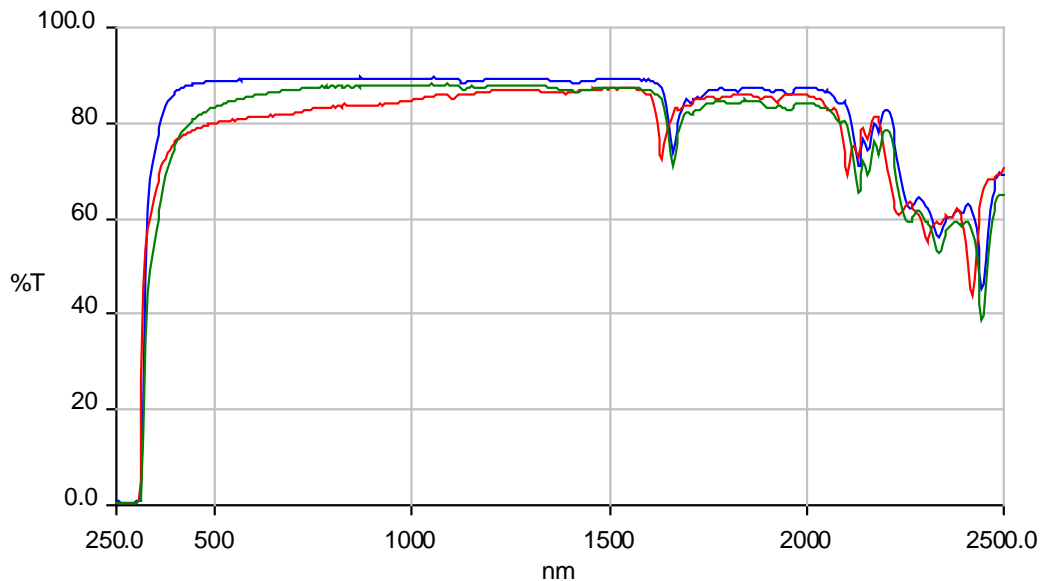
In Figure 7A yellowing of silver coating can be seen as a result of curing. This phenomenon can only be seen in thin transparent coatings and aroused considerable interest from NovaCentrix. To make sure all ethylene glycol was removed a second curing step was done at 300°C for 1hour, but produced no change in color of any of the silver coated slides. Eikos is currently working with NovaCentrix to determine the cause of this tinting.

5.1.5 CNT Comparison

Ink was formulated using Nanoledge CNT's for comparison with ITO and silver coatings. Coating deposition was done by spray coating on both glass and PET substrate. IPA/water solvent, in a 3/1 ratio, was used to formulate CNT ink was then driven off coatings by heating at 60°C for 20 minutes. Four-point probe testing was done to find the electrical resistivity of coated samples before transparency was measured by UV-Vis. Figure 8 shows % transmission across a wide spectrum from wavelengths of 250-2,500nm for ITO coated, CNT coated and uncoated glass and PET.



A.



B.

Figure 8: Transmission through uncoated (blue), 255 Ω/\square ITO coated (green), and 400-500 Ω/\square CNT coated (red) glass (A) and PET (B). Resistivity of CNT coating is 489 Ω/\square on glass and 405 Ω/\square on PET.

Results for CNT coated PET are disappointing, but the superior transparency of CNT coatings over a broad spectrum can be seen on glass (Figure 8A). ITO has a narrow window of optimal transmission in the visible light region (350-900nm). In the UV (<350nm) and IR (>1,000nm) CNT coatings outperform ITO. From these studies CNT TCC compare favorably with ITO and silver nanoparticulate dispersions.

ITO is too brittle to create flexible solar cells, and now represents one of the most expensive components in the module, as increased demand has caused a price increase of over 1600% in the last five years.³ SWNT electrodes are wet deposited, self assembling p-type conductors ideal for hole conduction at the transparent electrode.⁴ They have a high transmittance that is uniform across the solar spectrum. They are highly durable, mechanically flexible, and offer increased environmental stability for organic solar cells. Wet deposited silver dispersions are unable to match either ITO or CNT in terms of RT performance. While conductivity of these materials is good for thick coats, transparency is almost nonexistent. These properties make commercially available silver nanoparticulate good for electronic printing applications, but unsuitable for the PV industry.



5.2 Task 2: Development of Novel Nanomaterials for TCC's

Nanostructures made of noble metals such as gold and silver have been the focus of intense research because of their fascinating optical, electronic and chemical properties. Eikos investigated the use of metal nanoparticulate based conductive inks for TCCs. Size and shape of nanoparticulate is important.

Nanowires are better than more spherical particulates, as they can form a conductive network with less material (i.e. at a lower percolation threshold). Like a chain link fence, wires can form much more transparent network of connected conductors than highly packed particulates. Eikos successfully synthesized silver and gold nanowires.

5.2.1 Silver Nanowires

Silver nanowires (AgNW) represent a particularly interesting class of nanostructures to synthesize. Bulk silver exhibits the highest electrical and thermal conductivity among all metals. Silver is also an important material that has been used in a variety of commercial applications. Performance of silver in these applications could be potentially enhanced by processing silver into nanostructures with controllable dimensions and aspect ratio.

Among published literature, the most acceptable method of preparing AgNW is a soft (<200 °C) solution phase approach (1-3). This method is reported to yield silver nanowires with relatively uniform diameters, high aspect ratios, and large quantities. This so-called "polyol process" consist in reducing AgNO_3 in the presence of glycol and poly(vinylpyrrolidone) (PVP). Glycol serves as both a reducing agent and solvent. The first step of synthesis involves the formation of seeds from which silver nanowires will grow. The most often used glycol in this method is ethylene glycol (EG). Other glycols such as 1,2 propylene glycol or 1,3-propylene glycol can be used as well. The nature of glycols will affect the diameter, length and aspect ratio of AgNW. Two separate Ag NW syntheses were done.

The first synthesis was done by delivering all components consecutively by pipette only (2). The second was done based on a more recent method describing AgNW formation based on a modified polyol process, mediated by an anionic additive (4). Ionic additives promote the formation of a single morphology while discouraging other competing nanostructures. In this way a high concentration of nanowires was reportedly produced, with no or few nanoparticles.

Synthesis 1

1. In 25 ml flask 5 ml of EG was heated and stirred at 150 °C in sand bath for 1hr.
2. 40 μ L of 4mM $\text{CuCl}_2 \cdot 2\text{H}_2\text{O}$ was added and solution continued to be heated for 15 min.
3. Than 1.5 ml of 114 mM PVP (MW-58000) solution in EG was added, followed by 1.5 ml of 94mM AgNO_3 solution.
4. All reagents were delivered by pipette. The color of the mixture became yellow. Heating was continued until the solution became black-gray and the precipitate appeared (approximately 1h) at which time the reaction was stopped by submerging the flask in cold water.
5. Precipitate was separated from EG by centrifugation and washed twice with acetone and 3 times with DI water.
6. Glass slides were coated by dropcasting of the suspension in water and drying.
7. Slides were imaged via AFM.

According to AFM no AgNW were present, only Ag particles were seen. It is possible old AgNO_3 reagent is to blame for this unsuccessful synthesis.

Synthesis 2

1. In a 1000 ml flask, 4.17g PVP (MW 5800), 70mg Bu_4NCl , and 4.25g of newly ordered AgNO_3 were mixed into 500 ml EG.
2. The reaction mixture was stirred 15 minutes at room temperature until the color of solution was slight pink.
3. The flask was heated to keep internal temperature between 150-165 °C. After 30min of heating the reaction mixture has turned into gray-pink suspension.
4. After cooling the precipitate was separated from EG by centrifugation, and washed twice with acetone.
5. Drop casting was done to coat glass slides for AFM imaging.

AFM imaging indicated the successful synthesis of Ag NW. Most nanowires are small, some wires have very large aspect ratios of up to 125:1. By comparing the height of a long, well formed, AgNW from the substrate surface a diameter of 160nm was found (Figure 9 & Figure 10). The same nanowire from Figure 10 is too long to fit on a single AFM image. Splicing three images together enables a more accurate length of over 20 μ m to be seen (Figure 12).

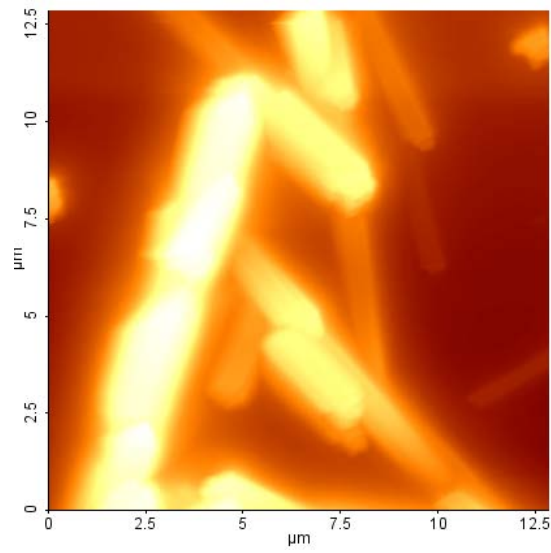


Figure 9: A cluster of silver nanowires grown from the polyol process.

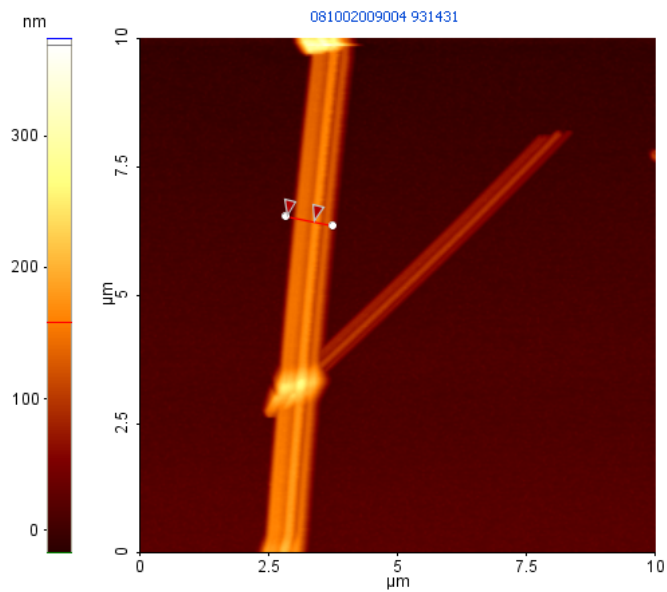


Figure 10: AFM image of silver NW

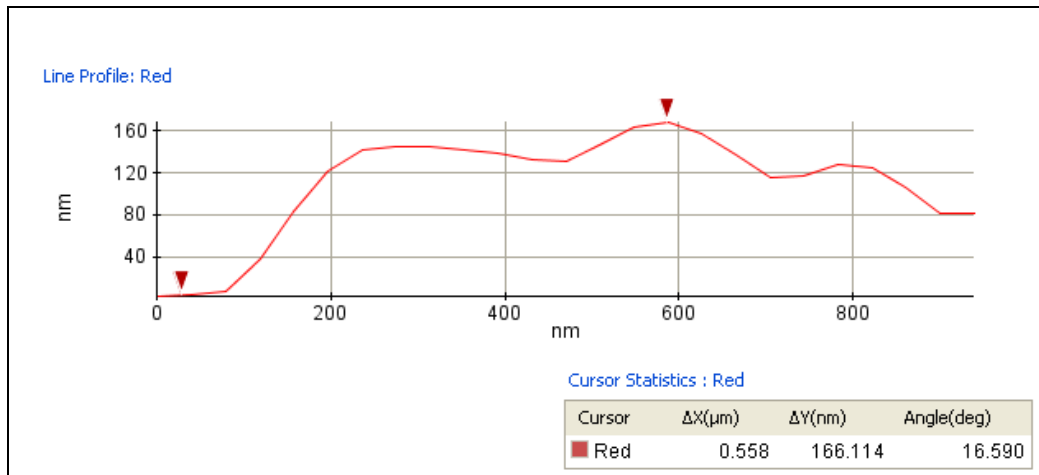


Figure 11: Diameter determination of a AgNW from AFM imaging. Red arrows from the width bar on the image correspond to the high peak and trough on the graph.

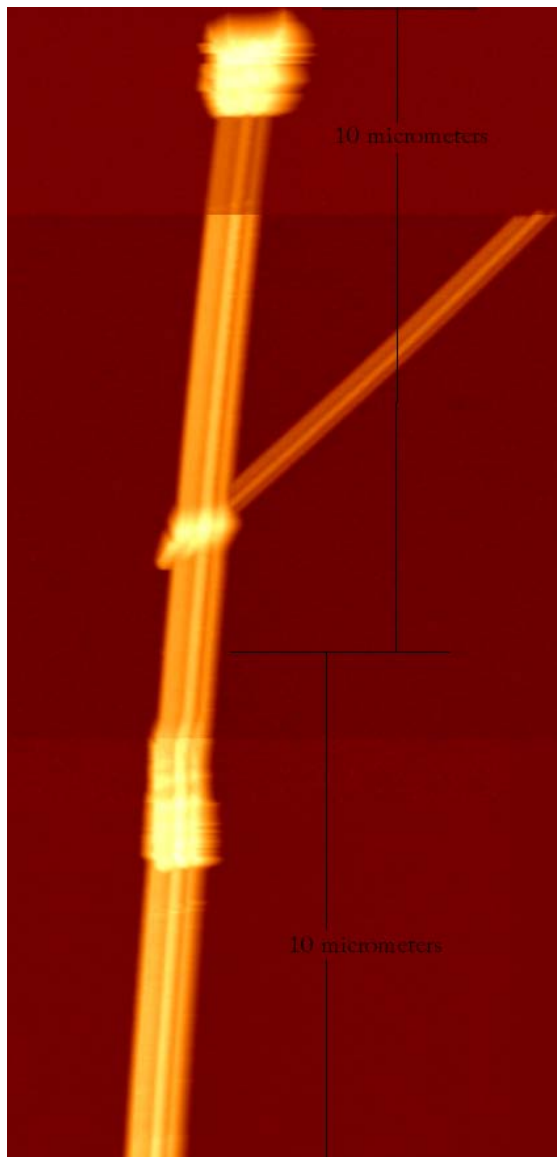


Figure 12: Spliced AFM images of a >20 μ m long AgNW.

Silver nanowires from synthesis 2 above were separated from acetone by centrifugation, washed twice in DI water and dried at room temperature. Recovered silver was first weighed then added to DI water to create a low wt% suspension. The mixture was sonicated for 30sec before a thin layer was cast on a glass slide and PET film. Transparency of coated samples was measured at a wavelength of 550nm with a Perkin Elmer UV/VIS Spectrophotometer. A total of seven castings were done (Table 3: Sheet resistance and transparency of AgNW coatings).

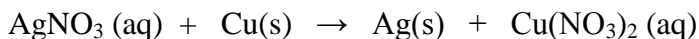
Table 3: Sheet resistance and transparency of AgNW coatings

| Solution (wt%) | Substrate | Drying Conditions | R (Ω/\square) | T (%) |
|----------------|-----------|-------------------|------------------------|-------|
| 0.5% in DI | PET | 130°C- 1hr | 113 | 22 |
| 0.5% in DI | Glass | 130°C- 1hr | Out of range | — |
| 0.5% in DI | Glass | 300°C- 3hr | Out of range | — |
| 0.017% in DI | PET | 130°C- 1hr | 2,000 | 20 |
| 0.017% in DI | Glass | 130°C- 1hr | 1×10^7 | 20 |
| 0.27% in IPA | PET | 130°C- 1hr | Out of range | — |
| 0.27% in IPA | Glass | 130°C- 1hr | 3×10^7 | 14 |

Transparency was not measured for coatings that had resistance over the range of the Ohm meter. The poor transmission measured samples was likely due to thick and non uniform casting layers resulting from non uniformity of the suspension. It was found resistances did not change after 6 days in standard atmospheric conditions.

5.3.2 Silver Nanowire/Carbon Nanotube Networks

Eikos explored the addition of AgNW to enhance or improve the RT performance of a CNT network. The method explored is a galvanic reaction whereby solid copper metal is immersed in an aqueous silver salt solution. The resulting reaction causes silver metal to plate onto the copper metal in an electro-chemical reaction. The utilization of this reaction is appealing because it occurs spontaneously, at room temperature, and in an aqueous solution. The specific reaction entails a solution of silver nitrate, AgNO_3 , in the presence of copper metal, where by Cu undergoes the galvanic reaction to produce silver metal, Ag, and solution of copper nitrate, $\text{Cu}(\text{NO}_3)_2$. This reaction is illustrated below:



The above precursor materials were mixed with CNT paste to induce a well integrated CNT/AgNW ink. Preliminary testing shows CNT stability is easily compromised by the ionic solution of silver nitrate. At some low level concentration, this salt solution will cause the CNT to crash out of solution and flocculate. To this issue the addition of materials previously tested for stability was explored. These additives are as follows:

- Surfynol ® 61 -- Air Products and Chemical, Inc
- Surfynol CT-121 -- Air Products and Chemical, Inc
- Surfynol CT-171 -- Air Products and Chemical, Inc
- Polyethylene Oxide (PEO) WSR-N70 – Dow, POLYOX Product Line
- Polyvinyl pyrrolidone (PVP) K-12 – International Specialty Products

Each stabilizer was added to CNT ink previously batched in a 3:1 solvent (IPA/water). Copper metal fragment and silver nitrate solution were then added (Table 4).

Table 4: Additives and Weights Along With Copper Metal Data

| Test Number | Material | Weight of Additive | Copper Metal Wire |
|-------------|-----------------|--------------------|-------------------|
| 1 | Surfynol 61 | 0.0174g | 0.0386g |
| 2 | Surfynol CT-121 | 0.0135g | 0.0390g |
| 3 | Surfynol CT-171 | 0.0131g | 0.0375g |
| 4 | PEO WSR-N750 | 0.0101g | 0.0378g |
| 5 | PVP K-12 | 0.0158g | 0.0389g |

For each mixture 10.0ml of CNT ink Batch #389 was dispensed using a volumetric pipette. Additive and CNT were sonicated for 40 seconds at 70% amplitude. Copper wire was cleaned using IPA and lab towels and coiled with an approximate diameter of 0.125” (1/8th inch). The purpose of coiling the copper wire is to provide more surface area exposed to the solution for reaction. Copper wire was added to the CNT solution and allowed to sit for one hour to establish equilibrium. After one hour 5mL of 0.1% AgNO₃ (0.1008g AgNO₃ in 100mL water) was added into each of the 5 test samples. No mixing was done for any of these samples after the addition of the silver nitrate solution. Solutions again remained idle for one hour after the addition of the AgNO₃ solution. Observations made on 15mL (total mixture volume) of each test sample, one hour after addition of silver nitrate, are as follows (Figure 13):

Test #1 - Surfynol 61 / CNT

Distinct Separation with clear fluid on bottom with an approximate volume of 5mL. The top layer was an approximate 10mL containing the CNT mixture. After a few minutes of handling the CNT layer became thinner and continued to float. Bubbles could be seen on the underside of the floating CNT layer. Silver metal is seen on the underside of the CNT layer as well as on the bottom of the test beaker near the copper coil.

Test #2 – Surfynol CT-121 / CNT

At first there was a separation similar to the Surfynol 61, Test #1. Like Test #1 the bottom layer was clear and at an approximated 5mL volume (~1/3rd). However, within the time frame as in Test #1, there is further separation of the 2 layers; whereby the bottom clear layer increased to approximately 10mL (~2/3rd). Some bubbles could also be seen on the bottom of the floating top CNT layer. Silver metal could be seen in the lower area of the CNT region.

Test #3 – Surfynol CT-171 / CNT

Some separation with clear bottom layer was observed, though not nearly as distinct as previous surfactant tests here. Roughly the bottom ¼ was clear. Overall, they were fairly well dispersed even after handling sample. Bubbles and silver were observed on the lower region of the CNT layer.

Test #4 - PEO N750 / CNT

Very similar to the Surfynol CT-171 test but even less layer separation. Though some separation can be discerned, it is not as clear-cut as other previous samples. Bubbles and silver metal was observed on lower region of CNT area.

Test #5 – PVP K-12 / CNT

At first this was a very homogeneous fluid. CNT well dispersed at initial observation. But upon handling the sample, significant layer separation developed. Bottom 1/3rd (5mL) is clear fluid. Bubbles on bottom but can also be seen throughout the CNT layer. The bubbles throughout the CNT layer may be a function of migration from the underside of the CNT layer. Silver metal can be seen on the bottom of the CNT layer.

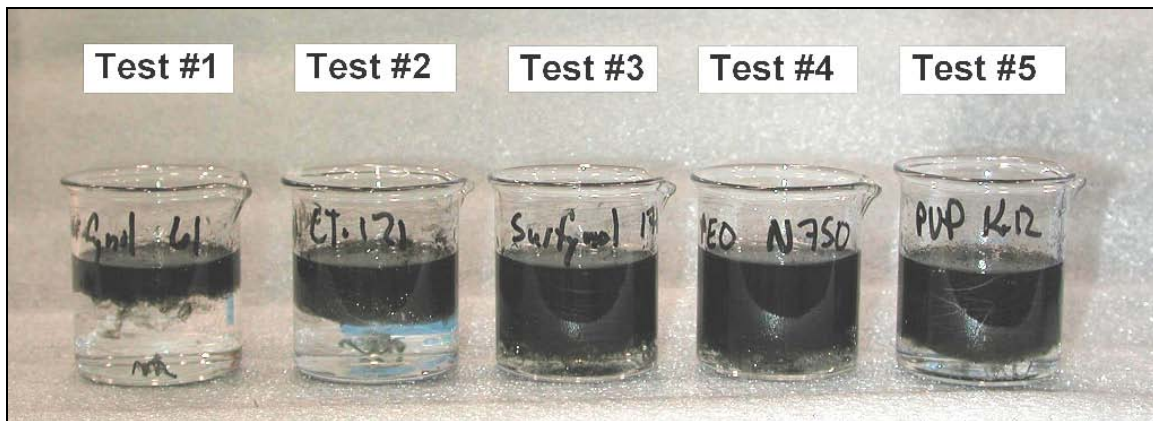


Figure 13: Silver / CNT / Additives – One Hour After Silver Solution

Each of the five samples was sprayed by air brush onto glass slides. Glass slides are 1” x 3” with silver electrodes painted onto the slide providing a sample area of 1” x 2”. The samples sprayed were measured for transparency and resistivity. A normalized calculation was done at 500Ω/□.

Table 5: Summary of Normalized Results for Silver/CNT testing

| Material | R _s ⁵⁰⁰ |
|---------------------------------|-------------------------------|
| Test #1 – Surfynol 61 / CNT | 18.5 %T |
| Test #2 – Surfynol CT-121 / CNT | 2.3 %T |
| Test #3 – Surfynol CT-171 / CNT | 1.8 %T |
| Test #4 – PEO N750 / CNT | 2.6 %T |
| Test #5 – PVP K-12 / CNT | 11.1 %T |
| Control – CNT base ink 100-2-01 | 80.5 %T |

As can be seen in Table 5, all mixtures have poor RT properties compared to CNT control ink. There are several factors that could be attributed to this. It is possible various stabilizing additives are too concentrated and thereby interfere with formation of the CNT network. This can be addressed by using fewer additives. Previous testing indicates additives can be added to a CNT solution and still allow a viable conductive network to be formed. Another potential is that the ionic nature of the silver nitrate solution causes flocculation of the CNTs. Once CNTs have flocculated, spraying becomes difficult and network formation is impeded. This could be addressed in a similar fashion as with the stabilizing additives, by using less, or more accurately, the *right* amount of silver nitrate. The amount of silver needed is linked to the metallic distribution ionically desired throughout the CNT material.

Another Trial at Combining NW and CNT

Eikos combined purified metallic NW with CNT to identify any additive affects these materials may have when used together. Three methods for NW and CNT coating integration were used. In the first method Eikos first deposited the NW then deposited the CNT layer on top. In the second method, a CNT coating was deposited first then NW was layered on top. Finally, in the third method NW and CNT were mixed and deposited as one homogenous. RT performance of these coatings was evaluated as a function of heating at 250°C for up to 2 hours. Heat treating lowered the resistivity of all NW-CNT samples. This was most profound for coatings made from the NW-CNT mixture. Table 6 compares RT performance, as a function of heat treatment, for homogeneous NW-CNT versus pure CNT coatings.

Table 6: RT performance of NW-CNT dispersion as coated on glass.

| Sample | Coating | Resistivity (Ω/\square) | | | | %T @ 550nm |
|---------|---------|----------------------------------|-----------|----------|-----------------|------------|
| | | Initial | 1hr@ 250C | 2hr@250C | 3 weeks storage | |
| 1012851 | CNT | 769 | 3110 | 3110 | 2630 | 74.6 |
| 1012853 | CNT | 388 | 707 | 707 | 949 | 76 |
| 1012854 | CNT | 743 | 1405 | 1330 | 1655 | 80.7 |
| 1012852 | CNT,NW | 3600 | 693 | 667 | 739 | 37.2 |
| 1012855 | CNT,NW | 3610 | 924 | 941 | 1148 | 56 |
| 1012856 | CNT,NW | 3010 | 529 | 527 | 610 | 42.3 |

The combined NW-CNT coating is initially less conductive than pure CNT by a factor of five (Table 6). However, where heat treatment causes the resistance of the pure CNT coating to increase, the same heat treatment causes resistivity of mixed NW-CNT to decrease to the point this coating is as conductive as or more conductive than the pure CNT coating. All mixed and layered NW-CNT coatings have significantly lower transparency than CNT coating alone. Nevertheless, this shows there is a beneficial interaction between NW and CNT in regards to lowering coating resistivity.



5.3.3 Gold Nanowires

Gold is chemically inert and has very low electrical resistivity. These properties make gold nanowires (AuNW) an ideal candidate as an additive for electrically conductive coatings, especially for PV applications in low earth orbit. Eikos synthesized AuNW. Gold nanowire synthesis was done by the reduction of HAuCl_4 in oleylamine or mixture of oleic acid and oleylamine (5). The goal of this process is to produce ultra thin (2.0 nm) wires with a length of several microns.

Using ultrasonication, $\text{HAuCl}_4 \cdot 3\text{H}_2\text{O}$ was dissolved in a oleylamine/ oleic acid solution to induce precipitate formation. This technique causes precipitate to slowly sink to the bottom of the flask and changes color from yellow to purple/dark red. Color change is indicative of completion of the reaction. This chemical process can be described in three steps:

1. Partial reduction of Au^{+3} to Au^{+1} by oleylamine/ oleic acid
2. Formation between Au^{+1} and oleylamine/ oleic acid leading to ordered mesostructure.
3. Slow reduction of Au^{+1} within mesostructure to form AuNW.

The colored deposit was separated from organic solvent by centrifugation and washed by mixture of ethanol and toluene several times to remove oleylamine. Centrifuge deposit was dispersed in hexane and suspension was sprayed out on glass slides. AFM imaging of coated slides indicates synthesis at 80 °C does produce AuNW (Figure 14).

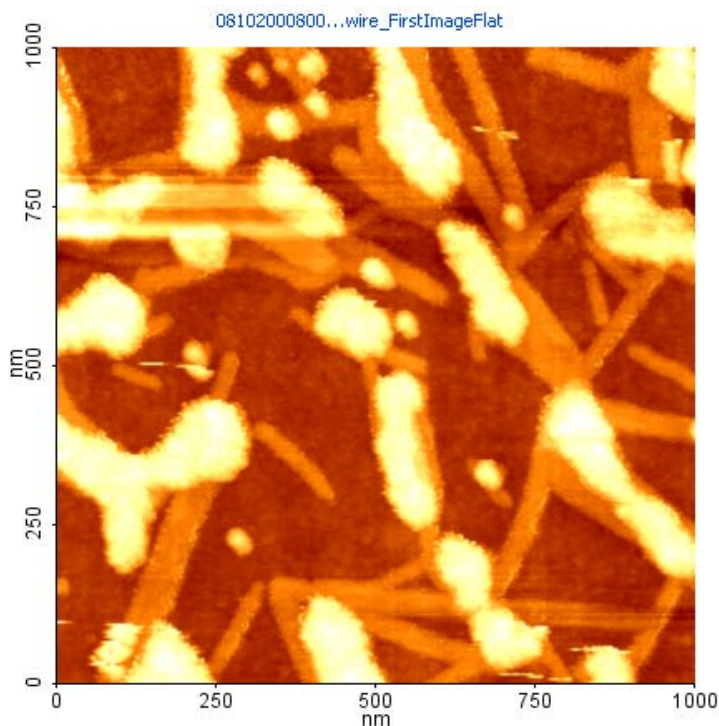


Figure 14: AFM image of gold nanowires.

Coated slides did not show conductivity as measured by Ohmmeter, or by 4 point probe. Based on AFM imaging, the aspect ratio of such wires is $\sim 20/1$, which would require a dense gold coating to produce a percolative (and thus conductive) network. Additionally, the removal of oleylamine presents a challenge, since it has strong affinity for gold, low solubility and is not volatile. The presence of residual oleylamine or other oils could electrically isolate gold nanowires and prevent conduction. From optical microscopy and AFM, Eikos have observed oily contamination on the slides. A high temperature treatment or solvent washing could remove some of this residue.

5.3.4 Synthesis of Gold Nanowires

Further effort was done to filter AuNW solutions through polymeric membranes and recover purified NW. New solvents were used to strip residual oleylamine other residuals from synthesis. Solvent such as acetonitrile, CS₂, DMSO and carbon disulfide have been identified as candidates for testing based on their ability to remove residuals without harming AuNW. Sonication was used to separate dissolved PC from AuNW in chloroform solvent. The sonicated dispersion were sprayed on slides and heated at elevated temperatures ($>500^{\circ}\text{C}$). Sonication breaks PC away from AuNW making the polymer readily burn off. Another approach is to evaporate chloroform off the filter cake. The cake is re-wet with other solvents, such as hexane. If needed the caked filter was sonicated in solution to re-disperse filtered AuNW. This new dispersion can then be spray coated on glass slides and tested for RT performance.

Efforts to scale synthesis of metallic nanowires focused on developing a reliable method to characterize NW growth. Published literature cites only the creation of AuNW, without the focus of applications.^{5,6} Indeed, only one paper even measured electrical resistance of AuNW coatings.⁷ Characterization is important before production scale up and application as a TCC are attempted. To perform proper characterization of NW for TCC applications Eikos must be able to determine the efficiency of NW synthesis and the physical form of the NW. Quantity of AuNW produced, as opposed to various other gold nanoparticulate, will determine purification methods needed to isolate NW and ultimately the feasibility of using AuNW as a TCC. The structure of AuNW is also important. High aspect ratio wires are ideal for producing high percolation threshold coatings with the least amount of deposited material, thus dictating thickness of the film, and in turn, transparency of the coating. Preparation of AuNW for characterization was done using two techniques.

Eikos made changes to our NW purification procedure in order to separate metallic NW from other materials produced during synthesis. New solvents were used for preparing the NW dispersion and other deposition methods were tried. Heat treatments were also tested to aid in purified NW layer formation. Three solvents were used to aid the dispersion of wet synthesized metallic NW. These solvents were carbon disulfide, Dimethyl sulfoxide and acetonitrile. It was found that Eikos are able to disperse and deposit NW on substrates using carbon disulfide. Heating this deposit at 300°C increases conductivity from an insulator into the $10^2/ \square$ range after 30 min and into the single $10^2/ \square$ range after 1 hour. AFM images of the sample heat treated at 300C for 1h suggest that the structure of NW is partially damaged, but solvent and other synthesis precursor materials have been burned off (Figure 15).

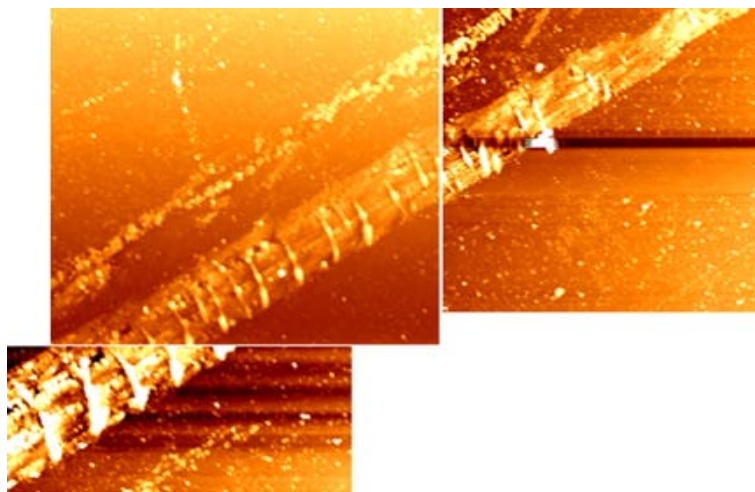


Figure 15 Carbon disulfide synthesized NW heat treated to 300C to remove impurities.



AuNW Purification/Characterization #1

A container with $\text{HAuCl}_4 \cdot 3\text{H}_2\text{O}$ dissolved in mixture of oleylamine and oleic acid was kept at 65C for 6-8 hours. The dark-red product of reduction (oleylamine serves both as solvent and reducing agent) was precipitated out by adding ethanol after finishing the reaction. Gold colored deposit was formed on the walls of the container. The reaction mixture was then separated into gold deposit and solvent using a centrifuge. The deposit was then washed three times with ethanol and sonicated for 30 seconds in ethanol to form dispersion.

The dispersion was centrifuged again to remove supernatant. Hexane was added to the collected gold deposit and sonication for 30 minutes producing a red colored dispersion. Dispersed AuNW was then deposited as a thin film of various thicknesses on glass slides for AFM imaging by spray coating or drop casting. Figure 2 shows there are still a lot of non AuNW particles present. Nevertheless, it is possible to see AuNW formed in the process. Four point probe resistivity testing indicates all coatings prepared by this method are not conductive, giving out of range readings.

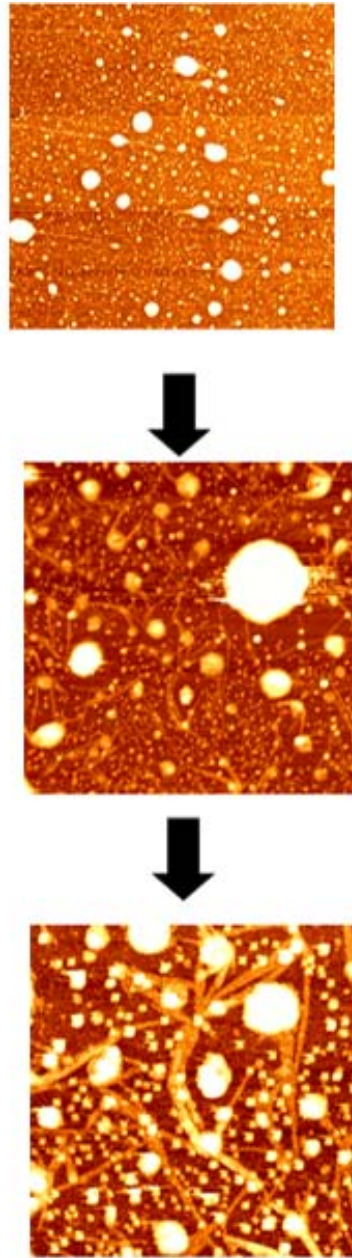


Figure 16: AFM image of AuNW and other nanoparticulate coating on glass substrate at $35 \times 35 \mu\text{m}$ (top), $8.5 \times 8.5 \mu\text{m}$ (middle) and $3.5 \times 3.5 \mu\text{m}$ (bottom) image size.

AuNW Purification/Characterization #2

After following the synthesis described above the reaction mixture was passed through polymeric (PC, PFC) filters of variable pore size (0.2, 0.4, 0.8 μm). After filtration the resulting cake was washed with EtOH and iPrOH to remove solvent. A final wash was done with Hexane to remove small particulate (i.e. smaller than the pore size). The beginning color of solution passing through the filter is yellow, indicating the removal of oleylamine, while the color of deposit on the filter turns from blue to pure gold. Hexane washing produces red filtrate, indicating removal of particulate. It was determined a PC filter of 0.2 μm pore size gives the best results. After washing with hexane (approximately 20 ml) and drying at 30°C for 1min it is possible to see a dense, thick, gold color circle of deposit. Four point probe resistance measurements indicate filtered cake is conductive. Depending on thickness of cake, resistance was measured to be from 500 $\text{K}\Omega/\square$ to 2 $\text{M}\Omega/\square$. Soaking in acetic acid followed by washing with DI water and IPA dropped resistivity by five orders of magnitude, into the single digit Ω/\square range. Filter cake was then transferred to a glass slide by smearing the cake on the slide. AFM images of covered slides show long bundles of AuNW (Figure 17).



Figure 17: A series of consecutive AFM images taken from the same region of a coated slide showing long bundles of AuNW. Each square is 20 μm x 20 μm .

Smearing of filter cake does not allow for uniform coatings, or collection of all the filter cake. Attempts were made to transfer the AuNW filter cake as a uniform layer on glass slides. PC filters made it possible to dissolve the filter in chloroform and disperse the cake for deposition on slides using spray coating or drop casting. Coatings made from this technique are dust black in color, rather than gold. Resistivity testing indicates no conductivity for these coatings. It is likely dissolved PC is being deposited along with AuNW and acting as an insulator. PC was burned off the slide by baking at 500C for 2 hours. Baked slides turned gold, indicating removal of PC, and producing a gold coating more uniform than smearing (Figure 18). Resistivity measurements show conductivity in spots, but not along the entire coating. Light transmission of the slide was measured to be 20% using UV-Vis.

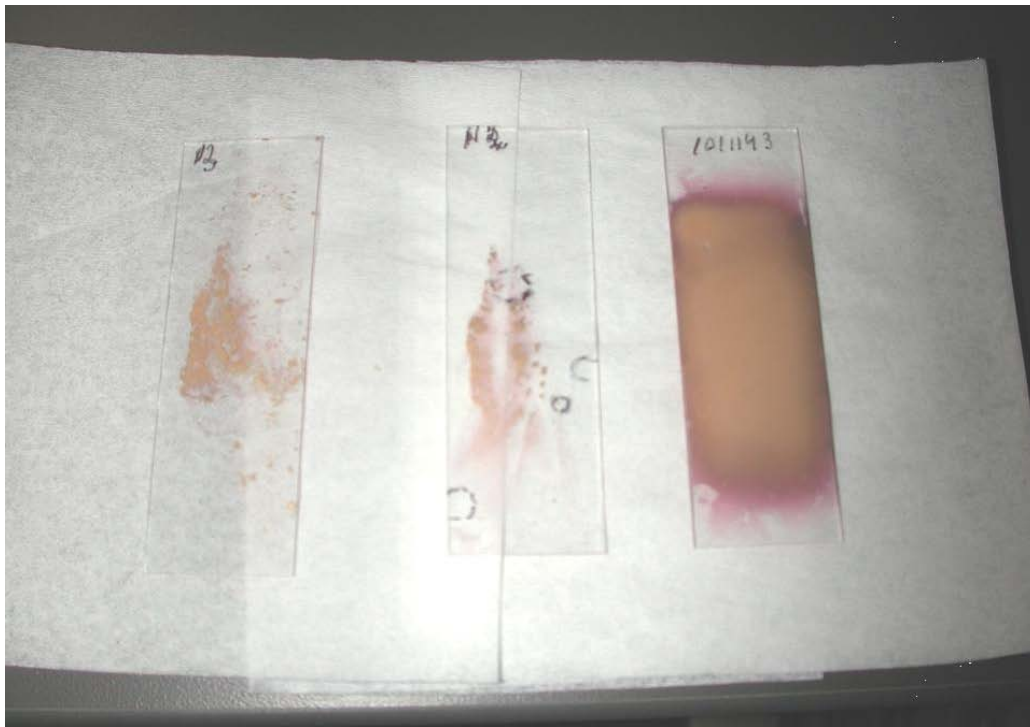


Figure 18: Comparison of a spray coated sample (right) and two samples that were prepared by smearing gold nanowire filter cake onto glass slides.

Eikos also focused on characterization of Cima Nanotech's SANTE™ Silver based thin film. SANTE films are made by allowing silver nanoparticles to self assemble into microscopic networks, thus providing simultaneous transparent and conductive networks. Cima claims SANTE films are durable and flexible coatings capable of replacing existing TCC technologies.⁸ SANTE film is deposited on PET by Cima and was tested by Eikos for a wide range of PV specifications. Tests included humidity resistance, adhesion and abrasion testing, RT performance before and after sample flexing, coating uniformity, optical distortion due to moiré effect, and color/haze changes as a result of environmental effects.

Resistivity of SANTE film is relatively uniform ranging from 8.0-12.8 Ω/\square . Flexing causes no change in resistivity. Moiré optical distortion was noticed by looking through three SANTE films stacked progressively $\sim 15^\circ$ to each other (i.e. 90, 105, 120°). Humidity testing has no effect on optical transmission of SANTE film if haze is ignored.

Utilizing the integrating sphere in our UV-Vis Spectrophotometer to factor out haze, CNT coated PET is 79% transparent at 550nm before and after 500 hours humidity testing. However, a visible haze was generated on the surface of the SANTE sample as a result of humidity testing. Figure 19 shows UV-Vis curves for SANTE film with and without haze included after humidity testing. Haze decreases transparency of SANTE film by 8% down to a total of 71% at 550nm.

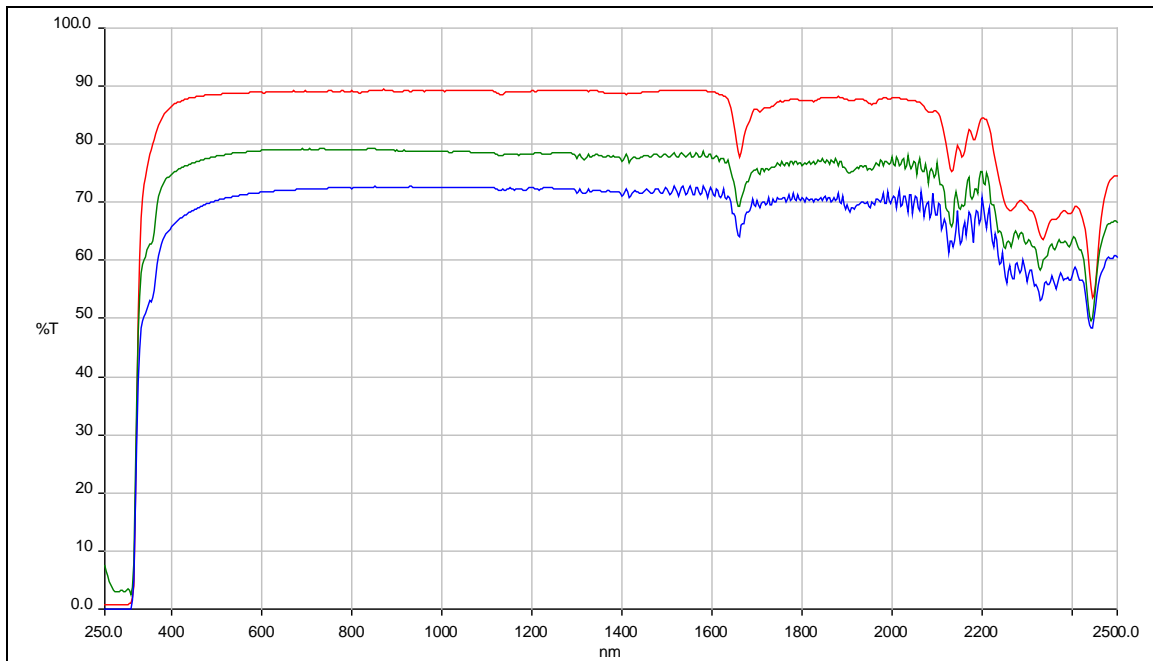


Figure 19: Spectrophotometer transmission curves for uncoated PET (red) and SANTE film after 500 hours humidity testing with haze (blue) and with haze factored out (green).

Adhesion and abrasion testing was done according to MIL-C-675C standard. While SANTE passed adhesion testing, it rubbed off easily during the more aggressive abrasion test. Samples are normally tested for 100 total cycles (one cycle equals front and back stroke) with resistivity testing done using the four point probe method after 10, 20, 40, 60, 80 and 100 cycles. SANTE coating was removed after only one test cycle.

Table 7 compares the ability of SANTE film with currently available TCC materials to meet PV applications. Properties for Invisicon® in this table are for CNT/binder on PET, developed by Eikos prior to this reporting period.

Table 7: Strengths and weaknesses of commercial TCC materials for PV requirements

| ○ Good ● Poor | Sputtered ITO | ITO dispersions | ICP dispersions | SANTE™ Film | Invisicon® Film |
|-------------------------|---------------|-----------------|-----------------|-------------|-----------------|
| Transparency | ○ | ● | ○ | ● | ○ |
| Conductivity | ○ | ● | ● | ○ | ● |
| Optical Distortion | ○ | ○ | ○ | ● | ○ |
| Cost | ● | ○ | ● | ○ | ○ |
| Color | ● | ● | ● | ○ | ○ |
| Flexibility | ● | ● | ○ | ○ | ○ |
| Environmental Stability | ○ | ○ | ● | ○ | ○ |
| Bonding/Adhesion | ○ | ○ | ○ | ● | ○ |

5.2.5 Characterization of Danubia SWCNT

This work included the characterization of materials from Danubia Nanotech, the commercial spin-off of Sineurop Nanotech. Prior results from testing of materials from Sineurop have been very promising (96%T @ 500 Ω/\square reported). During this effort, Sineurop Nanotech ceased production of SWCNT. A commercial spin-off, Danubia Nanotech, has taken over SWCNT production based on Sineurops growth process. Recently, Danubia scaled up production and is working with Eikos to optimize production of SWCNT from its new reactor.

Initial characterization of Danubia SWCNT indicates this material is inferior to that previously produced by Sineurop. Raman spectroscopy of each company's product showed that Sineurop SWCNT has a G/D ratio of 4.9 and G'/D ratio of 1.52 compared to Danubia's G/D ratio of 3.7 and G'/D ratio of 1.30. This indicates the Danubia SWCNT product has a higher percentage of lower grade carbon. Data from TGA indicates the Danubia SWCNT product has 28% residual catalyst compared to 18% for the Sineurop SWCNT product (Figure 20). Again, this indicates that the Danubia product has higher impurities content.

In addition, formulations of ink from Eikos purified Sineurop and Danubia SWCNT product yields RT performance of 96.2%T and 89.3% T @ 500 Ω/\square , respectively. At the time of this report, Danubia has not successfully scaled production of SWCNT to the quality of the previously tested Sineurop SWCNT.

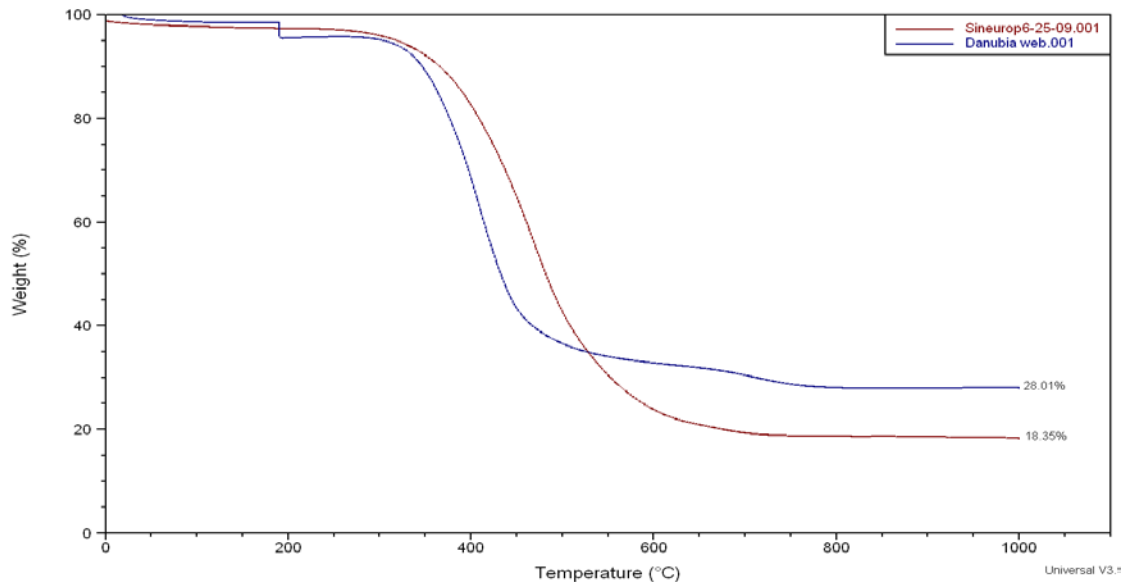


Figure 20: TGA curves for Sineurop (Red) and commercially scaled Danubia (Blue) SWCNT.

5.2.6 Purification of SWCNT via Heat Treatment

Eikos conducted heat treatment and characterization of SWCNT from a promising domestic supplier Carbon Solution Inc (CSI) from Riverside California. Eikos has previously done TGA and Raman characterization in addition to formulating inks to 95%t at 500Ω/□ with this material. Eikos used CSI SWCNT to conduct experiments to determine the effects of adding a heat treatment will result in better material purity and added benefits to ink yield and performance.

Eikos evaluated the purification of SWCNT via heat treatment. Under this effort, performed as part of our **NIST ATP Grant 70NANB7H7010 “Printable Electronic Nanotube Inks and Concentrates”**, five samples of as received Carbon Solutions batch AP-286 SWCNT were heat treated in either air or an inert atmosphere (argon). Eikos performed the air heat treatment with the intent to burn off amorphous carbon while oxidizing the SWCNT, and the inert atmosphere heat treatment to allow the SWCNT to anneal defects without inducing imperfections or SWCNT oxidization. Tried heat treatments are as follows:

- 1) 800mg SWCNT baked in air at 500°C for 20 hours (103-89-5)
- 2) 600mg SWCNT baked in argon at 500°C for 20 hours (103-89-1).
- 3) 600mg SWCNT baked in argon at 700°C for 20 hours (103-89-2).
- 4) 600mg SWCNT baked in argon at 900°C for 20 hours (103-89-3).
- 5) 600mg SWCNT baked in argon at 1100°C for 20 hours (103-89-4).

After heat treatment Eikos characterized each sample via Raman and TGA. Raman analysis determines the relative type and purity of carbon and TGA determines the amount of residual catalyst left in each sample after heat treatment.

Multiple Raman scans were done at various locations of within each sample, for both 633nm and 785nm lasers, to ensure an accurate characterization. Raman curves generated are near identical within each heat treatment, indicating a uniform material. Figures 1 and 2 show Raman curves for each sample using a 785nm laser (Figure 21) and a 633nm laser (Figure 22). The high radial breathing mode (RBM) seen in all samples from the 785nm Raman scan is normal for CSI SWCNT. The only other materials with this characteristic Eikos have encountered are SWCNT made by Hanwha Nanotech (formerly Iljin) and Sineurop Nanotech GmbH. The RBM peak is enhanced by heat treatments, especially oxidization. Higher RBM peaks indicate a material more in resonance with the wavelength of the scanning laser. In this case heat treated CSI SWCNT is in resonance with 785nm laser more than any other material Eikos has tested.

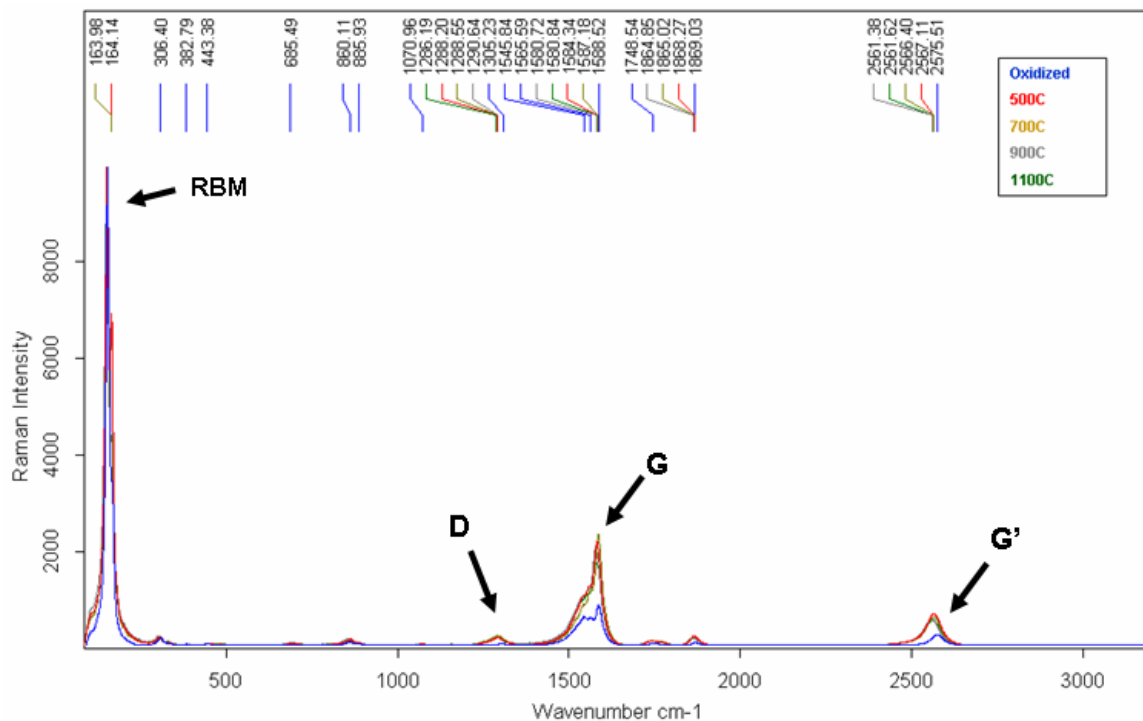


Figure 21: Raman Spectrum for annealed Carbon Solutions SWCNT using a 785nm laser.

The TGA curves for each sample after heat treatment are shown in Figure 3.

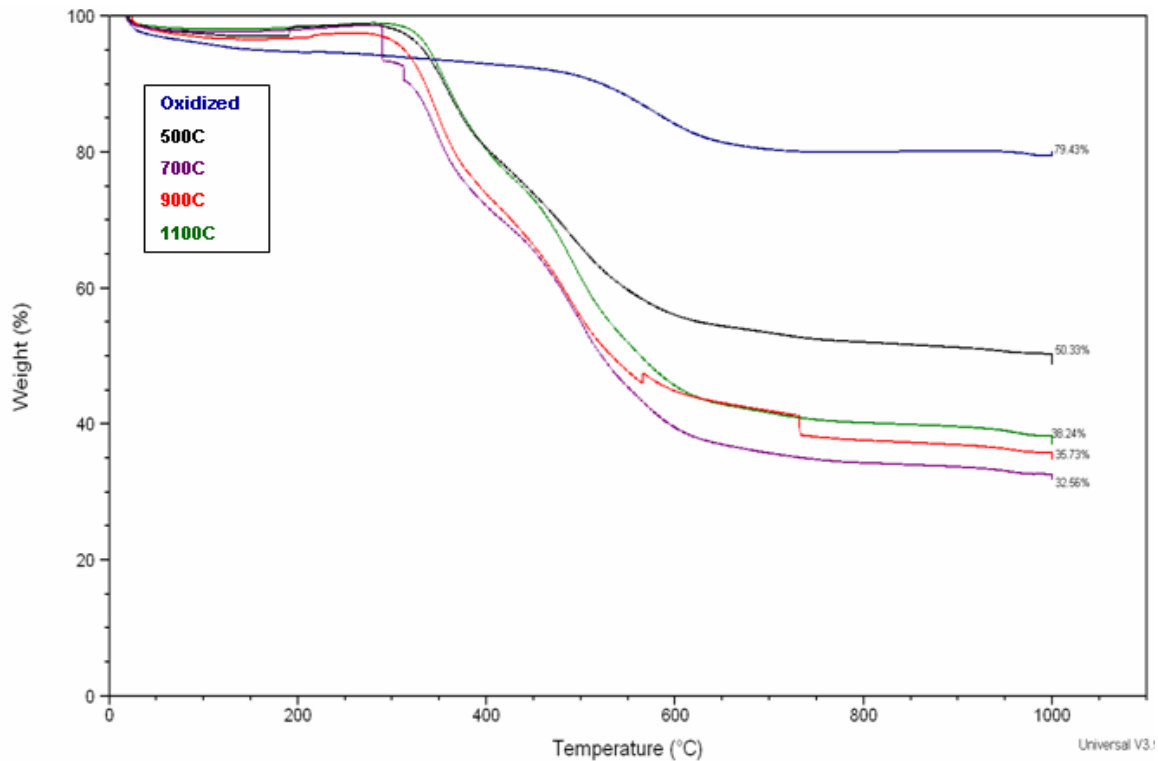


Figure 22: TGA curves for air oxidized and inert atmosphere annealed Carbon Solutions SWCNT.

Of interest, the residual catalyst content is highest for the air-oxidized SWCNT. This is expected since amorphous carbon and weaker-defect ridden CNT will be consumed by oxidation, leaving a higher concentration of catalyst. Of further note, the air-oxidized SWCNT is naturally more resistant to degradation at elevated temperatures than the SWCNT treated in an inert atmosphere because the carbon susceptible to oxidation degradation has already been removed.

Table 8 lists data obtained from Raman and TGA characterization. The top half of Table 1 lists Raman data from the 633nm laser and the bottom lists data from the 785nm laser. From Table 1 Eikos see no clear trend from increasing anneal temperature in regards to G/D or G'/D from Raman data. Only the air oxidized sample stands out with exceptionally good G/D and G'/D ratios, indicating better SWCNT purity than previously seen by Eikos in any CNT material. The air oxidized CSI SWCNT sets a new 100% pure SWCNT benchmark within our CNT purity curve, as reported last quarter.



Table 8: Raman and TGA data for heat treated Carbon Solutions SWCNT

| Annealing of Carbon Solutions for purification- Raman Data | | | | | | | | | | TGA Data | |
|--|--------------|------|-------|-----|---------|------|------|------|------|-------------|---------------------|
| Sample | Treatment | C | Laser | D | D-width | G | G' | G/D | G'/D | Burn temp C | Residual catalyst % |
| 103-89-1 | | 500 | 633 | 195 | 197 | 1741 | 1408 | 8.9 | 7.2 | 300 | 50.33 |
| 103-89-2 | | 700 | 633 | 635 | 195 | 6478 | 3864 | 10.2 | 6.1 | 300 | 32.56 |
| 103-89-3 | | 900 | 633 | 446 | 214 | 6322 | 3593 | 14.2 | 8.1 | 300 | 35.73 |
| 103-89-4 | | 1100 | 633 | 271 | 248 | 2306 | 1644 | 8.5 | 6.1 | 300 | 38.24 |
| 103-89-5 | air oxidized | | 633 | 187 | 149 | 4368 | 3119 | 23.4 | 16.7 | 500 | 79.43 |
| 103-89-1 | | 500 | 785 | 242 | 139 | 3298 | 1000 | 13.6 | 4.1 | 300 | 50.33 |
| 103-89-2 | | 700 | 785 | 216 | 150 | 2459 | 622 | 11.4 | 2.9 | 300 | 32.56 |
| 103-89-3 | | 900 | 785 | 261 | 157 | 2725 | 723 | 10.4 | 2.8 | 300 | 35.73 |
| 103-89-4 | | 1100 | 785 | 194 | 156 | 2132 | 653 | 11.0 | 3.4 | 300 | 38.24 |
| 103-89-5 | air oxidized | | 785 | 172 | 66 | 4623 | 1211 | 26.9 | 7.0 | 500 | 79.43 |

Table 9 gives carbon yield as a result from each heat treatment (bake). As anticipated, air oxidation results in a lower yield of higher quality SWCNT. Samples treated in an inert atmosphere show a decrease in carbon yield corresponding to an increase in the heat treatment temperature.

Note that the TGA data reveals material annealed at 500°C (inert atmosphere) yields a residual catalyst that does not fit with the trend from the inert atmosphere treated samples. Weight percent lost as a result of heat treatment in the inert atmosphere at 500°C is very low (5%), so a leak in the reactor can be ruled out as the cause of discrepancy in yield. Eikos suspect that the high residual content for this sample is likely an experimental anomaly, which in turn skewed the yield calculation.

Table 9: Yield for heat treatment of Carbon Solutions SWCNT

| Treatment (°C) | Start mass (mg) | End mass (mg) | Bake yield (wt%) | TGA residuals (wt%) | Total SWCNT yield (wt%) |
|----------------|-----------------|---------------|------------------|---------------------|-------------------------|
| Air 500 | 800 | 480 | 60 | 79.4 | 12.5 |
| Argon 500 | 600 | 572 | 95 | 50.3 | 47.2 |
| Argon 700 | 600 | 566 | 94 | 32.5 | 63.4 |
| Argon 900 | 600 | 522 | 87 | 35.7 | 55.9 |
| Argon 1100 | 600 | 546 | 91 | 38.2 | 56.2 |



5.3 Task 3: Inks and Dispersions from Novel Nanomaterials

It is important for Eikos to develop ink that can be printed with multiple methods (ink-jet, slot die, draw down, spray coating, roll/roll, etc.) in order to be positioned to provide cell manufactures a range of methods to integrate CNT coatings into their production process. One of the most attractive deposition methods to apply the transparent conductor is by wet roll coating, since that offers the lowest cost and largest scaling possible.

Investigation into draw-down deposition (typical industrial process serves as a model for roll coating) was done in parallel with current ink jet efforts. Using a Meyer Rod, Eikos looked into the viability of producing inks suitable for ink jet and roll-to-roll deposition. From this experiment it was learned current ink jetting ink does not readily transfer into other deposition techniques, although most 1st generation inks, not suitable for ink jet, do transfer between other deposition techniques (i.e. draw down→spray coating→slot die).

Additional work was done to remove additives from complex CNT ink formulations. These inks contain sufficient additives such as polymers and surfactants that yield excellent drop formation, surface wetting, and CNT dispersion and stability, but have limited or no conductivity.

Work was done to obtain conductivity by leaching out the insulating materials. This involved soaking the printed pattern in a bath of 50/50 IPA and water for up to 90 minutes. Another scheme is being explored to rid depositions from complex inks of additives in parallel with leaching. This process utilizes a device called a PulseForge[®] manufactured by NovaCentrix of Austin, TX. PulseForge tools deliver high-intensity strobes to drive off or cure additives, depending on intensity. The Photonic Curing process specifically targets inks and thin-film depositions, functionalizing them without heating or damaging the substrates.⁹ In total, 50 samples were sent to NovaCentrix for testing.

Ink stability is of great importance since it can lead towards achieving other improvements. Historically, additives, such as surfactants, provide excellent stability for a colloidal dispersion. In the case of CNT colloids, they reduce the RT performance. It is believed that the surfactant interferes with the formation of CNT network. Surfactant or other additive choice is often a function of ease of acquisition or a matter of reproducing previous work as a base-line, without perceived thought of interactions with the CNT system or material itself. The focus is to understand and control the effectiveness of colloid stabilizers for CNT systems.

It is important for TCC's to consist of small, and uniform, particles in order to avoid shunting between layers. The optical particle analysis method developed at Eikos has proven a consistent and reliable way of detecting particles of at least 175-200 nm in diameter. Initial particle reduction procedures have been successful, but room for



improvement remains. Surfactant treatment and high speed centrifugation have proven effective in these efforts, and these processes can be improved further.

Eikos conducted additional investigations of polymeric additives. Areas of further study are:

1. Explore ratios beyond 1:1, CNT to additive
2. Determine significance of additive molecular weight on target properties and characteristics
3. Discover and optimize stress testing procedures, heat, mechanical, storage vessel material, etc.
4. Utilization of larger batched, base ink for less variability within tests.
5. Continue to seek additional materials, such as more samples from the Surfynol family or other surfactants (fluorinated surfactants, bile salts)
6. Research existing literature on utilization of material choices in similar fields or industries (e.g. coatings)
7. Explore procedural steps in 'when' to add material to the batching process.
8. Investigate process energy needed for dispersion (sonication time and energy, spin speed, temperature, etc)
9. Use higher grade CNT paste (>87%T)
10. Employ recently acquired analytical equipment to aid in development and optimization of properties (Tensiometer)

Finding a reliable supply of high-performance CNT for future Invisicon® coatings is of great interest to Eikos. In related work done under NIST ATP contract 70NANB7H7010 Eikos continued purification and extraction experimentations with CNT from various suppliers with the end goal of creating coatings with RT performances greater than or equal to 95.0 %T @ 500 Ω/□.

Eikos continued its CNT purification efforts during with material from six separate CNT suppliers. Each material reacts uniquely when purified, and whenever possible, batches of material were split so extraction and separation experiments could be conducted in parallel to see which conditions produced the most favorable outcome. Both the CNT pastes and supernatant extracts were hand-sprayed after each extract to determine RT performance and separation efficiency. Coatings made from two of these CNT materials achieved RT performances of 96.2 %T @ 500 Ω/□ and 95.1 %T @ 500 Ω/□ respectively. Multiple batches of CNT from both suppliers were purified to 95.0 %T @ 500 Ω/□ or better.

Not only were paste RT performances favorable, but the conductivity of the supernatant extracts removed were quite low, suggesting that the separation techniques employed were highly efficient. Despite these facts, the yields of high-performance ink batches were all in the 0.30% - 0.90% range. Although these yields are rather common when separating tubes of this quality from larger masses of as-produced material, it makes producing large quantities of Invisicon® difficult and raises material costs dramatically.



Given the favorable results obtained, there are several areas of purification study that should be given attention. Most importantly, effort should be invested towards improving paste yield and securing a reliable and consistent supply of high-performance CNT. Two new CNT suppliers gave us good RT performance and have scaled, or in the process of scaling-up, production. Both suppliers have proven to be very open to working with Eikos to optimize their product for targeted applications. Once the RT performance consistency of one or both of these suppliers has been verified with the current purification process, additional experimentation should be attempted with less-aggressive reflux and extraction steps to determine if yield improvements are possible.

5.3.1 Ink Characterization

Resulting inks were coated via air-brush spraying on to borosilicate glass slides. After drying at 60 °C for 10 minutes slides were prepared for resistivity using painting silver electrodes spaced to provide a test area of 1 inch by 2 inches. Coated slides were then measured for light transmission in a Perkin Elmer UV/VIS Spectrophotometer.

A CNT concentration of 30 mg/L will yield an ink of absorbance = 1 for a 1cm path length, standard (PMMA or PS) Cuvette. Based on the measured absorbance, the ink concentration ranges from 60 mg/L to 165 mg/L see Table 10. Thus, the actual ration of additives to CNT varies from 1:3 to 1:5.5. These pastes likely have higher solids content than typical paste, resulting in higher absorbance after processing.

Table 10 RT performance of polymer additive/CNT inks

| Sample ID | Mix/Additive | R(Ω) | % T | Normalized RT | Abs |
|---------------------|-----------------|---------------|-------|---------------|------|
| PEO Control #1 | CNT / Water | 370 | 73.53 | 78.3 | 3.56 |
| PEO Control #2 | CNT / 3:1 | 1074 | 87.50 | 78.5 | 3.32 |
| PEO Test #1 | WSR-205 | 877 | 87.30 | 81.0 | 3.19 |
| PEO Test #2 | WSR-N80 | 1056 | 73.30 | 58.4 | 3.10 |
| PEO Test #3 | WSR-N750 | 566 | 89.50 | 88.5 | 3.08 |
| | | | | | |
| Surfynol Control #1 | CNT / Water | 1817 | 91.10 | 77.4 | 3.40 |
| Surfynol Control #2 | CNT / 3:1 | 1361 | 88.90 | 77.2 | 3.36 |
| Surfynol Test #1 | Surfynol 61 | 1207 | 87.30 | 76.4 | 3.78 |
| Surfynol Test #2 | Surfynol 420 | 1164 | 85.60 | 74.2 | 3.46 |
| Surfynol Test #3 | Surfynol 440 | 1153 | 83.30 | 70.8 | 5.54 |
| Surfynol Test #4 | Surfynol 465 | 1222 | 83.10 | 69.3 | 3.03 |
| Surfynol Test #5 | Surfynol CT-121 | 1160 | 86.80 | 76.1 | 3.60 |
| Surfynol Test #6 | Surfynol CT-171 | 1140 | 83.80 | 71.6 | 3.40 |
| | | | | | |
| PVP Control #1 | CNT / Water | 1032 | 86.70 | 77.7 | 3.73 |
| PVP Control #2 | CNT / 3:1 | 1055 | 84.40 | 74.0 | 4.45 |
| PVP Test #1 | K-12 | 1044 | 87.60 | 79.0 | 4.07 |
| PVP Test #2 | K-15 | 1079 | 80.00 | 67.1 | 3.82 |

Highlighted in the table above are samples whose RT performance is approximately the same or better than control CNT paste. In the case of the PEO WSR-N750, it is higher than the control. The CNT paste is rated at 87.4% T and the N750 measures at 88.5% T.

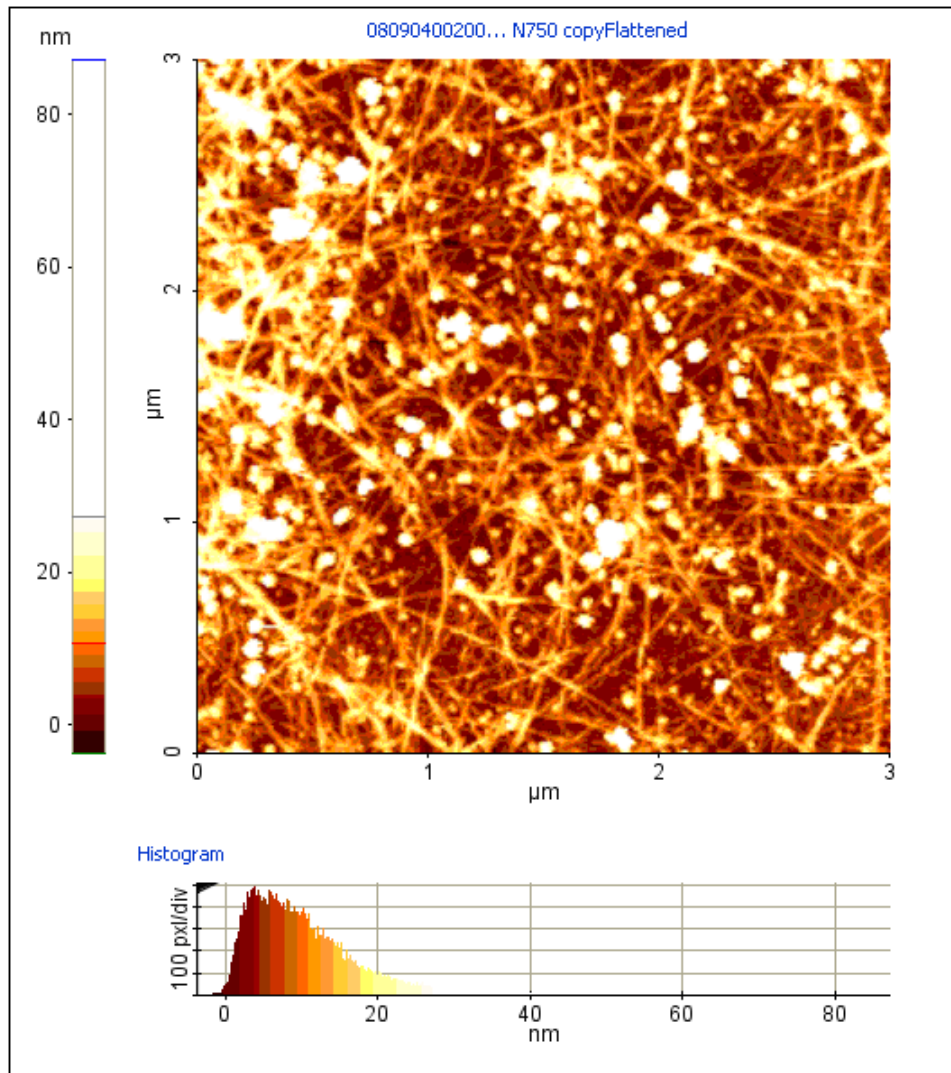


Figure 23: AFM Image of PEO Test #3, CNT & PEO WSR-N750 on Glass Slide

From the Atomic Force Microscope (AFM) image in Figure 1 it can be seen that a large MW polymer such as PEO does not impede formation of a CNT network. Carbon nanotubes do join together to form rope-like structures. Depth in the network matrix can also be observed from this image. White peaks seen in Figure 2 are believed to be contamination from graphitic shells remaining after the purification process.

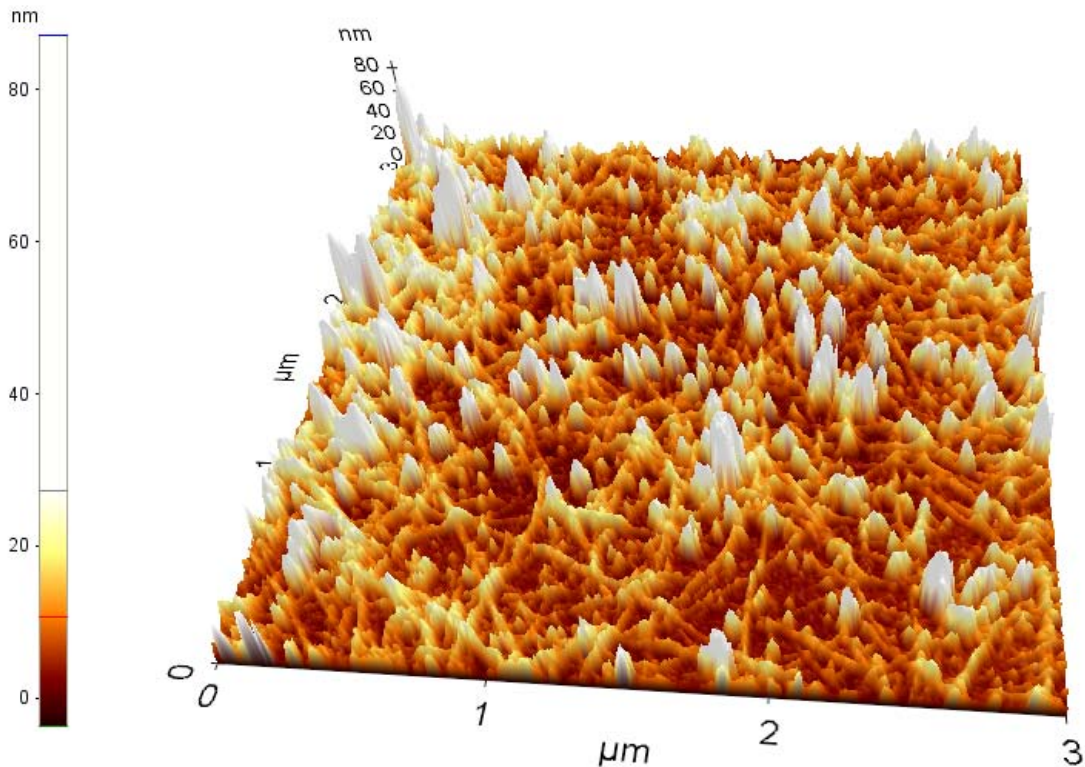


Figure 24: 3D View of AFM Image of PEO Test #3, CNT & PEO WSR-N750 on Glass Slide

Particle Reduction

Eikos continued to optimize particle reduction techniques for cleaner CNT inks. Samples of 40ml were centrifuged up to 120 minutes at 25,000 CFM. Counting of particles was performed by taking 5 pictures of the particles at 1000x in a known area. Software was used to count the particles via the method described in our 1st quarter report. The 5 particle values were then averaged to get the particle count per set area. Resulting particle reduction is listed in Table 11 for several suppliers of good quality CNT.

Table 11: Particle reduction via centrifugation for four manufactures of carbon nanotubes.

| CNT Supplier | Number of Particles at Start | Lowest Number of Particles (2 hours) | Particle Reduction (%) |
|------------------|------------------------------|--------------------------------------|------------------------|
| Nanoledge | 384 | 40 | 89.6 |
| Swan | 226 | 30 | 86.7 |
| NanoC | 386 | 11 | 97.2 |
| Carbon Solutions | 519 | 13 | 97.5 |



Ink samples were then prepared by spraying on glass slides to 94% T @ 550 nm and then the particles were counted on each slide using Eikos SOP. This procedure was successfully scaled to 200ml by adjusting centrifuge time to 180min. Scale up of particle reduction in our CNT ink is potentially very valuable. Less ink particles decrease the resulting surface roughness of a coating, making these layers more compatible in multi-junction PV cells. Samples sprayed down to less than $7\Omega/\square$ exhibited less haze than non centrifuged ink due to less particles in the film.

5.3.2 Sonication study

To identify the potential process related causes for particle formation and to help in scaling up of CNT ink production the sonication step involved in ink production was evaluated. Extending the time of sonication is desirable for improved CNT dispersion during ink production. During sonication trials it was observed that sample inks generated heated as with longer sonication times. An ice bath was used to cool some of the samples to determine the effect of heat generation on RT performance and particle generation.

The resistance and transparency at 550 nm were recorded for sprayed sample after sonication and again four days later, to help determine ink stability. Figure 25 shows transparency data normalized to $500\Omega/\square$ as versus sonication time for these samples. The samples exhibit a downward trend in transparency until ice is used to reduce the heating of the sample. Trends seen in Figure 25 indicate controlling the temperature will allow for longer sonication times. When ice was used the transparency improved over longer sonication times. Comparison of data taken on day 1 and after day 4, indicate this CNT dispersion has limited shelf life.

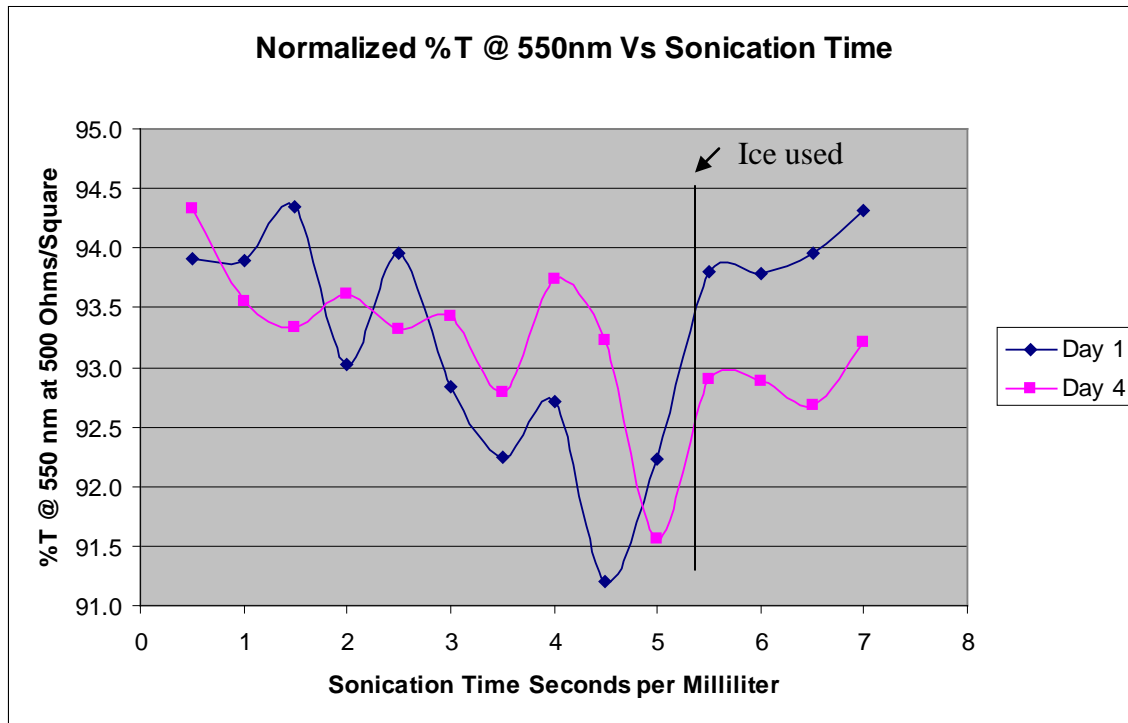


Figure 25: CNT data normalized to 500 Ohms/Square. The same CNT ink was sprayed on the preparation day and then four days later. Ice was used during the higher sonication times.

Particle characterization was done using the standard Eikos procedure of five separate pictures taken at 1000X before converting the image and counting the particles using ImageJ software. The particles were counted for each sample and the results of the five readings were averaged. Particle count results are shown in Figure 26. This data does not show a trend of increasing or decreasing particle counts with sonication. The samples sprayed with four day old ink show a slightly higher trend of particles compared to the samples sprayed on the first day. This is likely an issue with ink stability rather than a result of sonication.

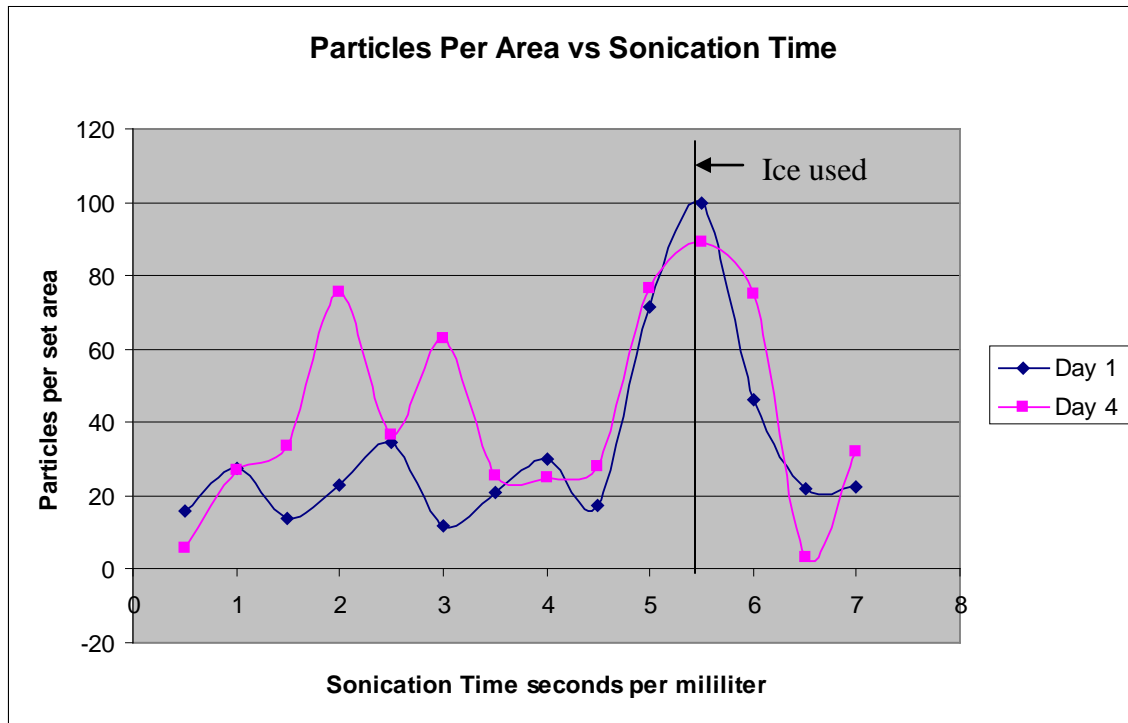


Figure 26: Particles present in the final CNT coating. From the data there was not a general trend for particles present due to sonication time.

5.3.3 Ink Additives

Eikos made significant advancements developing CNT ink dispersions with additive surfactants and leveling agents. Both additives greatly increase the ability to deposit a uniform CNT layer using ink jet printing or roll-roll coating. Once deposited, however, these additives act as insulators interfering in the formation of CNT conductive pathways across a surface.

Efforts were undertaken to determine the best method to wash surfactant and leveling agent additives out of the coating after deposition. Five washing solutions, listed in Table 12, were used in this effort.

Table 12: Solutions used to remove trace surfactants and Leveling agents

| Rinsing Solution | pH |
|-----------------------|-----|
| DI Water | 4.0 |
| Ammonia Water | 10 |
| HCl Water | 1.5 |
| Potassium Bicarbonate | 8.2 |
| DI water w/Sonication | 4.0 |

A total of thirty 1” x 3” PET samples were coated with CNT inks containing surfactants and leveling agents. All samples were then dried at 120C for 10 minutes to enable the CNT coating to set. Once set, the pre-wash sheet resistance of each sample was taken. Samples were then washed with one of the solutions in Table 12 for 30, 60, 300, or 600 seconds. Through this study it was found that while short term washing benefits the conductivity of the CNT layer, long term washing (>30 sec) starts to wash away the CNT network.

The three wash solutions that produced the greatest drop in resistivity in the first experiment, DI water, dilute ammonia, and dilute HCL, were reevaluated, using the method described above, at 10 and 30 seconds. The results of this evaluation are shown in Figure 27

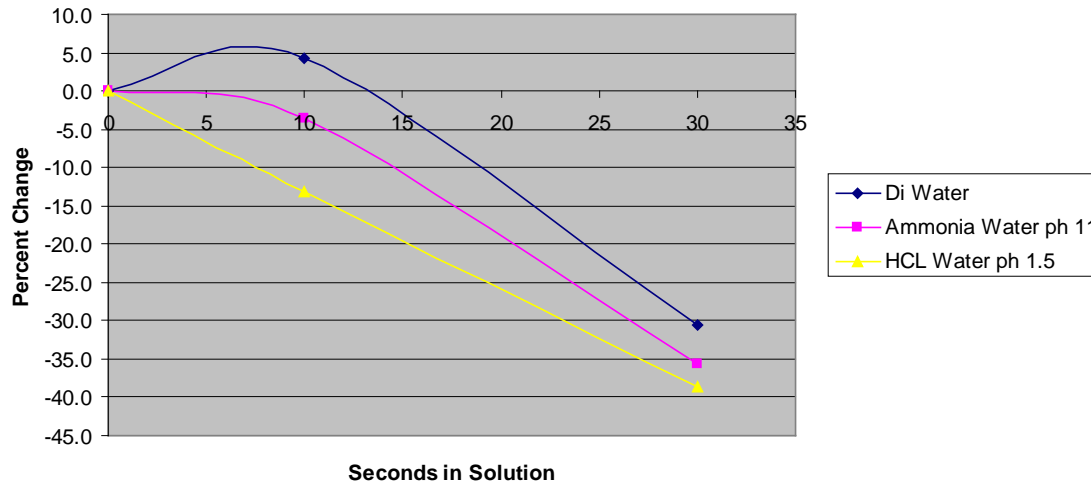


Figure 27: Resistance change using DI water, Ammonia water, and HCL water wash for 10 and 30 seconds

5.3.4 Curing to Remove Ink Additives

Several CNT inks were formulated to readily print using a Dimatix Spectra SE-128AA inkjet printer. Based on Eikos formulations these inks exhibit several desirable characteristics for printing including:

- Good drop formation
- Extended dispersion of CNT producing better ink stability
- Flow properties enabling continuous printing without clogging of print head
- Favorable wetting of substrate
- Minimal migration of deposited ink
- Fast drying on substrate

All of these properties enable Eikos to deposit a thin, uniform and integrated conductive pattern on polymer and glass substrate. Once ink has been deposited the substrate is then cured to remove additives and set binder included within the ink to enable printing.

Curing is usually done in two steps, for three distinct purposes. The first step, low temp curing, is used to drive off solvent and other ‘low boilers’ with low boiling points. Often, this curing is done at room temperature in atmosphere, for solvents such as IPA. Conditions for curing of low boilers are usually 25-80°C for no more than 2 hours. Solvents with high boiling points, known as high boilers, and additive polymers needed to provide surface tension and viscosity are then driven off at higher temperatures. Polymer binders are sometimes added that form a protective hard coat when cured, giving the printed conductive layer improved protection from the environment. Curing conditions needed to drive off high boilers and form hard coats range between 150-300 °C for 1-3 hours. It is important to note the curing process is one step heating, relying on the fact that low boilers will be removed as the oven ramps to temperatures needed to remove high boilers and polymers.

While additives are crucial to providing good CNT ink these same additives impair the conductivity of CNT networks. Insulation is a result of the very mechanism that enables the dispersion of CNT and the stability of the ink; by coating, wrapping or statically separating CNT. The challenge Eikos faces is to enable deposition of uniform and stable coatings and patterns while not insulating the inherent conductivity of CNT.

Eikos also conducted experiments to determine optimum curing conditions to remove insulating additives from CNT ink jetted coatings. Curing methods tested were curing samples in a vacuum oven and utilizing a new curing technology known as the PulseForge[®] produced commercially by NovaCentrix. PulseForge tools work because of the energy delivered by the high-intensity strobes at the heart of the system (Figure 28). The strobes are driven by high-powered pulse electronics technology resulting from years of engineering, and are unlike anything on the market today. The strobes deliver energy to the target surface, selectively heating and fusing ink particles, and forming highly conductive pathways.

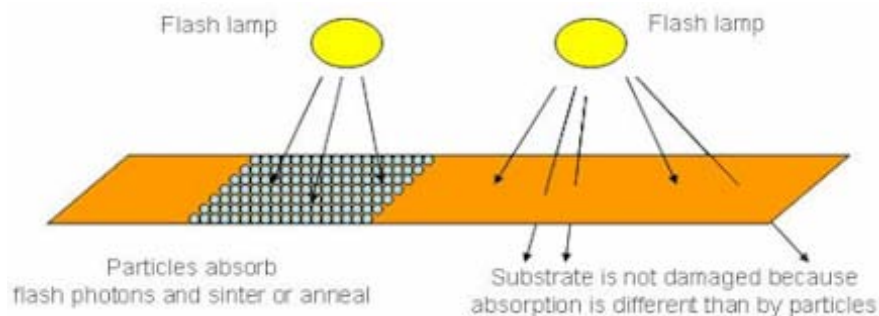


Figure 28: Photonic curing as a result of strobes of high powered flash lamps.



The photonic curing process specifically targets inks and thin-film depositions, functionalizing them without heating or damaging the substrates on which they are printed, or affecting nearby thermally sensitive components. This allows a large-area complex pattern to be instantly cured even on low temperature substrates. PulseForge technology is effective with all types of particle-based inks, whether nanoparticle-based or metal-based.¹⁰ Traditional curing up to 250°C is done using a vacuum oven. For higher temperatures a standard box oven was used. Both PulseForge and heat curing was done in parallel to determine the best method of additive removal. CNT ink formulation relies on five types of material additive. These include: pigment; low boiler solvent, high boiler solvent, polymers; and surfactants.

Three of these additives are, for the sake of this experiment, remain constant. Set materials include:

1. Pigment: CNTs are the core technology of Eikos and the keystone of all industrial applications.
2. Low boiler solvents: this is a proprietary mixture of water, DMF and IPA that makes up the majority (by volume) of the solution.
3. Surfactants: Surfynol 61 was used when a surfactant is added.

This leaves the composition of high boilers and polymer additives the focus of formulation experiments. Several high boilers and two grades of PVP were tested (Table 13).

Table 13: High boiler and polymer additives to be tested for formulation of CNT ink.

| High Boilers | Importance |
|-----------------|--|
| Ethylene Glycol | This is the high boiler NovaCentrix uses in their inks. |
| 1,4 Butadial | Eikos staff has experience using this additive to produce inks. |
| Cyclohexanol | Eikos has used this additive to produce CNT inks. |
| | |
| Polymers | Importance/MW |
| PVP K-12 | MW of 6,000, has been used in high concentrations (5%) |
| PVP K-90 | MW of 400,000; tested to determine dilution and effect on ink. |
| PVP K-120 | MW of 1,200,000; tested to determine dilution and effect on ink. |

The first stage of this work was to determine optimum formulations. Eikos has the ability to formulate CNT inks that readily print using Cyclohexanol and Ethylene glycol as high boiler solvents and PVP K-12 as a polymer additive. Eikos sought to determine if 1,4-Butanediol would enable stable formulations. In addition, higher MW PVP was incorporated into CNT inks to determine if higher MW allows lower overall polymer concentration while maintaining ink viscosity, surface tension and stability.



Ink deposition was done on 1 x 3" borosilicate glass slides using the Dimatix Spectra SE-128AA ink jet printer. CNT ink coatings were then oven cured or PulseForge cured in parallel. The temperature of oven curing depends on the boiling point of ink additives. After curing coated slides were resistivity tested using a hand held voltmeter. NovaCentrix claims heat cured conductive coatings will often benefit from re-curing in the PulseForge, to further lower resistivity. Therefore, heat cured CNT coated slides were sent to NovaCentrix after resistivity testing to be re-cured using the PulseForge to determine additive effect. An outline of work is included below:

Step 1: Determination of Optimum PVP Polymer Additive

PVP of MW 6,000, 400,000 and 1,200,000 were used to formulate CNT inks. The goal of this task is to find a MW of PVP that allows for lower overall polymer concentration while maintaining ink viscosity, surface tension and stability. Formulations were formulated with and without Surfynol to determine if surfactant is needed with the addition of PVP.

Step 2: Determination of High Boiler

CNT inks were formulated with Ethylene Glycol, 1,4 butadiol and Cyclohexanol at concentration of 4%. Each of these formulations were tested for stability, and printing effect on the ink. Those additives that are found to produce a stable ink that is readily printed, and produces an even coating on multiple slides were selected for curing trials.

Step 3: Curing Trials

Favorable CNT ink formulations were heat cured or using the PulseForge, in parallel. Heat cured coatings were tested for resistivity using a hand held voltmeter then re-cured by the PulseForge and re-tested for resistivity. Samples cured using only the Pulse Forge were resistivity tested and compared to heat cured and dual cured samples.

Step 4: Imaging of CNT Coatings

Cured samples were imaged using AFM to determine overall if a residual coating of additive is still present. Specific points of interest are thickness, uniformity and degradation of additive coatings.



5.4 Task 4: Coating/Deposition Development

5.4.1 Ink-Jet printing

Work started with investigation of materials for what is referred to as First Generation Printing Inks. These simple systems consist of solvent and water mixed at 1:1 ratio with a stable amount of CNT, at approximately \approx Abs 1. Candidate solvents must be determined before any addition of CNT material is done to produce a workable ink. Candidates were chosen based on materials that are known as either beneficial to CNT systems or viable for ink jetting application. Polyethylene Terephthalate (PET) was chosen as a substrate since it is a common media for flexible electronic circuits. Historically, conductivity of printed electronics on PET is lower than on glass substrate. So, though more challenging than glass, it seemed more accurate and realistic to conduct our investigations on PET.

Work done is outlined below:

1. Explore ratios beyond 1:1, CNT to additive
2. Utilization of larger batches, base ink for less variability within tests
3. Explore procedural steps in 'when' to add material to batching process
4. Investigate process energy needed for dispersion of ink [components] (sonication time and energy, [centrifuge] spin speed, temperature, etc.)
5. Use higher grade CNT paste ($> 87\%T$)
6. Employ recently acquired analytical equipment to aid in development and optimization of [ink] properties (Tensiometer).

Table 14: Summary of Solvent/Water (1:1) Mixtures on PET 453 at 60°C

| Material | Solution Observations | Pass / Fail | PET Wetting (5min) | PET Drying (20 min 60°C) |
|---------------------------|--|-------------|--------------------|----------------------------------|
| DMF | Homogeneous solution | Pass | Poor – fair | <i>Good – excellent</i> |
| Triethanolamine | Well dispersed/dissolved blue solution | Pass | Poor – fair | <i>Better wetting</i> |
| Triethylamine | Layer separation – [vapors] dissolve Parafilm® | Fail | - | - |
| GBL | Homogeneous solution | Pass | Fair – good | <i>Good – excellent</i> |
| Ethanol | Homogeneous solution | Pass | Excellent | <i>Dry</i> |
| 1-Hexanol | Layered solution/mix | Fail | - | - |
| Cyclohexanol | Layered solution/mix | Fail | - | - |
| 2-Pyrrolidinone | Homogeneous solution | Pass | Poor – fair | <i>Fair – good</i> |
| Ethylene Glycol | Homogeneous solution | Pass | Poor | <i>N Better wetting o change</i> |
| Propylene Glycol | Homogeneous solution | Pass | Poor – fair | <i>Better wetting</i> |
| 1,3-Propanediol | Homogeneous solution | Pass | Poor | <i>Better wetting</i> |
| 1,4-Butanediol | Homogeneous solution | Pass | Poor - fair | <i>Better wetting</i> |
| 1,5-Pentanediol | Homogeneous solution | Pass | Fair | <i>Better wetting</i> |
| Diisopropylamine | Layering but not even cut – more like 70:30 with clear (solvent) on bottom | Fail | - | - |
| <i>Ethyl Acetoacetate</i> | <i>Layered solution – not severe but noticeable</i> | <i>Fail</i> | - | - |

No noticeable difference in wetting and drying could be discerned for tested solvents on PET substrate. A “Fail” in Table 14 indicates the 1:1 mix of that solvent, with water, does not result in a solution structure that would be viable for future testing. In this instance, the mode of failure is the inability of the solvent to mix homogeneously with water. These components may have some future value as small percentage additives in a more complex ink formulation. ‘Fail’ ranked materials were excluded from further testing. From this PET wetting/drying testing four viable solvent candidates were determined. They are classified as “A” and “B” candidates. Primary or “A” candidates are Dimethylformamide (DMF) and Gamma-Butyrolactone (GBL). These “A” candidates were chosen on the basis of both wetting the PET substrate and being volatile enough at 60°C. The secondary or “B” candidates are 1,4-Butanediol and 1,5-Pentanediol. These “B” candidates were chosen on the wetting characteristics, but also are significantly less

volatile than the “A” classed materials. As such, these –diol compounds were explored but at much lower concentrations than the 1:1 tested here.

1st Generation Inks

All “A” and “B” candidates explored above were then printed in a Dimatix Spectra SE-128AA industrial piezo jetting head assembly (Figure 29) to tune printing technique and ease of printing.

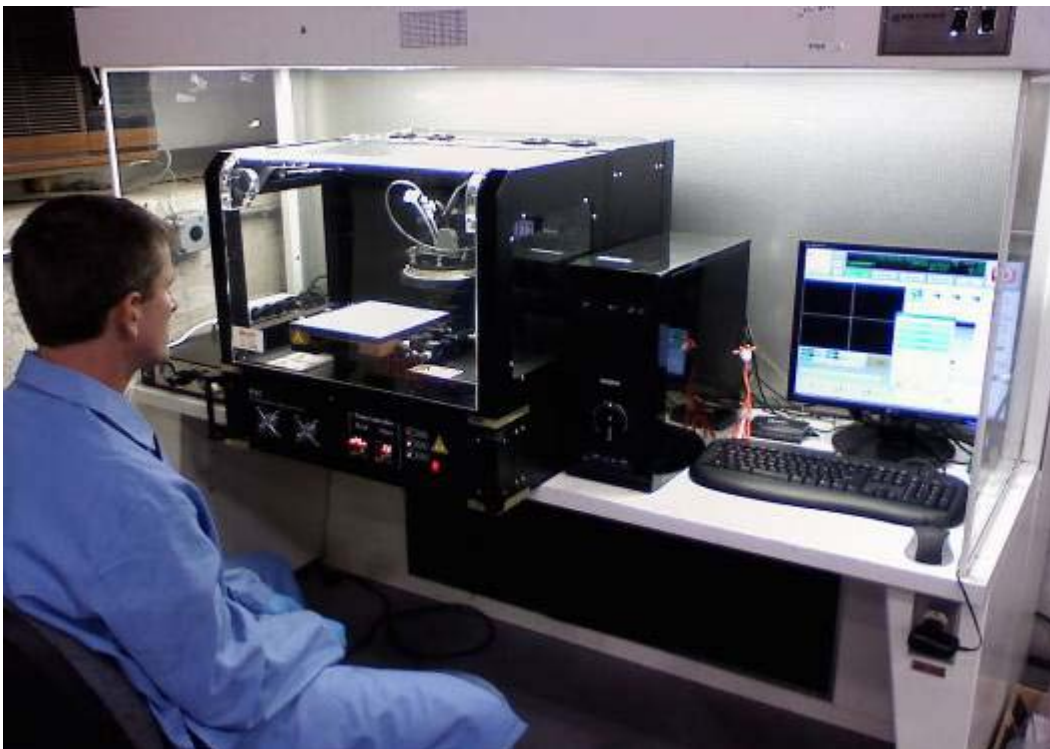


Figure 29: Dimatix Spectra SE-128AA industrial piezo jetting head assembly for inkjet printing.

Of the four solvents tested, DMF/water solution more readily printed. CNT were then added to this system for printing trials. Clogging of the nozzles and ink flocculation was found to be a significant problem. To resolve this issue various DMF/water concentrations were explored. It was found that DMF/Water at 3:1 provided good CNT stability along with reasonable R/T performance and printing properties. A 1.035 ABS CNT ink at 93.2 %T, normalized at $500 \Omega/\square$ was formulated using a 3:1 DMF/water solvent solution. This is less than the target of 1.0 ABS at 95%T, but still significant progress for printing CNT inks. Ink-jet printing of CNT's is notoriously difficult because of flocculation and clogging of the print head.

It was noticed the material would coat the inside of the print head and can exacerbate these problems. To help resolve this issue a by-pass reservoir, hereby referred to as the

“By-Pass”, was engineered onto the printer. This was accomplished by not using the body assembly to hold fluid but a 30mL polypropylene vial plumbed directly into the housing just behind the junction where the print head attached to the mechanism that affixes it to the printer.

This By-Pass greatly reduced the exposure of the CNT ink to the offending coating. It is still believed that some coating is still in the fluid path of the ink, but significantly less than originally designed. Additionally, the operator can visually inspect the ink in the By-Pass for any flocculation. All functions of the Printer, such as maintaining the meniscus (via vacuum) or purging (via positive pressured air), are not affected with this By-Pass.

2nd Generation Inks

Simple ink formulations do not print well. In order to achieve better printing properties more complex ink formulations are necessary. Ink-jet printing requires inks with specific properties such as drop formation, surface tension, and viscosity. Common materials used to tune these formulations, and what they do, are listed in Table 15.

Table 15: Classifications and Components of Printing Ink.

| | Classification | Function | Example |
|---|-----------------------|---|----------------------------|
| 1 | Primary Solvent | Carrier of additives | Water |
| 2 | Humectants | Keep ink from drying on surface of nozzle plate | Glycerol |
| 3 | Drop Modifiers | Aid in creation of ideal drops in jetting | Polymers – PVP |
| 4 | Surfactants | Aid in controlling surface tension – flow characteristics | SDS |
| 5 | Co-solvents | Aid in dispersions and/or other characteristics | DMF, IPA, 2-pyrrolidinone |
| 6 | Biocides | Preservatives | Parabens, Sorbates, or CNT |

Several iterations of solvents/additives were formulated to tune ink properties based on the additives listed in Table 15. The Protocol for formulation is as follows:

1. Batch blank ink at 1000g size, mixing with magnetic stirrer, unheated
2. In predetermined size, gravimetrically add (weigh) CNT paste to batched blank
3. Sonicate 4 minutes at 70% power, rotating
4. Centrifuge 4250RPM, 15°C for 60 minutes
5. Decant supernatant, associate all into one vessel
6. Sonicate again 2 minutes at 40% power, rotating.

One formulation consisting of Water/DMF/IPA solvent with 4% 1,4-Butanediol, 2% 2-Pyrrolidinone, 0.5% PVP K-12, and 0.1% Surfynol surfactant did allow for complex patterns to be printed. This mixture is able to make a very stable, very well behaved CNT ink at a very high absorbance of 42.3 ABS. The benefit from this stability is more efficient printing. At higher concentrations it would require less printing for a given pattern since more CNT material is being dispensed per pass. The stability of this ink was shown to have no flocculation or other issues after 30 days of manufacture. Some 1st Generation Inks do not last a single day, a week at best. Also, a 1st Gen Ink would typically start to clog nozzles on the first pass with full head failure (all nozzles blocked) within 5 passes. This 2nd Gen ink will print for nearly a week with 40 – 50 passes. Several RFID 01-400DPI patterns, chosen to determine bulk and complex patterning ability, were printed with CNT ink on glass and PET substrate (Figure 30).

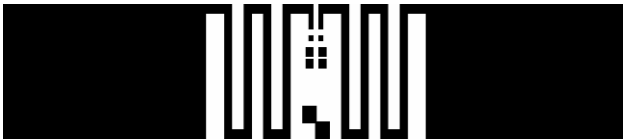


Figure 30: RFID tag used to print CNT pattern.

Unfortunately, there is no conductivity for these printed circuits. It is likely that the PVP and Surfynol insulate the CNT network. This explains the excellent stability and printing properties. In effect, the same properties that enable additives to make a stable dispersion, coating and separating the CNT network, hinder the formation of a CNT on CNT network. To solve the problem of left over insulation on printed coatings Eikos attempted to leach or flush away some of the insulating components and increase conductivity. Several different solvents and mixtures were used to flush insulating additives (Figure 31).

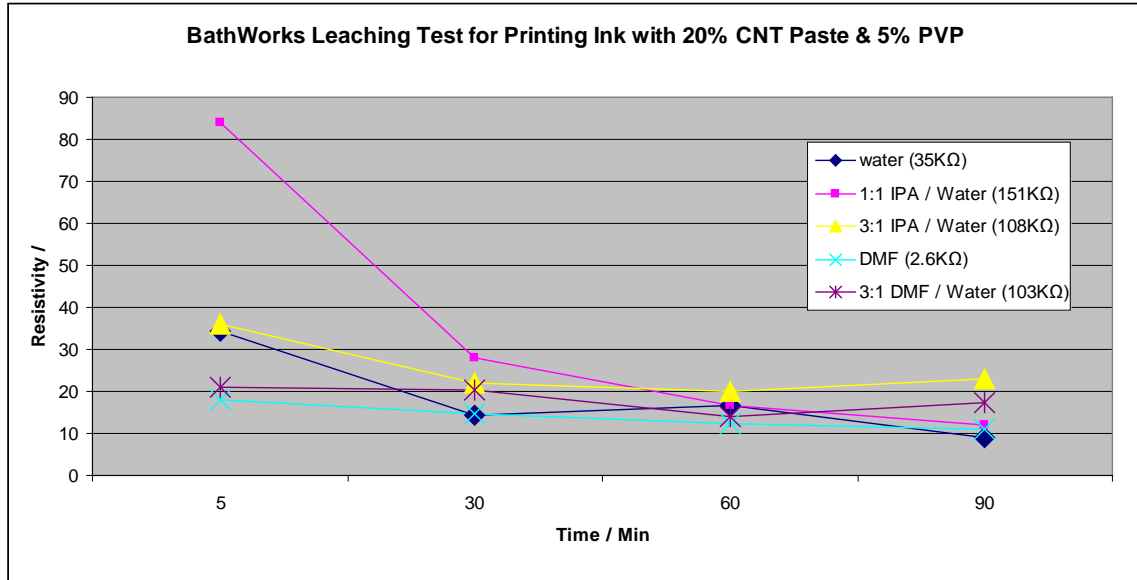


Figure 31: Leaching of polymeric additives from printed CNT coating.

From testing done in Figure 31 it was decided to focus on soaking for 90 minutes in 1:1 IPA/Water for leaching experiments. After leaching, coated samples were dried at 100°C for 60 minutes. Samples were allowed to cool to room temperature prior to RT performance characterization. Resistivity and transparency were measured before and after leaching. The performance of these patterned samples is not yet desirable. However, what these experiments do show is the possibility to remove insulation from a CNT pattern, still maintain a pattern (visually), and increase the key performance properties of transparency and conductivity (Table 16).

Table 16: Summary of Applied BathWorks to Patterned Samples – Same Ink in Initial BathWorks Testing

| Substrate | Before | | After | |
|-------------------|-------------|--------------|-------------|--------------|
| | Resistivity | Transparency | Resistivity | Transparency |
| PET | 0 – Zero Ω | 29.0 %T | 21KΩ | 94.5 %T |
| Glass – 5 Passes | 0 – Zero Ω | 67.9 %T | 7.0KΩ | 92.2 %T |
| Glass – 10 Passes | 17MΩ | 46.0 %T | 5KΩ | 89.6 %T |

Summary

To solve the problem of insulated CNT networks Eikos investigated other ink formulations. Eikos achieved some success in the past with 3:1 IPA/Water with 4% of the humectant Cyclohexanol. This formulation was used as the new start point for new formulations. Eikos continued to explore Cyclohexanol and other Humectants in order to see if a simplified CNT printing ink can be developed without insulating additives. However, the additives that do cause insulation do also increase stability and printability.

5.4.2 Inkjet Deposition and Evaluation

After several months of ink-jet printing CNT, using numerous ink formulations, the print quality was not yet acceptable, even though progress was made to improve the coatings. By formulating inks with surfactants, leveling agents and other additives, together with the tuning of the printing parameters, Eikos were able to ink-jet print complex and highly conductive CNT circuits (Figure 32).

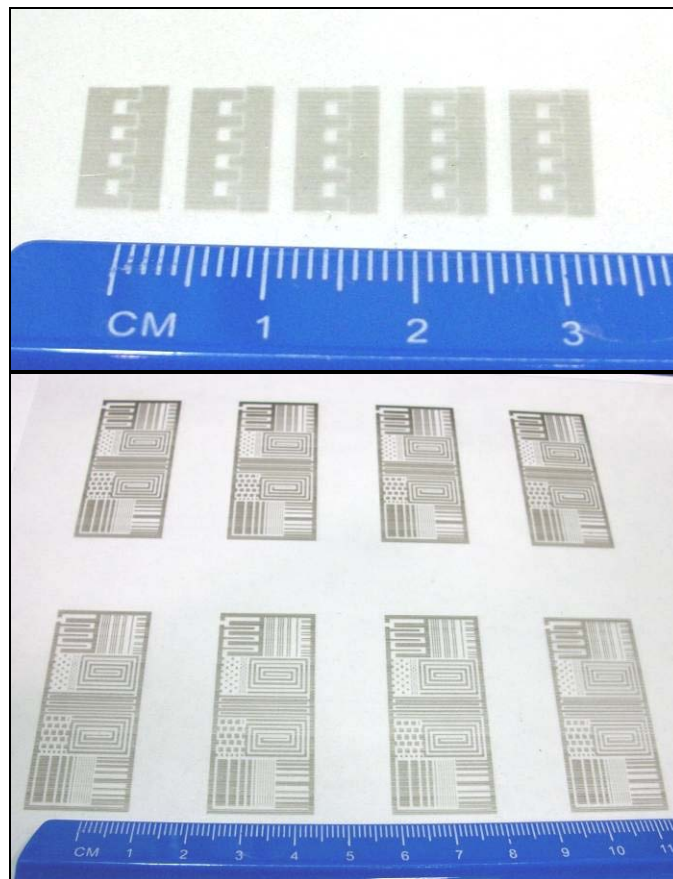


Figure 32: Complex CNT circuits deposited on transparent PET using ink-jet printing.

5.4.3 Inkjet Deposition in Practice

For several months advancements in printing CNT patterns on polymeric film were made using the Dimatix printer. The best CNT coatings were formed by applying a leveling agent to a substrate and then printing onto the leveling agent. The film is then washed multiple times to consolidate the CNT network and to remove the surfactant and leveling agents.

Eikos sought to adapt this technique to the fabrication of a four layer FET device. Success in doing so would open the door to direct fabrication of printable electronic devices including OPV stacked cells, FET's, flexible LED's, sensors and more. Figure 33 illustrates the bitmap(s) used to deposit individual printed layers using the Dimatix printer for the fabrication of this device.

Printed Four Layer Field Effect Transistor using Dimatix Printer

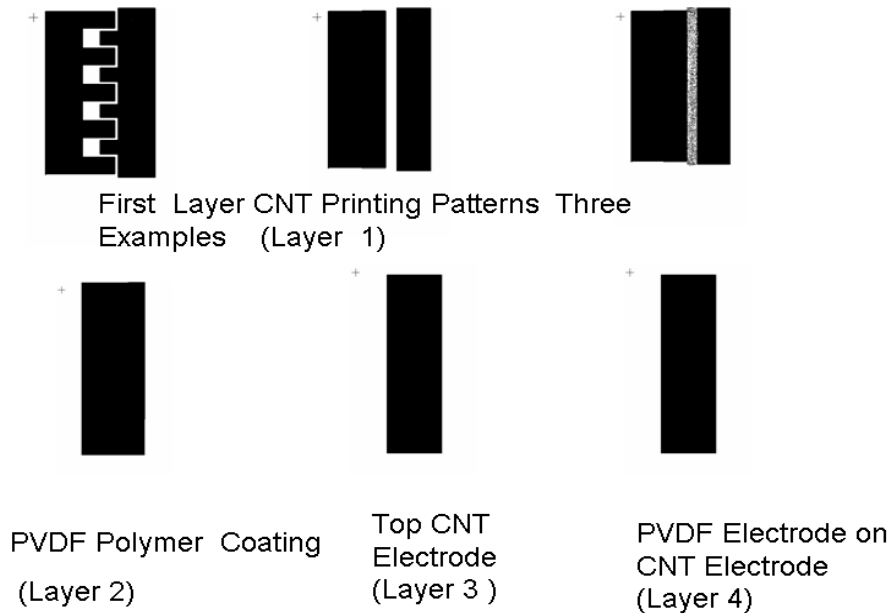


Figure 33: Printed Four Layer Field Effect Transistor Consisting of First CNT Layer then PVDF Polymer Layer Followed by a Top CNT Electrode which is then Over Coated with PVDF.

Printing on PET film is a challenge in that water born inks tend to de-wet at the surface, which prevents the formation of a conductive network. The additional of leveling agents, such as those utilized in our roll-to-roll formulations discussed above in Task 3, tend to destabilize the inks when used in an ink-jet formulation. To circumvent this problem, Eikos has developed a method whereby the leveling agent is first applied to the PET film, and then is removed after CNT network deposition. Eikos applied this technique to the fabrication of FET device, as depicted in Figure 34.

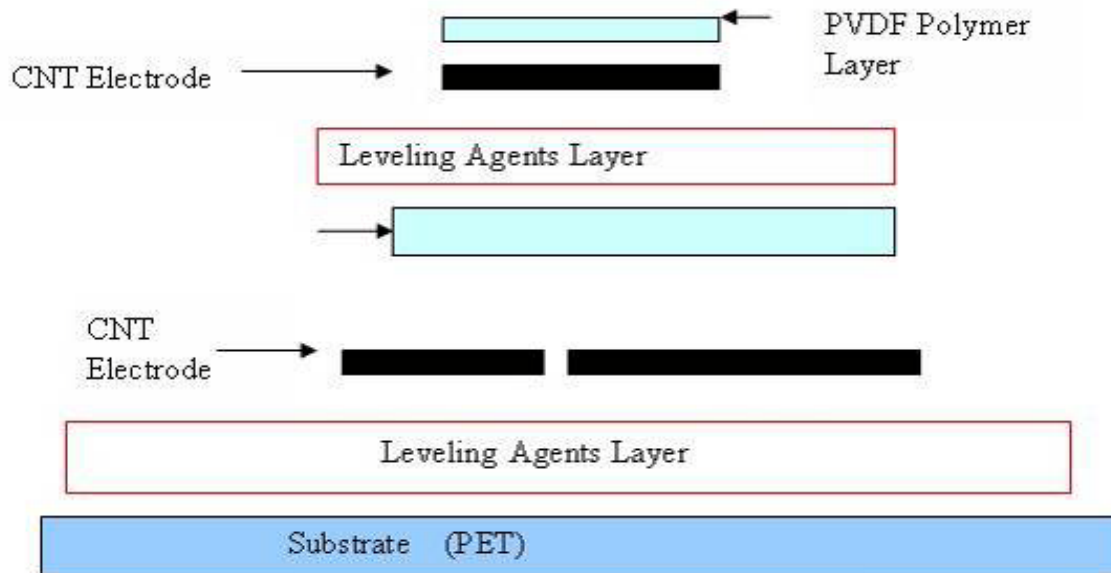


Figure 34: Printing process involves coating PET substrate with leveling agent before CNT.

Here, four layer coatings were applied to PET film in the following sequence:

- 1) Leveling agent is applied to the surface of PET substrate.
- 2) Treated PET film is then dried.
- 3) Using the Dimatix layer 1 is printed on the treated PET (Figure 35).
- 4) Leveling agents and other ink additives are then washed off and the sample is dried.
- 5) Layer 2 PVDF coating is then printed on from a dilute PVDF solution.
- 6) Layer 3 top CNT electrode is then printed.
- 7) Ink additives from step 6 are washed out, and the sample is dried.
- 8) The top PVDF coat is applied (Layer 4).

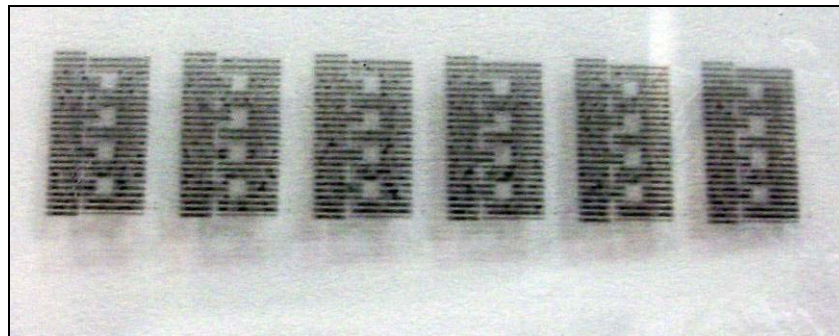


Figure 35: First layer of fingered electrodes printed using CNT ink

The completed device is shown in Figure 36. From this image only the CNT circuit and electrode layers are visible due to the transparency of the polymeric layers and substrate.

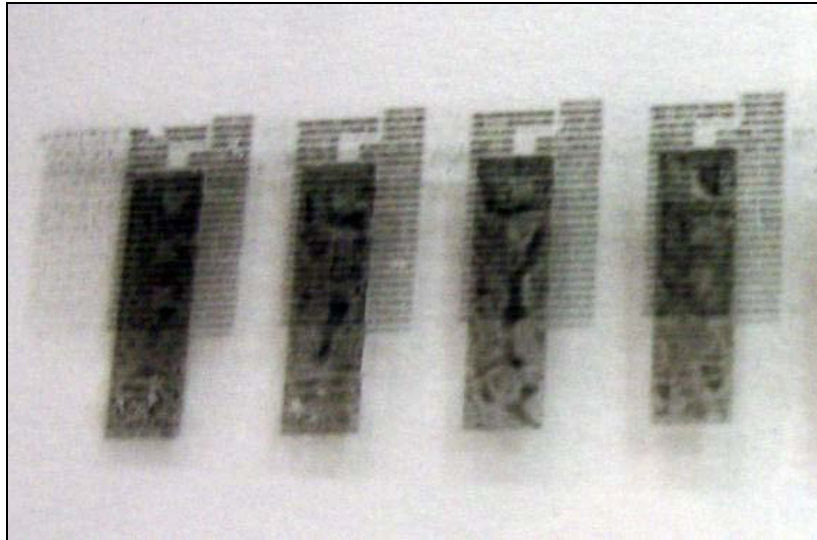


Figure 36: Example of a completed four layer device made with CNT. Note- the polymer layers are transparent.

Further Inkjet Development

Eikos' investigation of nanotube inks for printing spanned organic solvent dispersions, mixed solvent suspensions and aqueous phase inks. Inks that were stable for inkjet printing were not conductive after deposition. Conversely, conductive inks were found to be unstable. Another issue was the concentration of carbon nanotubes in the ink. The organic solvents do not give high concentrations of carbon nanotubes, whereas the water based suspensions can achieve relatively high loading.

After many attempts to develop an inkjet able ink, an alternate method of patterning was developed that utilized the Dimatix Spectra SE-128AA printer for its direct writing capability, high resolution and convenient rapid prototyping. A printable resist was formulated and used to print a negative image of the desired pattern. A high concentration nanotube ink was sprayed on the pattern until the desired sheet resistance was achieved. The coated substrate was then washed in a developing solution to remove the mask and the surfactant. The positive image is obtained during this lift off step. Several mask formulations were tested. Organic solvent based masks were an obvious choice, as the nanotubes were coated from an aqueous suspension.

Eikos also found that aqueous based mask formulation was compatible with the water based nanotube inks. The first films were 250 ohm per square. Repeated attempts enabled us to drop the resistance by a factor of five to 50 ohms per square.

Eikos has been able to print very complex circuit patterns (Figure 37). The electrical resistance of these patterns is in the Kilo Ohm range. In the future Eikos aim to lower this to below $200 \Omega/\square$.

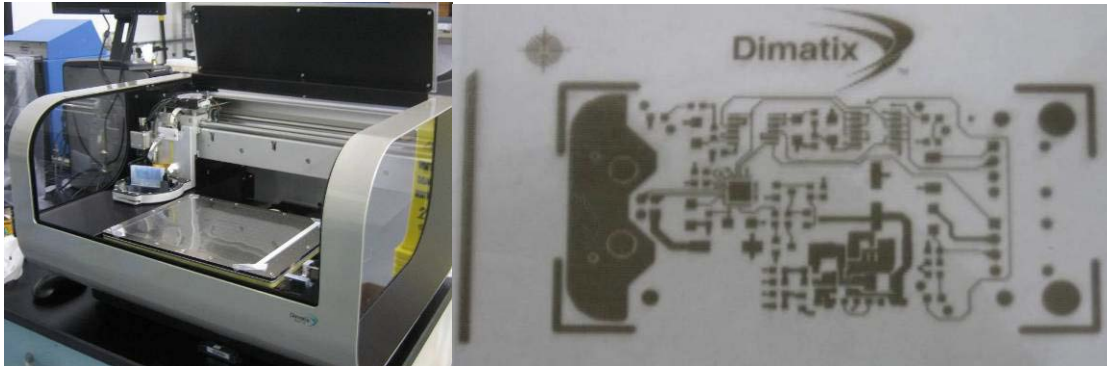


Figure 37: Dimatix DMP-2800 Series Printer and complex CNT pattern printed with this instrument.

5.4.4 PV Cell fabrication and Testing

Eikso worked with NREL to fabricate and test OPV cells using CNT TCC as an electrode. For this effort, nine glass slides were coated with CNT by Eikos according to NREL specifications. A total of 6 patterned samples and 3 blanket-coated witness samples were sent to NREL to be integrated into OPV cells as an electrode layer for comparative testing versus ITO.

Coatings were patterned using the electrode mask designs provided by NREL. Three of the samples were coated with high-conductivity ink to a resistivity of $65.7 \Omega/\square$, another three were coated with the same ink to a resistivity of $154.5 \Omega/\square$, and the final three were coated with a different, low-particle ink to a resistivity of $87.5 \Omega/\square$. All coatings were deposited onto 3" x 1" borosilicate glass slides pre-cleaned according to NREL suggested cleaning procedure.

Surface imaging of these samples by NREL over the entire sample used for device fabrication (magnification of 2.5X) shows these coatings to be reasonably uniform in thickness (Table 17). For surface uniformity/roughness characterization, the average mean surface deviation (R_q) and the Maximum height between the highest and lowest point (R_t) are the most important parameters. As expected, the thinner coating made from lower particulate CNT ink has a more uniform surface.



Table 17: Surface roughness data at 2.5x for a high conductivity thicker layer of CNT and a thinner layer deposited from low particle CNT ink.

| Coating | Ra (nm) | Rq (nm) | Rz (nm) | Rt (nm) |
|-------------------|---------|---------|---------|---------|
| High conductivity | 7.11 | 9.17 | 57.62 | 61.23 |
| Low particle | 2.33 | 3.08 | 25.4 | 27.84 |

Ra = Average roughness over the entire area
 Rq = RMS average between mean surface and height deviations
 Rz = Average maximum profile of the ten greatest peak-to-valley separations
 Rt = Maximum height between the highest and lowest points

Of note, these patterned CNT samples were provided to NREL without a binder coat to eliminate the risk of its interference with device fabrication or testing. The trade off in doing so is that the CNT network conductivity will drift over time without binder coats protection from the environment. Unfortunately, these samples were tested three weeks after being received by NREL. Table 18 shows the discrepancy in resistivity of each coating measured the same day it was coated is compared to resistivity values tested by NREL three weeks later.

Table 18: Rs drift in CNT TCC on glass, without protective a top coating.

| Sample ID | Ink | Transmission | Rs (Eikos) | Rs (NREL) |
|-----------|-------------------|--------------|------------|-----------|
| 113-11-1 | High Conductivity | 82.9 % | 65.7 Ω/□ | 106.8 Ω/□ |
| 113-11-2 | High Conductivity | 88.2 % | 154.5 Ω/□ | 172.7 Ω/□ |
| 113-11-3 | Low Particle | 80.2 % | 87.5 Ω/□ | 110.9 Ω/□ |

OPV cells using coatings made from the lower particulate ink performed the best. In fact, these out performed cells made with ITO. Testing from NREL revealed OPV cells using Eikos CNT low particle ink as a transparent electrode have an energy conversion efficiency of 3.09% compared with 2.85% for cells made with ITO. This is *despite* the poor conductivity of the samples as a result three weeks of environmental exposure. Figure 38 compares the performance of all the samples tested in this experiment.

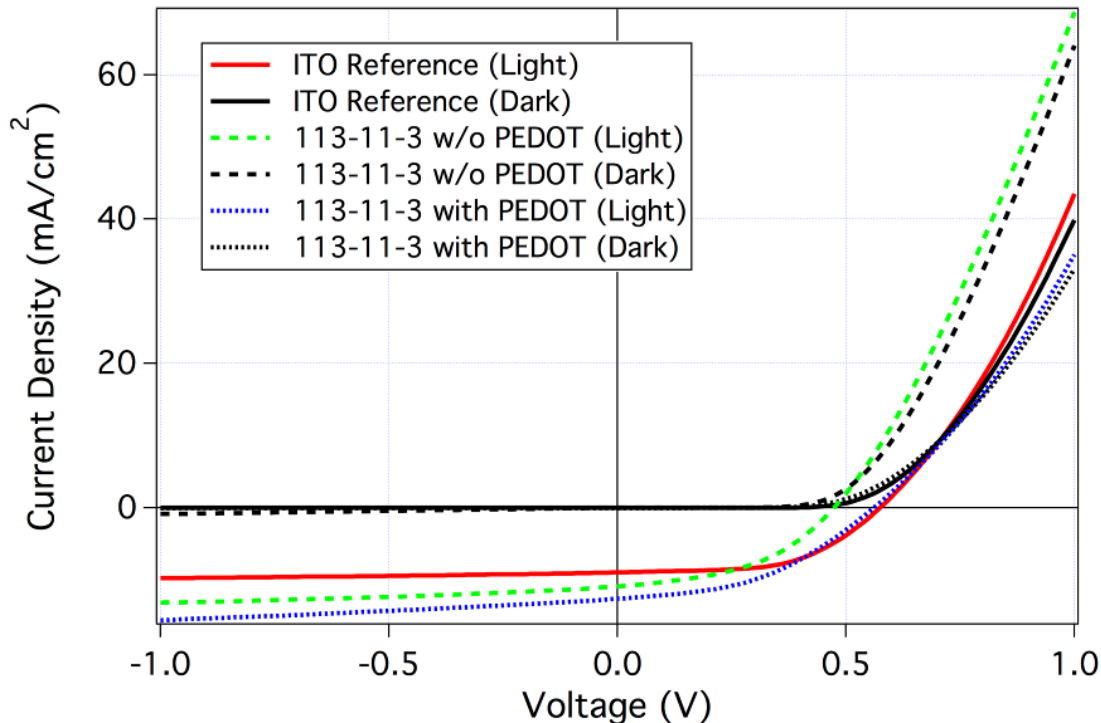


Figure 38: Comparison of performance between OPV cells made with ITO versus CNT electrodes.

5.4.5 CNT Coatings for PV Applications

NREL utilized Eikos CNT coatings as a back contact in a Cadmium Telluride (CdTe) multi-junction device. Characterization, done by NREL, shows our CNT coating outperforms ITO. Given the fact that CdTe is the dominant thin film PV cell and that ITO is, by far, the dominant TCC material, this result demonstrates the potential commercial applicability of CNT coatings for PV applications in place of ITO. This quarter Eikos focused on integrating Eikos technology into OPV cells, again made by NREL.

Four slides were coated with CNT by Eikos. The coated slides consist of two standard borosilicate microscope slides cleaned in house by Eikos using a standard surfactant wash protocol, then spray coated to the resistance specification of 75-100 Ω/\square , as requested by NREL. The other two coated slides were obtained pre-cleaned from VWR, then spray coated to the above resistivity specification. Two separate batches of VWR slides were used. Three uncoated slides were included as an optical reference. All seven sample slides listed in

Table 19 were delivered to NREL.



Table 19: R/T performance of 75-100 Ω/\square SWCNT film coated on borosilicate glass slides.

| Sample # | Substrate Type | Resistivity (Ω/\square) | AVG %T (no Ref) | AVG %T (w/ Ref) |
|---------------|-------------------------|----------------------------------|-----------------|-----------------|
| 97-292-2A | Standard slide | 86.3* | 76.0 | 82.7 |
| 97-292-2B | Standard slide | 91.0* | 76.2 | 83.1 |
| 97-292-3A | VWR-batch1 | 86.3* | 76.3 | 83.4 |
| 97-292-3B | VWR-batch2 | 91.0* | 75.1 | 81.7 |
| 97-292-1Ref | Uncoated standard blank | N/A | N/A | N/A |
| 97-292-3Ref A | Uncoated VWR-batch 1 | N/A | N/A | N/A |
| 97-292-3Ref B | Uncoated VWR-batch 2 | N/A | N/A | N/A |

* Based on reference slides coated under the same conditions.

NREL conducted AFM surface analysis of the coatings along with performing R/T and sheet resistance measurements. NREL also built OPV small (.1cm²) and large (1cm²) devices on the coated substrates. Device performances were compared with devices made using NREL CNT coatings and commercially available ITO.

5.4.6 Building PV Devices with NREL

Eikos work with NREL produced evidence that the roughness of our CNT coatings is the limiting factor for device performance when they are used as the top electrode in PV cells. The optimal resistivity of CNT coatings used in this fashion is 60 – 100 Ω/\square , and even when using highly-conductive inks of 4000 S/cm, this resistivity level necessitates depositing a significant amount of CNTs.

As measured by AFM, the peak-to-valley surface roughness of these coatings is approximately 190 – 290 nm. When used in the stringent structure of an OPV cell, Eikos hypothesize that this surface morphology restricts current flow and causes contact resistance losses.

There are several methodologies that can be employed to solve this problem, including ink particle reduction, coating deposition technique, surface polishing, and post-processing procedures. Currently, Eikos are investigating the effectiveness of "CNT substrate transfer" where CNTs are deposited normally onto a smooth substrate but are then transferred onto another substrate, causing the smooth side of the coating to be inverted and make contact with the rest of the OPV cell during device fabrication. The general procedure of this experimental technique is as follows:



1. spray-coat CNT coatings of $50 \Omega/\square$ onto 1" x 3" substrates;
2. for some samples, dip-coat thick ($\gg 100$ nm) binder coatings and cure for 1 hour at 125°C ;
3. measure the resistivity of each sample with a four-point probe;
4. transfer the deposited coating(s) onto another 1" x 3" substrate (so that the side of the coating that originally faced the smooth substrate surface is now exposed) using one of three methods:
 - A. heat the uncoated substrate to its softening point with a hot press, and press the two substrates together,
 - B. cover the coated substrate with a liquid plastic material, and allow it to integrate into the CNT network and harden,
 - C. adhere the coated substrate to an uncoated substrate, and dissolve the original substrate with chemical rinsing and/or heat;
5. measure the new resistivity of each sample with a four-point probe;
6. measure the surface roughness of each sample via AFM.

The end result sought from this technique is a conductive coating with an exposed surface that matches the low/uniform roughness of the substrate it was originally deposited onto. Coatings are deposited to $50 \Omega/\square$ to offset an expected increase in resistivity from the processing and handling this procedure requires; the optimal resistivity level for coating deposition was determined when the experiment was completed. There are a number of characteristics that will influence the effectiveness of this technique, including the roughness of the substrate the CNTs are originally deposited onto, the preferential adhesion of the CNTs and/or binder to one substrate material versus another, and the effect of the processing and handling on coating resistivity. To evaluate the effectiveness of this technique, the best transfer method, and the optimal combination of substrate materials, the experimental matrix shown in Table 20 is being executed.

Table 20 - CNT Substrate Transfer Experimental Matrix

| Coating Substrate | Binder Coating | Transfer Substrate | Transfer Method(s) |
|---------------------------|----------------|-----------------------------------|--------------------|
| Borosilicate Glass | No | Melinex® 453 Polyester | A |
| | | Lexan™ 8010 Polycarbonate | A |
| | | Crystal Clear® 202 Liquid Plastic | B |
| Melinex® 453 Polyester | No | Melinex® 453 Polyester | A |
| | | Lexan™ 8010 Polycarbonate | A |
| | | Crystal Clear® 202 Liquid Plastic | B |
| | Yes | Borosilicate Glass | A |
| | | Melinex® 453 Polyester | A |
| | | Lexan™ 8010 Polycarbonate | A |
| Mylar® A Polyester | No | Melinex® 453 Polyester | A |
| | | Lexan™ 8010 Polycarbonate | A |
| | | Crystal Clear® 202 Liquid Plastic | B |
| | Yes | Borosilicate Glass | A |
| | | Melinex® 453 Polyester | A |
| | | Lexan™ 8010 Polycarbonate | A |
| Lexan™ 8010 Polycarbonate | No | Crystal Clear® 202 Liquid Plastic | B |
| | | Melinex® 453 Polyester | A |
| | | Lexan™ 8010 Polycarbonate | A |
| | Yes | Crystal Clear® 202 Liquid Plastic | B |
| | | Melinex® 453 Polyester | A |
| | | Borosilicate Glass | A |
| Wafer-Mount™ 559 | No | Borosilicate Glass | C |
| | | Crystal Clear® 202 Liquid Plastic | B,C |
| | Yes | Borosilicate Glass | C |
| | | Crystal Clear® 202 Liquid Plastic | B,C |

The coating substrate must allow adequate CNT network formation but then subsequently allow the removal of the CNT and/or binder via their preferential adhesion to the transfer substrate. The transfer substrate must be optically transparent and allow adhesion of the CNT and/or binder coating(s). For these reasons, a variety of substrates were chosen for both coating deposition and CNT transfer to determine the best combination in terms of feasibility, smoothness, and resistivity stability.

No binder-coated samples are being made on borosilicate glass substrates because the chemistry of the binder causes it to bond strongly to the borosilicate. Mylar® A polyester is typically used as a release layer in cast molding, but it is not being tested as a transfer substrate because it is opaque. Crystal Clear® 202 is an aliphatic diisocyanate-based liquid plastic produced by Smooth-On that hardens at room temperature in 9 minutes. Wafer-Mount™ 559 is a substrate that can be dissolved at room temperature by washing with acetone. Figure 39 is a picture of the substrate materials being utilized for this experiment.



Figure 39 - CNT Transfer Experiment Substrate Materials

5.4.7 PV Test results

Eikos previously reported efficiencies of 3.1% for OPV cells fabricated by NREL using CNT coated substrate provided by Eikos. Tests done by NREL compared CNT directly against ITO as a TCC using NREL's standard R&D OPV cell construction. Results of these tests indicate our CNT coatings compare favorably to ITO (Figure 38). The maximum efficiency obtained from OPV cells using ITO was 3.0%. While this shows CNT can provide a materials advantage over ITO, these results are still very far from the world record efficiencies of 7.9% set by commercial OPV cell manufacturer Solarmer.

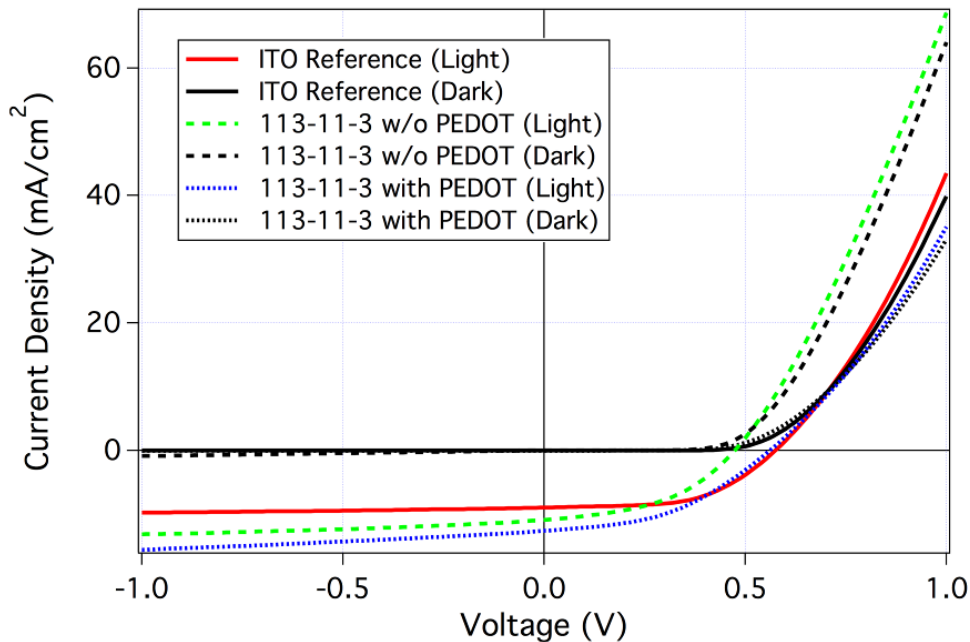


Figure 40: Comparison of performance between OPV cells made with ITO versus CNT electrodes.

NREL identified surface roughness of the CNT coating as an impediment to optimal cell performance. Optical profilometry shows asperities on the surface of the CNT conductive layer are large enough to significantly hinder the ability of the CNT layer to evenly contact the active layer. In effect the ability of the CNT conductive layer to transport electrons is limited by the area of each asperity point in contact with the active layer. The result is very inefficient power conversion efficiency.

Aiming to optimize the value of the CNT electrode Eikos then developed a method of flattening the CNT layer last quarter. The result of this process is an extremely durable conductive coating of CNTs with a surface roughness nearly equal to that of glass. Samples were delivered to NREL for device fabrication and testing near the end of the last reporting period. Optical profilometry characterization indicates press polished samples have less than 32nm Rpv surface roughness compared to previous coatings containing asperities over 300nm (Figure 41).

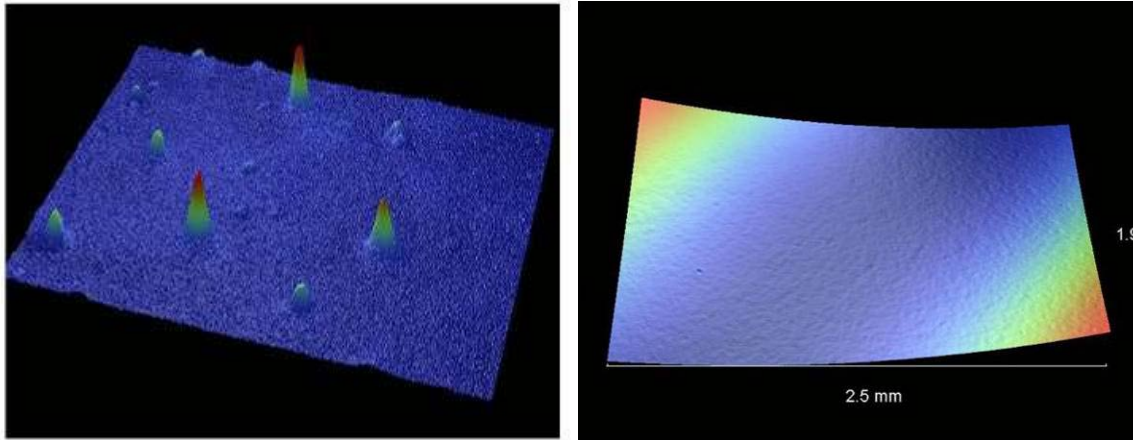


Figure 41: Optical profilometry images depicting surface roughness of CNT coatings with (L) and without (R) Asperities

Flattening of the CNT layer requires the use of the press polishing technique. Press polishing is performed by depositing a CNT coating on a thermoformable substrate, cushioning the coated substrate with ultra-smooth glass backed by flat steel, and applying modest heat and pressure with a hot press. During pressing, the thermoformable substrate conforms to the surface of the ultra-smooth glass cushions surrounding it, and the CNTs present on the substrate become partially embedded within it.

In order to utilize the press polish technique Eikos substituted PET substrate, commonly used for OPV cell fabrication, with glycol doped PET (PETG). The glycol acts as a plasticizer enabling PET to thermoform without hazing. During this quarter flattened CNT coatings on PETG were integrated into OPV cells and evaluated. Results of these tests indicate cells made with PETG act as resistors with no recorded power output (0% efficiency). Figure 42 compares the power output of cells made with PETG with previous 3.1 % efficient OPV cells made with CNT on PET.

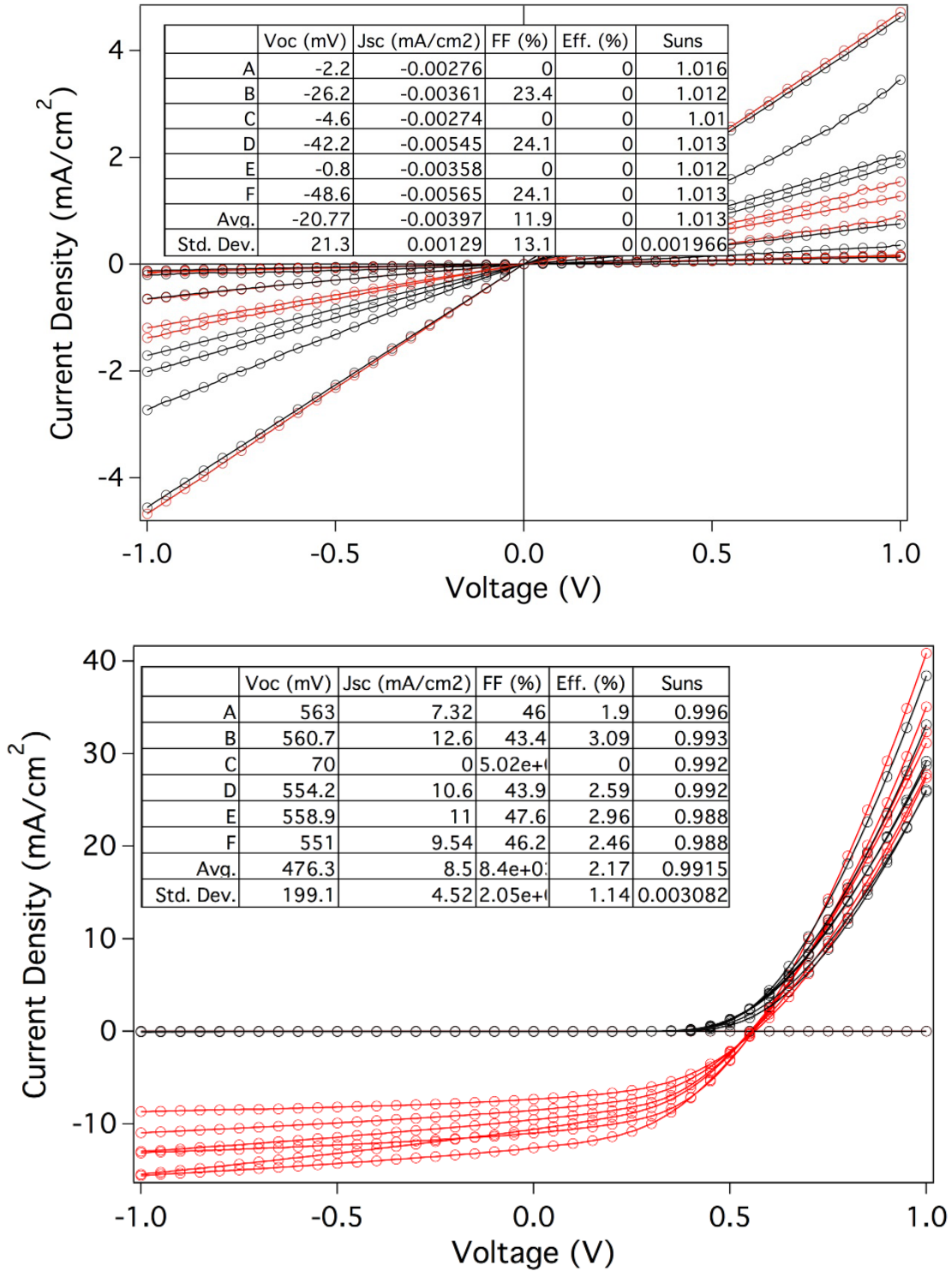


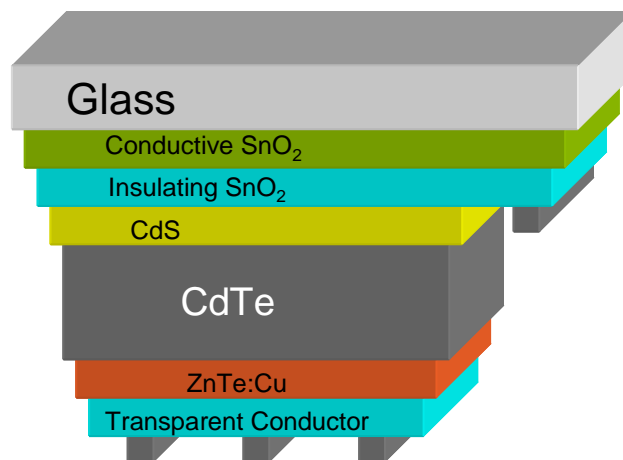
Figure 42: Power output from OPV cells made with ‘flattened’ CNT coatings on PETG (top) and ‘rough’ CNT coatings on PET.

It was surmised by NREL scientist the poor performance of these devices is a result of chemical incompatibility of the glycol with solvents used to make the cells. Given NREL's reluctance to change solvents used in cell fabrication, new materials to replace PETG were sought. Any new material must be thermoformable at temperatures below 200C, so as not to damage the CNT, and be chemically compatible with all solvents used by NREL for OPV cell fabrication.

Additional example of CNT based PV

Eikos provided NREL with carbon nanotube coatings on CdTe devices. The device work was led by Joel Duenow, and was supported by Teresa Barnes and Jeremy Bergeson of NREL. To make transparent back contact devices, NREL used standard processing for CdTe cells. A schematic diagram of the device is shown in Figure 43 . Both the thickness and copper percentage of the ZnTe:Cu layer was varied to determine its effect on the transmission of the layer and the performance of the device.

NREL made devices with a variety of different back contacts, as well, to determine the effect of the contact on device efficiency. Specifically NREL tested ZnO:Al, ITO, and SWNTs transparent contacts and titanium as an opaque contact. ZnO:Al and ITO were deposited by RF magnetron sputtering. Nanotube coatings were deposited by the membrane transfer method and spray coating from surfactant suspension by NREL, and spray coating from a water-alcohol suspension by Eikos.



Eikos coatings were deposited using Eikos standard ink graded at 95.7%T at 500 Ω/\square . As requested by NREL, two $\frac{3}{4}$ " x $\frac{3}{4}$ " CdTe devices and one $\frac{3}{4}$ " x $\frac{3}{4}$ " glass slide were spray coated to 102 Ω/\square . Subtracting the glass slide, the coating transmission was measured to be 82%T, which renormalized to 94.5%T at 500 Ω/\square . It should be noted that the carbon nanotubes used to make this coating were not from Eikos' typical nanotube supplier. Devices were fabricated and tested under AM 1.5 illumination. Current-voltage curves were measured under both light and dark and are shown in the Table 21 and Figure 44 below.

Table 21: Summary of best device performances using different back contacts and ZnTe:Cu layer thickness.

| ZnTe:Cu, Substrate Temp. 360 °C, 4% Cu, 0.4% H ₂ /Ar Sputtering Ambient | | | | | | |
|--|-------------|---------|----------------------|---------------------------------------|--------|----------|
| | ZnTe:Cu | Back | V _{oc} (mV) | J _{sc} (mA/cm ²) | FF (%) | Eff. (%) |
| | Thick. (nm) | Contact | | | | |
| — | 500 | Ti | 775 | 20.1 | 70.0 | 10.9 |
| - - - | 500 | ZnO:Al | 798 | 20.8 | 61.7 | 10.3 |
| - - - | 500 | ITO | 821 | 19.7 | 69.7 | 11.3 |
| Best Thin ZnTe:Cu | | | | | | |
| ⋯ | 200 | ITO | 772 | 20.5 | 61.2 | 9.69 |
| SWCNT Network Films | | | | | | |
| - - - | 500 | NREL | 800 | 21.3 | 42.2 | 7.19 |
| — | 500 | Eikos | 818 | 20.2 | 71.7 | 11.8 |

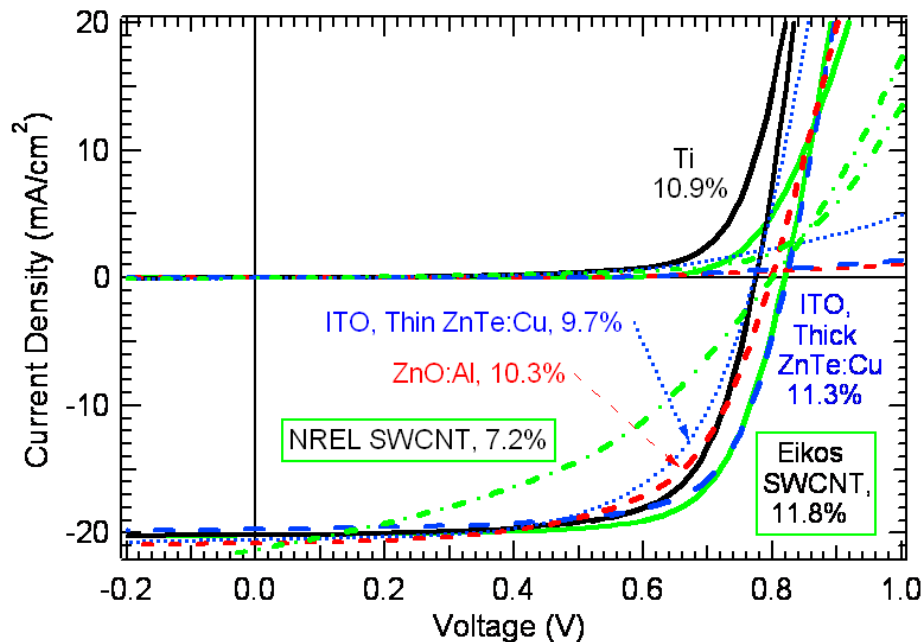


Figure 44: I-V Curves for Best CdTe Devices with Various Back

Devices with Eikos SWNTs had both the highest fill factor (71.7%) and also the highest efficiency (11.8%). This efficiency is higher than the best transparent device (ITO, 11.3%) and the opaque device (Ti, 10.9%). Eikos noted that devices with NREL SWNTs resulted in devices with 7.2% efficiency. It was postulated that Eikos materials result in higher performance devices because the nanotubes are in more intimate contact with the substrate and also because Eikos do not use surfactants to disperse the nanotubes, which



could create charge barriers. This experiment demonstrates the value of using carbon nanotubes as a back contact to achieve high device efficiency.

5.4.8 Reducing Roughness

Our work with NREL produced evidence that the roughness of our CNT coatings limits device performance when the CNT coatings are used as the top electrode in OPV cells. This is in large part because all the OPV layers are deposited on top of the electrode and any defect or contaminate in the electrode will interrupt the formation of the remaining layers. The optimal resistivity of CNT coatings used in this fashion is $60 - 100 \Omega/\square$, and even when using highly conductive inks of 4000 S/cm , this resistivity level necessitates depositing a significant amount of CNTs.

As measured by AFM, the peak-to-valley surface roughness (R_{pv}) of these coatings is approximately $190 - 290 \text{ nm}$. The high R_{pv} is attributed to a low density of relatively large asperities in the coating. When used in the fine layered structure of an OPV cell, Eikos hypothesize that this surface roughness causes penetration between layers resulting electrical shunting or at least in poor layer definition.

Essentially, the roughness is greater than the layer thickness and thus the peaks are protruding into the active layer and possible through to the opposite electrode leading to shorting. Eikos investigated several techniques to solve the problem:

1. CNT-Substrate Transfer
2. Blade Leveling
3. Binder Topcoat Addition
4. Chemical-Mechanical Polishing
5. Press Polishing

1: CNT-Substrate Transfer

Eikos investigated the effectiveness of "CNT substrate transfer" where CNTs are spray coated onto a smooth substrate and are then transferred onto another substrate, thus causing the smooth side of the coating to be inverted and make contact with the active layer of the OPV cell during device fabrication. The techniques general procedure is as follows:

1. Spray-coat CNT coatings of $50 \Omega/\square$ onto $1" \times 3"$ substrates;
2. For some samples, dip-coat thick ($\gg 100 \text{ nm}$) binder coatings and cure for 1 hour at 125°C ;
3. Measure the resistivity of each sample with a four-point probe;
4. Transfer the deposited coating(s) onto another $1" \times 3"$ substrate (so that the side of the coating that originally faced the smooth substrate surface is now exposed) using one of three methods:

- A. heat the uncoated substrate to its softening point with a hot press, and press the two substrates together,
 - B. cover the coated substrate with a liquid plastic material, and allow it to integrate into the CNT network and harden,
 - C. adhere the coated substrate to an uncoated substrate, and dissolve the original substrate with chemical rinsing and/or heat;
5. Measure the new resistivity of each sample with a four-point probe;
 6. Measure the surface roughness of each sample via AFM.

The transfer substrate must be optically transparent and allow adhesion of the CNT and/or binder coating(s). To determine the best combination in terms of feasibility, smoothness, and resistivity stability, a variety of substrates were chosen for both coating deposition and CNT transfer. Five separate substrate materials were used to deposit the starting CNT coating. In order to evaluate the effectiveness of this technique, the best transfer method, and the optimal combination of substrate materials, coated substrates were pored with up to four transfer substrates according to the experimental matrix shown in Table 20.

Table 22 - CNT Substrate Transfer Experimental Matrix

| Coating Substrate | Binder Coating | Transfer Substrate | Transfer Method(s) |
|---------------------------|----------------|-----------------------------------|--------------------|
| Borosilicate Glass | No | Melinex® 453 Polyester | A |
| | | Lexan™ 8010 Polycarbonate | A |
| | | Crystal Clear® 202 Liquid Plastic | B |
| Melinex® 453 Polyester | No | Melinex® 453 Polyester | A |
| | | Lexan™ 8010 Polycarbonate | A |
| | | Crystal Clear® 202 Liquid Plastic | B |
| | Yes | Borosilicate Glass | A |
| | | Melinex® 453 Polyester | A |
| | | Lexan™ 8010 Polycarbonate | A |
| Mylar® A Polyester | No | Melinex® 453 Polyester | A |
| | | Lexan™ 8010 Polycarbonate | A |
| | | Crystal Clear® 202 Liquid Plastic | B |
| | Yes | Borosilicate Glass | A |
| | | Melinex® 453 Polyester | A |
| | | Lexan™ 8010 Polycarbonate | A |
| Lexan™ 8010 Polycarbonate | No | Melinex® 453 Polyester | A |
| | | Lexan™ 8010 Polycarbonate | A |
| | | Crystal Clear® 202 Liquid Plastic | B |
| | Yes | Borosilicate Glass | A |
| | | Melinex® 453 Polyester | A |
| | | Lexan™ 8010 Polycarbonate | A |
| Wafer-Mount™ 559 | No | Borosilicate Glass | C |
| | | Crystal Clear® 202 Liquid Plastic | B,C |
| | Yes | Borosilicate Glass | C |
| | | Crystal Clear® 202 Liquid Plastic | B,C |

This experiment produced some success leveling the CNT layer, but at the cost of raising resistivity of the coating. All transfer methods attempted raised the resistivity by a factor of 2-3 (into the hundreds of Ohm), rendering these samples unusable for PV cell optimization.

2: Blade Leveling

Blade scraping is used in the OLED community to remove asperities on the surface of ITO conductive layers. This straight forward mechanical method involves running an angled blade across the surface of a rough planer coating to cut off high points and leave the bulk of the coating intact (Figure 45). Blade leveling is a quick and easy method to remove relatively large asperities from thin coatings.

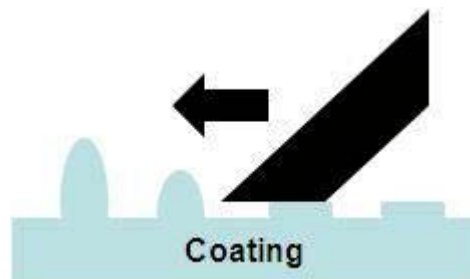


Figure 45: Removal of surface asperities by blade leveling

During this period Eikos modified the blade leveling technique to remove high points on the surface of our CNT coatings. While peak-to-valley surface roughness dropped from 190-290nm to 60-80nm as a result of blade leveling, tests done by NREL indicate this is still too rough for use as an electrode layer in OPV cells. However, blade leveling was used as a precursor for further leveling experiments such as binder addition and polishing.

3: Binder Topcoat Addition

Dip coating of a binder topcoat was investigated in an attempt to level the surface in contact with the PV active layer. Two oxide based sol-gel binders, Binder A and Binder 3, were chosen for this experiment based on these binders ability to evenly topcoat CNT without substantially affecting the conductivity of the CNT network.

All coatings were deposited onto pre-cleaned 3" x 1" borosilicate glass slides to $60 \Omega/\square$, within 10% variability. Slides were pre-cleaned using the following procedure:

1. sonicate slides in a mild detergent solution for 20 minutes at 30°C,
2. sonicate slides in clean DI H₂O for 20 minutes at 30°C,
3. individually rinse each slide with high-pressure DI H₂O,
4. individually rinse each slide with filtered IPA, and

5. individually dry each tube with filtered, compressed air at 40 psi. After CNT deposition samples were post treated to remove large particulate using the blade leveling technique.

Initial work shows single dip coatings, thick enough to cover asperities from the CNT layer, amplify surface roughness. Therefore, multiple thin binder topcoat layers were used an effort to level out surface roughness. Slides were dip coated with one, two and three thin layers of Binder A or Binder 3. Eikos found even thin layers of Binder A increase the overall surface roughness. Additional layers of Binder A further increase roughness (Table 23). In addition, subsequent layering of Binder A causes surface hazing due to crystallization at the interface of each binder topcoat layer.

Table 23: Effects of oxide binder topcoat on surface roughness

| Top Coat | Sample | Rpv(nm) | Rq(nm) | Ra(nm) | Resistivity (Ohm/sq) |
|------------------------|----------|---------|--------|--------|----------------------|
| Binder A Single dip | 1 | 74 | 9.6 | 7.3 | 65 |
| | 2 | 112 | 9.6 | 7 | |
| | 3 | 72 | 9.5 | 7.1 | |
| | Average: | 112.00 | 9.57 | 7.13 | |
| Binder A Three dips | 1 | 200 | 22.3 | 15.1 | 72 |
| | 2 | 181 | 15 | 10.7 | |
| | 3 | | | | |
| | Average: | 200.00 | 18.65 | 12.90 | |
| Binder 3 Single dip | 1 | 93.8 | 9.9 | 7.4 | 70 |
| | 2 | 88 | 8.5 | 6.5 | |
| | 3 | 154 | 12.8 | 8.9 | |
| | Average: | 154.00 | 10.40 | 7.60 | |
| Binder 3 Three dips | 1 | 74 | 6 | 5 | 77 |
| | 2 | 67 | 7 | 5 | |
| | 3 | 74 | 6.4 | 5 | |
| | Average: | 74.00 | 6.47 | 5.00 | |

Surface roughness increases with the initial layer of Binder 3, but levels off considerably with the addition of multiple coatings. Peak to valley roughness is lowered from 154-74nm. In addition, mean (Rq) and average roughness (Ra) both become uniform over the sample. This phenomenon can be seen visually with the help of AFM imaging (Figure 46).

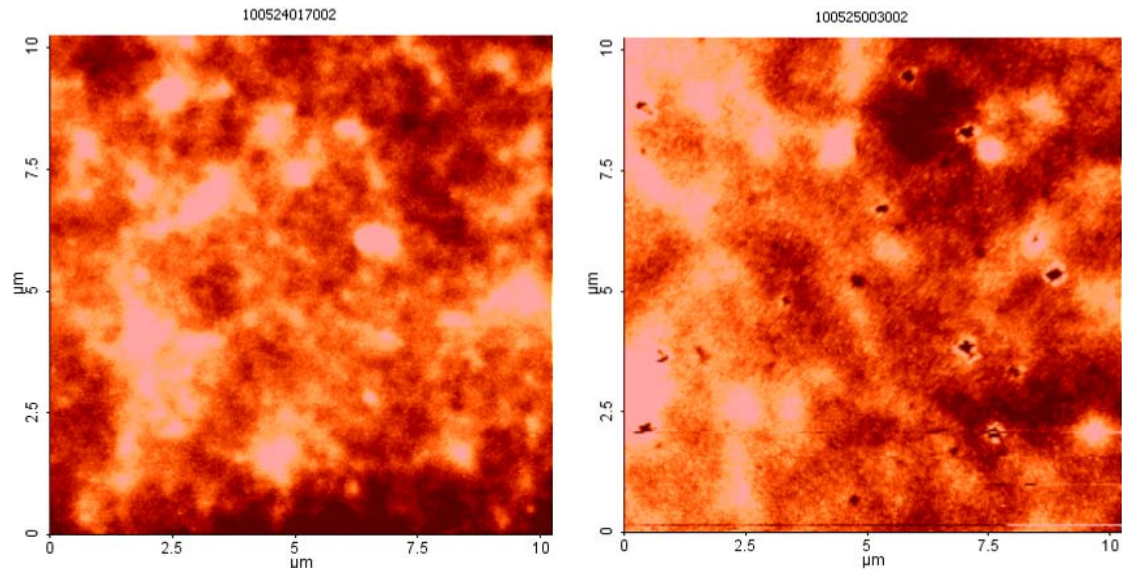


Figure 46: Surface roughness of CNT/binder topcoat for one dip of sol-gel binder 3 dip (left) versus three daps of Binder 3 (right)

While R_q and R_a values are excellent for triple coated Binder 3 samples the R_{pv} is still too high. This indicates large asperities are still protruding through the binder topcoat layer. It may be possible to continue dip coating additional binder topcoat layers until all asperities are covered. However, this would result in binder topcoats that match the thickness of the highest asperity. Multiple binder topcoats at this thickness would adversely affect the RT performance to the point of eliminating these coatings from useful performance in PV cells.

4: Chemical-Mechanical Polishing

Chemical-Mechanical Polishing (CMP) is used extensively in the microchip fabrication industry to polish the surface of silicon wafers to tolerances of $>10\text{nm}$. Silicon wafers are mounted face down on a rotating platen covered with an absorbent pad. A slurry of small particulate abrasive is continuously fed on the pad to induce wafer polishing (Figure 47).

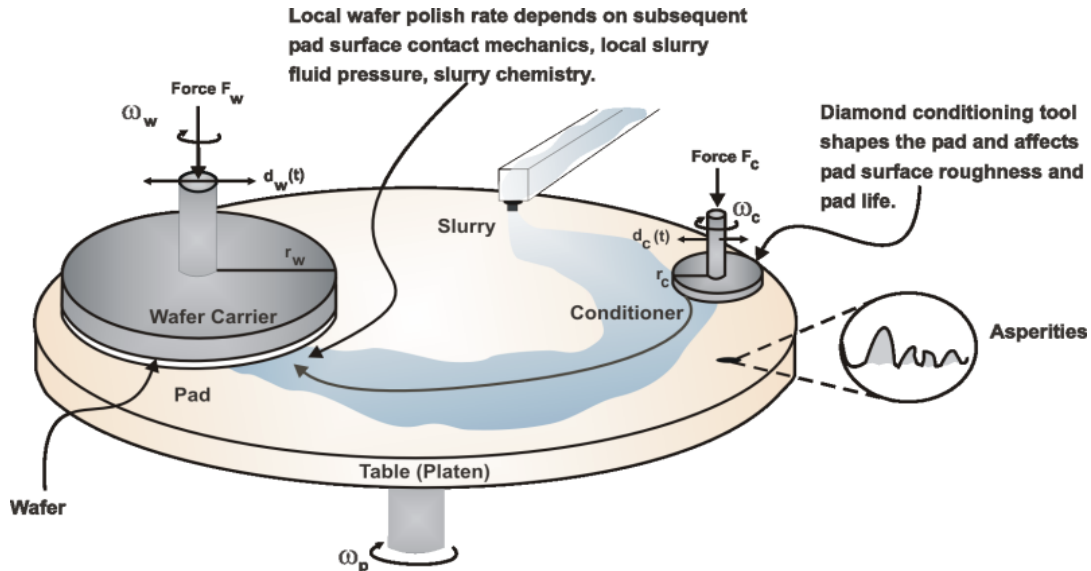


Figure 47: Diagram for silicon wafer polishing, via CMP, used in the microchip industry¹¹

Glass slides were spray coated with CNT to 50 Ohm then dip coated in a sol-gel to form a Binder A or Binder 3 topcoat. Instead of using a rotating platen slides were polished by hand rubbing the coated side against a microfiber cloth pre-wet with a slurry of either 50nm diamond or 20nm silicon dioxide particulate. To maintain a stable and uniform polish the microfiber cloth was backed by a ¼" thick flat glass plate. Slides were polished to 10, 20 and 50 strokes (one stroke = forward one inch then back) and imaged using AFM after each stage.

Results from this experiment are disappointing. AFM imaging indicates polishing with SiO₂ has little or no effect reducing surface roughness and starts to rub the CNT-binder layer off after 50 strokes. The diamond slurry entirely removes the CNT-binder coating after only a few strokes.

5: Press Polishing

Optical profilometry shows asperities on the surface of the CNT conductive layer are large enough to significantly hinder the ability of the CNT layer to evenly contact the active layer. In effect the ability of the CNT conductive layer to transport electrons is limited by the area of each asperity point in contact with the active layer. The result is very inefficient power conversion efficiency.

Press polishing is performed by depositing a CNT coating on a thermoformable substrate, cushioning the coated substrate with ultra-smooth glass backed by flat steel, and applying modest heat and pressure with a hot press. During pressing, the thermoformable substrate conforms to the surface of the ultra-smooth glass cushions surrounding it, and the CNTs present on the substrate become partially embedded within it. **The result of this process**

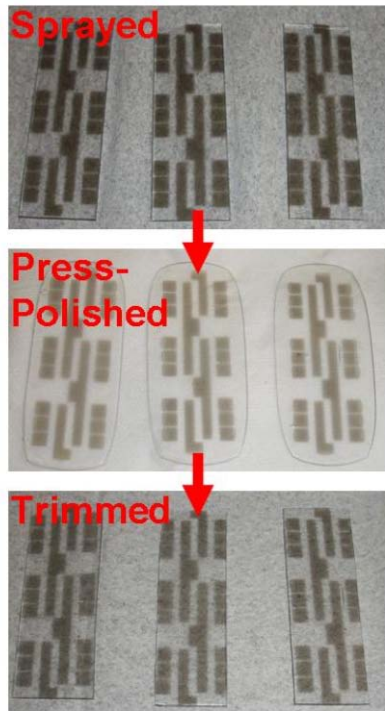


is an extremely durable conductive coating of CNTs with a surface roughness nearly equal to that of glass.

Press polishing can be performed on any substrate with a softening point significantly lower than that of the glass cushions used for the procedure (820°C for borosilicate). However, damage to CNT coating conductivity increases with temperature, so substrates with softening points as low as possible are optimal. In addition, a major motivation behind surface roughness reduction is the anticipated gain in PV device performance that could result from using an ultra-smooth CNT coating.

Furthermore, since NREL performed device fabrication and testing with our patterned samples, Eikos sought to utilize a substrate compatible with their solvent chemistries. Substrate screening tests were performed using polycarbonate (PC), polyethylene terephthalate (PET), and glycol-modified polyethylene terephthalate (PETG) as substrates. Ultimately, Eikos chose PETG for NREL sample production because it retains the high chemical compatibility of PET, possesses an extremely low softening point of 83°C, and has an amorphous structure that will not haze or discolor during heat treatment.

Figure 48 shows a visual progression of patterned CNT samples on PETG at different points during press polishing. The detailed procedure used for NREL sample production is as follows:



1. Spray-coat patterned CNTs onto 3" x 1" PETG samples using negative stainless-steel templates of the NREL "racetrack" pattern;
2. Place two 6" x 6", 1/4"-thick pieces of flat tool steel on a hot press, and preheat its top and bottom platens and the tool steel to 120°C;
3. Place up to three patterned samples between two 6" x 6" pieces of ultra-smooth LCD glass, leaving at least 1" of space between samples;
4. Place the samples and glass between the two pieces of tool steel on the hot press;
5. Apply 10,000 lb_f for 30 seconds;
6. Remove the glass and samples from the hot press and allow them to return to room temperature for 5 minutes;
7. Soak the glass and samples in neat DI H₂O for 5 minutes to separate; and
8. Trim the press-polished samples back down to 3" x 1" in size with a razor.

Figure 48: Visual Progression of Press-Polishing Procedure

All NREL samples were coated with "A+" CNT ink (>96.0 %T @ 500 Ω/□, ~4000 S/cm). The press-polishing procedure increased their initial resistivity by ~50%; from ~30 Ω/□ to ~45 Ω/□. Despite this minimal increase in sample resistivity, the effect of the press polishing procedure is obvious even to the naked eye. Figure 49 shows 1000x magnification pictures of a blanket-coated reference sample taken both before and after press polishing.

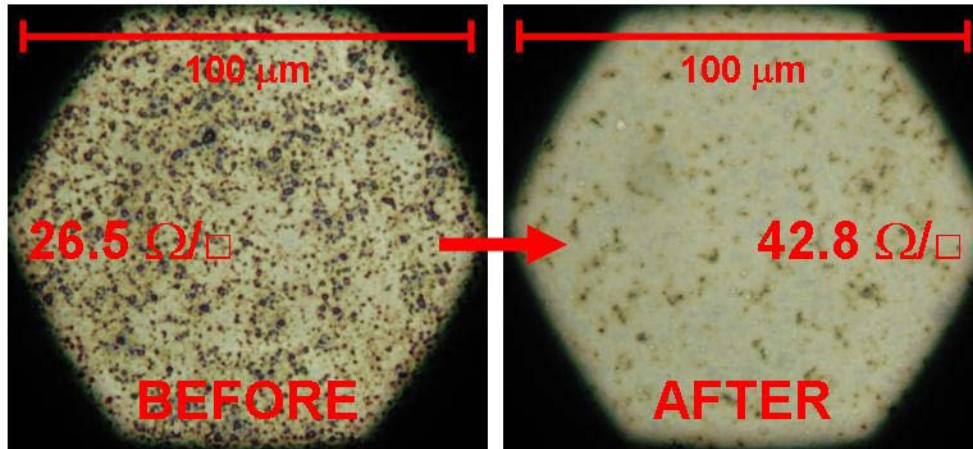


Figure 49: CNT on PETG Before (Left) and After (Right) Press Polishing

The samples produced are approximately an order of magnitude smoother than any previous samples delivered by Eikos to NREL for testing. According to AFM analysis of our retained control sample, this press polishing procedure resulted in $\sim 45 \text{ } \Omega/\square$ coatings with surface roughness of only 36.3 nm R_{pv} and 3.2 nm R_q. A 10 μm^2 AFM image of our control sample is shown in Figure 50.

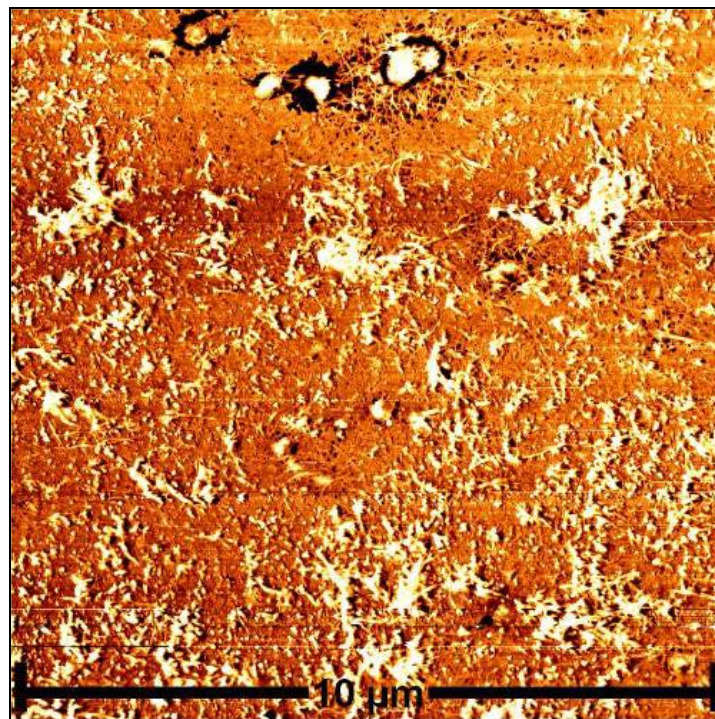


Figure 50: AFM Image of Blanket-Coated, Press-Polished PETG Sample



Overall, press polishing dramatically reduced surface roughness with very little impact on the other properties of our CNT coatings. Table 24 summarizes the effect of press polishing.

Table 24: Characterization of Blanket-Coated, Press-Polished PETG Sample (#113-91-2)

| When Measured | Substrate Thickness (inches) | Resistivity (Ω/\square) | %T vs. PETG Reference | Sample %T (vs. Air) | Max Rpv Roughness (nm) | Ave. Rq Roughness (nm) |
|------------------|------------------------------|----------------------------------|-----------------------|---------------------|------------------------|------------------------|
| Before Polishing | 0.053 | 31.11 | 58.8 | 53.0 | N/A | N/A |
| After Polishing | 0.029 | 43.81 | 60.7 | 54.2 | 36.3 | 3.2 |

Samples were delivered to NREL for device fabrication and testing near the end of the reporting period. Optical profilometry characterization indicates press polished samples have less than 32nm Rpv surface roughness (Figure 51).

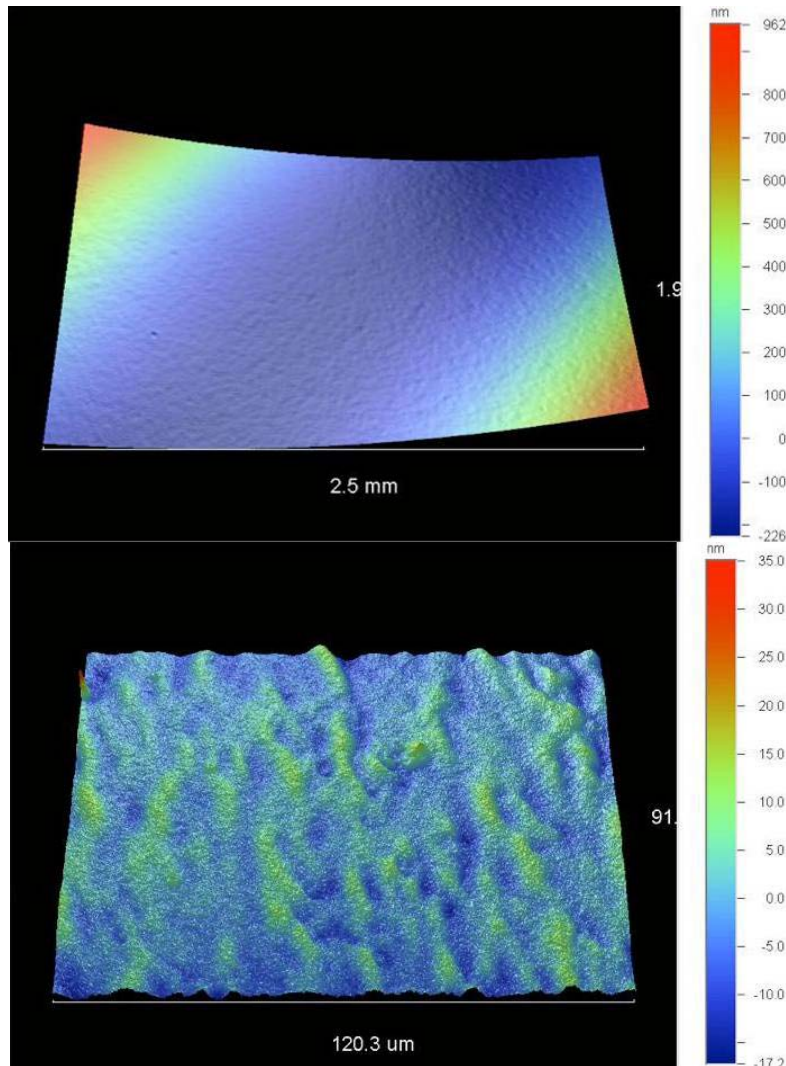


Figure 51: Optical Profilometry image of press polished CNT coating imbedded on the surface of PETG at 2.5X magnification (top) and 50X magnification (bottom)

Aiming to optimize the value of the CNT electrode Eikos then developed a press polishing method of flattening the CNT layer already report above. The result of this process is an extremely durable conductive coating of CNTs with a surface roughness nearly equal to that of glass. Optical profilometry characterization indicates press polished samples have less than 32nm Rpv surface roughness compared to previous coatings containing asperities over 300nm (Figure 52).

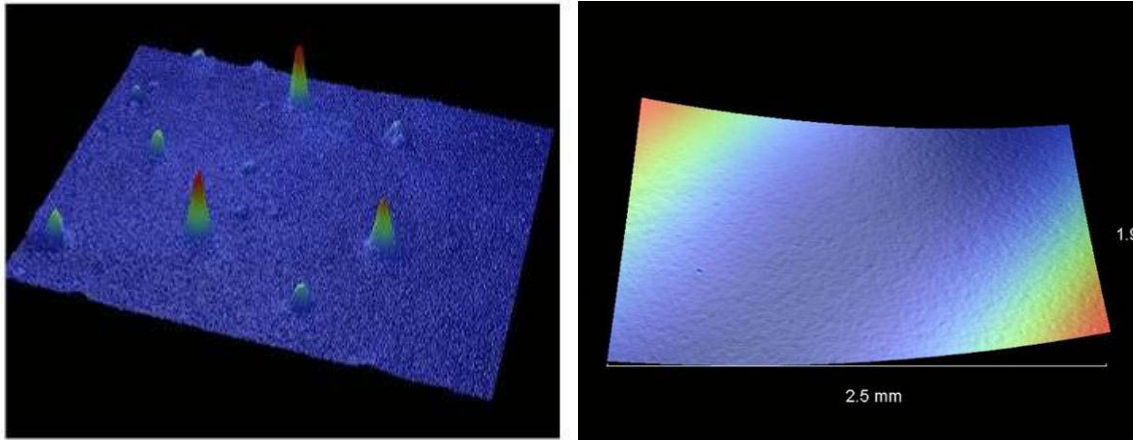


Figure 52: Optical Profilometry of CNT coatings with (L) and without (R) Asperities

In order to utilize the press polish technique Eikos substituted PET substrate, commonly used for OPV cell fabrication, with glycol doped PET (PETG). The glycol acts as a plasticizer and Tg reducer, enabling PET to thermoform at low temperatures without hazing. During last quarter, flattened CNT coatings on PETG were integrated into OPV cells and evaluated. Results of these tests indicate cells made with PETG act as resistors with no recorded power output (0% efficiency). It is surmised by NREL the poor performance of these devices is a result of chemical incompatibility of the glycol with solvents used to make the cells. Given NREL's reluctance to change solvents used in cell fabrication, Eikos are currently investigating new materials to replace PETG.

Eikos identified several candidate polymers to replace PETG in our press-polishing procedure based on the desired characteristics of a (relatively) low softening temperature, an amorphous structure (to prevent hazing), and chemical resistance to NREL's ortho-dichlorobenzene fabrication solvent. Initial screening tests were performed by submerging samples of ethylene-vinyl acetate (EVA), cyclic olefin copolymer (COC), and polymethyl pentene (PMP) in o-dichlorobenzene for several minutes to test their compatibility. Of these materials, only PMP did not dissolve. Although PMP is a crystalline polymer, preliminary press-polishing trials suggest that with the proper processing conditions, it can be put through our procedure without hazing. PMP has a melting point of 230°C, but softens at temperatures as low as 47°C, making it compatible with our press-polishing technique.

Press-polishing trials using PMP as a substrate were completed. First, Eikos adjusted our processing conditions for PMP by adjusting the platen temperature of our hot press, determining an acceptable press time based on resulting CNT conductivity and sample flatness, and investigating a post-press cooling procedure to ensure no hazing occurs.



Second, Eikos used these optimized parameters to produce CNT-patterned samples for NREL. Prior to being press-polished, some samples were coated with CNTs, and others were coated with both CNTs and one of several Eikos-proprietary binder systems. While our binders are normally cured in an oven after deposition, leaving the binder coatings on these samples uncured and investigate the use of the press-polishing method itself as an “instant cure” technique.

5.4.9 Reducing Roughness Part II

Eikos work with NREL produced evidence that the roughness of our CNT coatings limits device performance when the CNT coatings are used as the top electrode in OPV cells. The optimal resistivity of CNT coatings used in this fashion is 50 – 100 Ω/\square , and even when using highly conductive inks of 4000 S/cm, this resistivity level necessitates depositing a significant amount of CNTs. As measured by AFM, the peak-to-valley surface roughness (R_{pv}) of these coatings is approximately 190 – 290 nm. The high R_{pv} is attributed to a low density of relatively large asperities in the coating. When used in the fine layered structure of an OPV cell, Eikos hypothesize that this surface roughness causes penetration between layers resulting electrical shunting or at least in poor layer definition. Essentially, the roughness is greater than the layer thickness and thus the peaks are protruding into the active layer and possible through to the opposite electrode leading to shorting and adversely effecting cell performance.

Previous efforts to reduce or eliminate asperities were marginally successful. One method, Press Polishing, eliminates the roughness issue, but has been frustrated by material incompatibility. Substrate materials used for press polishing of CNT, which allow for hyper flat and uniform conductive layers, are not chemically compatible with NRELs current method for cell fabrication.

Eikos met with NREL to determine the path forward in light of the technical difficulties this program has encountered. From this meeting three parallel efforts were pursued to overcome these difficulties and, simultaneously, find a path toward improving the performance of current OPV cells. These three efforts are:

- *Formulate and deposit binders as a substitute for PEDOT/PSS within OPV cells.*
- *Press Polish using new substrate material(s).*
- *Incorporate binders into the press polish technique.*

Potential Binder Replacements for PEDOT:PSS

NREL expressed great interest in using Eikos’ sol-gel based oxide binders as a substitute for PEDOT:PSS within OPV cells. PEDOT:PSS has two functions within a OPV cell: 1) To facilitate charge transfer between the active layer and the conductive layer; and 2) to help cushion/reduce the surface roughness of the conductive layer from the active layer.



Based on a literature search of oxides used to supplant PEDOT:PSS and our own internal knowledge of binder chemistry, a total of six sol-gel based oxide binders were down selected for sample production and testing. Samples were produced in three batches on slides of 3"x1" borosilicate glass that were pre-cleaned and then coated with CNT and/or binder; CNT coating was accomplished via spraying, binders were dip-coated. Batch #1 samples were coated with one of our six candidate binders, and some samples were dipped multiple times to gauge its effect on surface roughness. Table 25 below lists each coated slide from Batch #1 with the corresponding transparency measurements made by Eikos.

Table 25: Sample Batch #1 - Binder Coated Samples

| Binder Coating of Blank Slides | | | | |
|---------------------------------------|---------------|------------------|---------------|-----------|
| <i>Sample</i> | <i>Binder</i> | <i>Dip Speed</i> | <i>Layers</i> | <i>%T</i> |
| 103-178-01 | Z1 | 250 | 7 | 93.0 |
| 103-178-14 | V1 | 100 | 1 | 90.9 |
| 103-178-18 | V1 | 200 | 2 | 80.9 |
| 103-178-19 | V1 | 200 | 1 | 87.7 |
| 103-178-20 | A2 | 100 | 1 | 91.0 |
| 103-178-21 | A2 | 200 | 1 | 91.4 |
| 103-178-22 | A1 | 200 | 1 | 82.1 |
| 103-178-23 | A1 | 100 | 1 | 87.5 |
| 103-178-24 | 3.2 | 200 | 2 | 93.6 |
| 103-178-25 | 3.2 | 200 | 1 | 90.2 |
| 103-178-26 | 3.1 | 200 | 1 | 94.8 |
| 103-178-27 | 3.1 | 200 | 2 | 98.8 |
| 103-178-28 | 3.2 | 100 | 2 | 90.5 |

Batch #2 samples were blanket-coated with both CNT and binder. Slides were spray-coated to $50 \Omega/\square$, scraped to remove asperities using an in-house technique, dipped with one of our candidate binder coatings, and then cured. Table 26 lists all Batch #2 samples and the results of the RT characterization done at Eikos.

Table 26: Sample Batch #2 - CNT & Binder Coated Samples

| Binder Top Coat of CNT Coated Slides | | | | | |
|--------------------------------------|--------|-----------|--------|------|------------|
| Sample | Binder | Dip Speed | Layers | %T | R (Ohm/sq) |
| 103-178-02 | A1 | 200 | 1 | 62.2 | 59 |
| 103-178-03 | A1 | 100 | 1 | 60.7 | 69 |
| 103-178-04 | A1 | 200 | 2 | 64.3 | 70 |
| 103-178-05 | A2 | 200 | 1 | 61.5 | 56 |
| 103-178-06 | A2 | 100 | 1 | 60.4 | 52 |
| 103-178-07 | A2 | 200 | 2 | 61.2 | 60 |
| 103-178-08 | 3.1 | 200 | 1 | 64.8 | 62 |
| 103-178-09 | 3.1 | 200 | 2 | 71.2 | 64 |
| 103-178-10 | 3.2 | 200 | 1 | 63.8 | 62 |
| 103-178-11 | 3.2 | 200 | 2 | 66.0 | 66 |
| 103-178-12 | V1 | 200 | 1 | 57.8 | 75 |
| 103-178-13 | V1 | 100 | 1 | 62.0 | 70 |
| 103-178-15 | V2 | 200 | 1 | 61.7 | 76 |
| 103-178-16 | V2 | 100 | 1 | 62.8 | 79 |
| 103-178-17 | V2 | 100 | 2 | 61.8 | 77 |

Batch #3 samples were spray-coated with CNT to $50 \Omega/\square$ in the “racetrack” pattern furnished by NREL, dip coated with candidate binders, scraped, and then cured. With the exception of samples coated with V1, all binder coatings applied to Batch #3 slides correlate to the same coatings deposited on Batch #2 samples; for example, Batch #2 sample 103-178-04 was coated with the same CNT-binder layer that was applied to Batch #3 sample 103-178-31. Figure 53 shows the physical appearance of slides that have been coated with a “racetrack pattern,” and Table 27 lists the details of the Batch #3 samples.

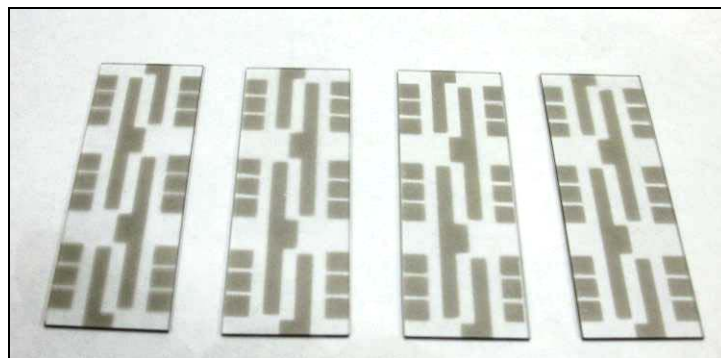


Figure 53: Glass Slides Coated with CNT to $50 \Omega/\square$ in a ‘Racetrack’ Pattern



Table 27: Sample Batch #3 - Patterned CNT & Binder Coated Samples

| Binder Top Coat of CNT Patterned Slides | | | |
|--|---------------|------------------|---------------|
| <i>Sample</i> | <i>Binder</i> | <i>Dip Speed</i> | <i>Layers</i> |
| 103-178-29 | A1 | 200 | 1 |
| 103-178-30 | A1 | 100 | 1 |
| 103-178-31 | A1 | 200 | 2 |
| 103-178-32 | A2 | 200 | 1 |
| 103-178-33 | A2 | 100 | 1 |
| 103-178-34 | 3.1 | 200 | 1 |
| 103-178-35 | 3.1 | 200 | 2 |
| 103-178-36 | 3.2 | 200 | 1 |
| 103-178-37 | 3.2 | 200 | 2 |
| 103-178-38 | V2 | 200 | 1 |
| 103-178-39 | V2 | 100 | 1 |
| 103-178-40 | V2 | 200 | 2 |

All samples were delivered to NREL for testing. Characterization of these samples included resistivity, transparency, surface roughness, and work function evaluation. NREL also fabricate the patterned Batch #3 samples into actual OPV devices but did not provide their performance characterization in the form of current vs. voltage curves and power conversion efficiencies.

5.4.10 Particle Reduction

Eikos focused on optimization of CNT inks by particulate reduction. Eikos has developed an optical particle analysis procedure capable of detecting particles 175-200 nm in diameter and larger in its CNT coatings, and has used it to evaluate our efforts to reduce at particle size and surface roughness. Initial material analyses suggest AIF processed inks contain many more particles than corresponding Ex. 7 processed inks, despite Ex. 7 inks' lower RT performance. Differences in overall particle count and average particle size between different materials also exist, and there is variability in particle count within coatings themselves. Initial particle reduction experiments involving sodium deoxycholate monohydrate surfactant treatment and high speed centrifugation have given promising results. The most successful of these experiments has shown the ability to reduce the particles present in Nanoledge Ex. 7 ink from 33 particles per $7250 \mu\text{m}^2$ and an area fraction of 0.10% to 10 particles per $7250 \mu\text{m}^2$ and an area fraction of 0.04%.

CNT and Binder Deposition

A coating evaluation was performed at Euclid Lab Coaters in Bay City, Michigan, on March 26 at one of their company's facilities. The objective of this trip was to evaluate the coating capability of the Euclid gravure/roll-roll coaters as a processing technique to allow for low cost/low temp coatings that can easily be scaled. To perform the valuation,

three different polymer substrate films were selected (ST505, Kimoto #188 G1DST, and Kapton). Each was spray coated with carbon nanotubes before gravure coating for top coat (binder) evaluation. In addition, bare ST505 was run through the gravure to determine coating of CNT via roll processing. The specific coating machine evaluated was a 12 inch, 3 Roll offset Gravure coating system made by Euclid. This system comprises a six inch gravure bottom roller, a 6 inch E.P.D.M center roller, a three inch stainless steel top roller, a wiper blade and a stainless steel coating pan (Figure 54).

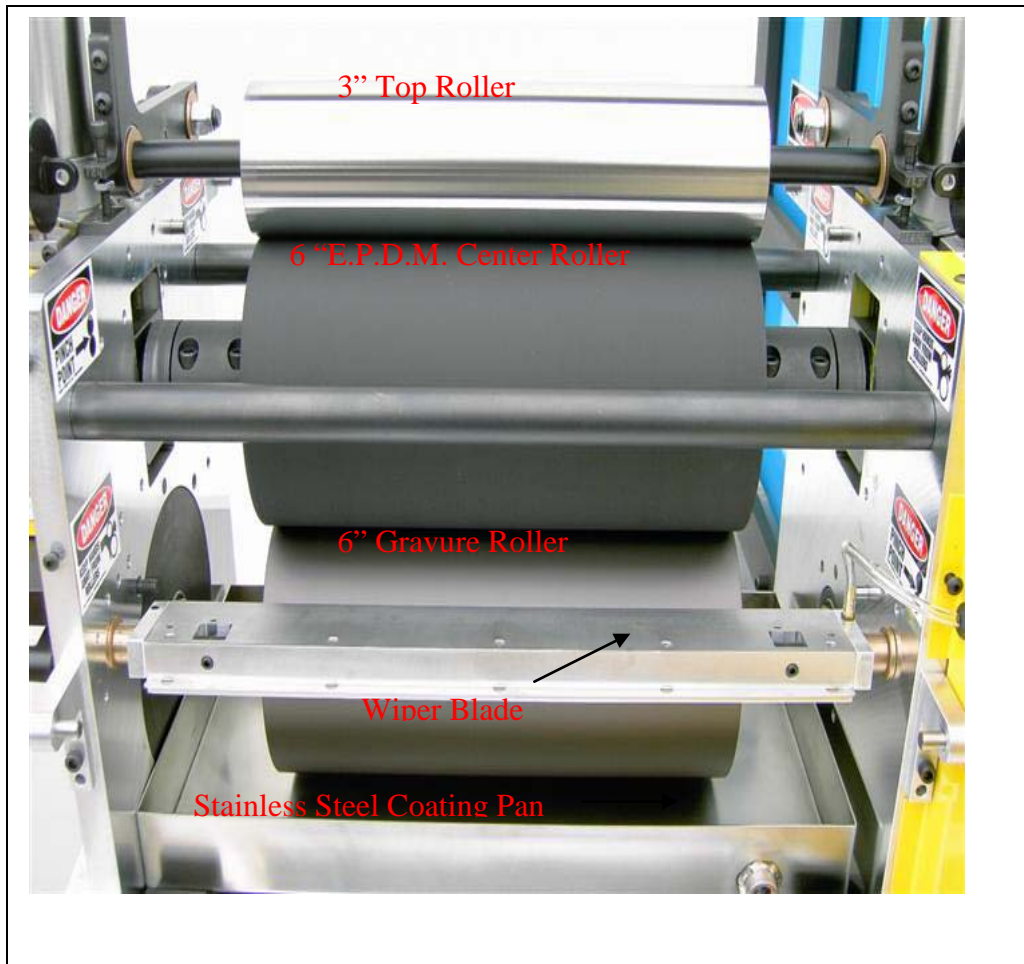


Figure 54 Euclid three roll offset Gravure Lab Coater with parts marked

Roll coated samples look similar in appearance to the coatings produced by Eikos' ultrasonic spray coating deposition. 4% TiAlZn top coats show uniformity and thickness issues from the gravure roller. Streaks in the coating and also blue colored spots in the coating are present. These may be due to not enough coating being applied on the film. A newer roller or a different concentration of solution may help to resolve this issue. A formulation of binder designed for use as anti reflective layer coated very well giving a uniform coating on bare and CNT coated substrates. CNT/binder gravure coated samples



were washed on site and also back in the laboratory to remove surfactants that were added to the CNT ink. The percent transmittance was taken at 550 nm along with four point probe resistivity measurements for each sample. The results are reported as the actual number and also calculated for the percent transmittance at 500 Ohms/Square and 550 nm to normalize results (Table 28).

Table 28 Resistance values and transmittance for Gravure CNT coated PET after washing with and without top coatings.

| Top Coating | 4 Point Ohms/Square | %T of CNT layer @ 550 nm | %T @ 500 Ohms/Square |
|-----------------------|---------------------|--------------------------|----------------------|
| None | 2184 | 96.5 | 89.1 |
| None | 618 | 88.2 | 86.2 |
| None | 1302 | 93.9 | 87.4 |
| 6% Anti Reflective SI | 1481 | 90.6 | 79.3 |
| 6% Anti Reflective SI | 567 | 93.4 | 92.7 |
| 6% Anti Reflective SI | 2023 | 93.5 | 81.6 |
| 6% Anti Reflective SI | 2192 | 93.3 | 80 |
| 4% TiAlZn | 742 | 93.8 | 91.6 |
| 4% TiAlZn | 1035 | 94.5 | 90.4 |
| 4% TiAlZn | 1084 | 91.2 | 84.4 |
| 4% TiAlZn | 1513 | 92.1 | 82.1 |

Abrasion testing was done on roll coated samples by rubbing 1 lb_F-weighted cheese cloth over the coated surface. Readings were taken at 0, 1, 3, 5, 7, 10, 20, 30 and 60 cycles. Pristine (not abrasion tested) CNT/binder samples made by roll coating were humidity tested at 85/85 for 300 hours. Tested samples did not perform well in the abrasion and environmental procedure. There are many potential reasons for poor adhesion to the surface, many of which cannot be verified without more trials. Eikos purchased a roll coater like that used herein to conduct future trial runs and work out processing and formulation issues in house where Eikos have access to the full characterization capabilities of our lab.

Overall the gravure/roll process needs some fine tuning to meet the specifications required for PV, but initial results are very promising. For a first try R/T performances listed in Table 28 are good. Streaking and blue interference dots on the films may be reduced with a courser roller or by adjusting the drying time. Anti-reflective Si coated well and gave a uniform coating.



5.4.11 Roll-to-Roll Coating

Eikos performed coating trials via our pilot scale roll-to-roll coater. Eikos produced the multi-foot long 12-inch wide films by using a deposition, wash, binder coat process analogous to that described in Task 3 above. Eikos then evaluated CNT-binder Rs uniformity by *first* assessing Rs at one-foot increments along the length of the film at the films center, and *secondly* assessing an Rs matrix of seven across the width of the film by three (over a 12” length) taken incrementally along the length of the film.

The coated film samples average Rs and coefficient of variation over the length of the film is derived from the *first* set of data.. The coefficient of variation reflects the standard deviation divided by the average resistance of the sample group multiplied by 100. The project target was 20% with a goal of less than 10 %. Noted in Table 29, the coefficient of variation at the center of each sample was below 20 % and achieved less than 10 % for two of the four samples.

Table 29: Length Data

| Sample ID | Average Rs Length | STD Length | % CV Length |
|-----------|-------------------|------------|-------------|
| 114-14-1 | 1453 | 173 | 12 |
| 114-14-2 | 873 | 72 | 8 |
| 114-14-3 | 485 | 66 | 14 |
| 114-14-4 | 1372 | 19 | 6 |

The *second* set of data was used to derive the uniformity of the coating across the width of the sample. Eikos took Rs data incrementally along the samples length at 1, 8, 12, and 20-foot increments. For each area three sets were measured down the film with 7 measurements across the film at the 38, 76, 114, 153, 191, 229 and 267 mm areas. The average resistance, standard deviation, and coefficient of variation were derived for each matrix increment (i.e. 1, 8, 12, etc...) and a total for all data points was derived as well. . This sample group used 21 different points for each testing area with a total of 84 to 105 total points used for the overall measurements. For the discrete matrix areas down the length of the film, the coefficient of variation was under 20 % except for one area on sample 3, which was at a Coefficient of variation (CV) of 27 %. Notably, some of the discrete areas presented a CV of less than 10%.

Table 30 identifies the overall average Rs, Rs standard deviation, and CV using all of the data points for the matrix pattern measurements. The overall coefficient of variation for matrix was higher than that of the discrete areas. Additionally the average values are consistently higher for the grid testing, indicating the resistance increases when moving out from the center of the sample.

Table 30: Overall Grid Data

| Sample ID | Average Rs Matrix | STD Matrix | % CV Grid |
|-----------|-------------------|------------|-----------|
| 114-14-1 | 1788 | 397 | 22 |
| 114-14-2 | 1036 | 212 | 20 |
| 114-14-3 | 505 | 56 | 11 |
| 114-14-4 | 1598 | 305 | 19 |

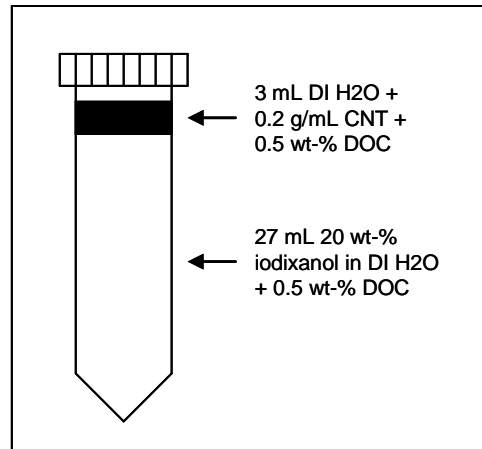
Some of the variation could be attributed to visually evident CNT streaking on the samples, thought to be caused by particle accumulation of the coaters Mayer rod.

5.4.12 Particle Reduction by Fractionalization

The investigation of particle reduction and length fractionalization using a density gradient in a high-density carrier solution with a surfactant is only in the preliminary stages. Centrifugation speed and time can be adjusted, CNT loading can be changed, and carrier solution density can be modified. In addition, several other variations of this experiment could be tried. If conditions are properly optimized, it should be possible to achieve bidirectional material transport by injecting the CNT layer in the middle of a series of stratified layers of different-density solutions. In addition, it is possible to apply this principle to as-produced CNT material instead of Eikos' processed CNT pastes, which may result in a higher yield of length-separated tubes and a more cost-effective process.

Eikos conducted its particle reduction and length fractionalization experiment by processing a nanotube ink in a high-density carrier solution with a surfactant additive using ultracentrifugation. The theory behind this experiment is that density of carbon nanotubes vary from graphitic/other particles and among the nanotubes themselves based on length, and that this results in the transport through a high-density solution to occur at different speeds for the different types of material present in Eikos' nanotube inks. If successful and optimized properly, this could enable ultracentrifugation to create a density gradient of material and effectively separate tubes by length. The desired lengths of tubes could then be collected and used to increase the RT performance and reduce the particles of Eikos' transparent conductive coatings.

The setup of this experiment required careful layering of two different solutions in 35 mL high-speed centrifuge tubes. First, a 20 wt-% iodixanol solution ($\rho=1.11$) with a 0.5 wt-% sodium deoxycholate additive was prepared, and 27 mL of this solution was pipetted into each of several centrifuge tubes. Next, a solution with a 0.2 g/mL loading of CNT paste in DI H₂O ($\rho=1.00$) with a 0.5 wt-% additive of sodium deoxycholate was prepared, and 3 mL of this solution was carefully layered on top of the higher-density iodixanol solution in each centrifuge tube. A representation of this experimental setup is shown in Figure 55.



3 mL DI H₂O +
0.2 g/mL CNT +
0.5 wt-% DOC

27 mL 20 wt-%
iodixanol in DI H₂O
+ 0.5 wt-% DOC

Figure 55 - Iodixanol/CNT Experimental Setup

The centrifuge tubes containing these layered solutions were subjected to 4 hours of 27,500 RCF centrifugation using a Sorvall RC6 centrifuge with an HB-6 swing-bucket rotor. After centrifugation, it was clear to the naked eye that downward CNT transport through the higher-density iodixanol solution had occurred. A clearly-visible color gradient in the resulting solution would have been indicative of different rates of transport for tubes and particles of different lengths, but the resulting solution appeared to be relatively uniform in color. Photos of two centrifuges tubes before and after centrifugation are shown in Figure 56.

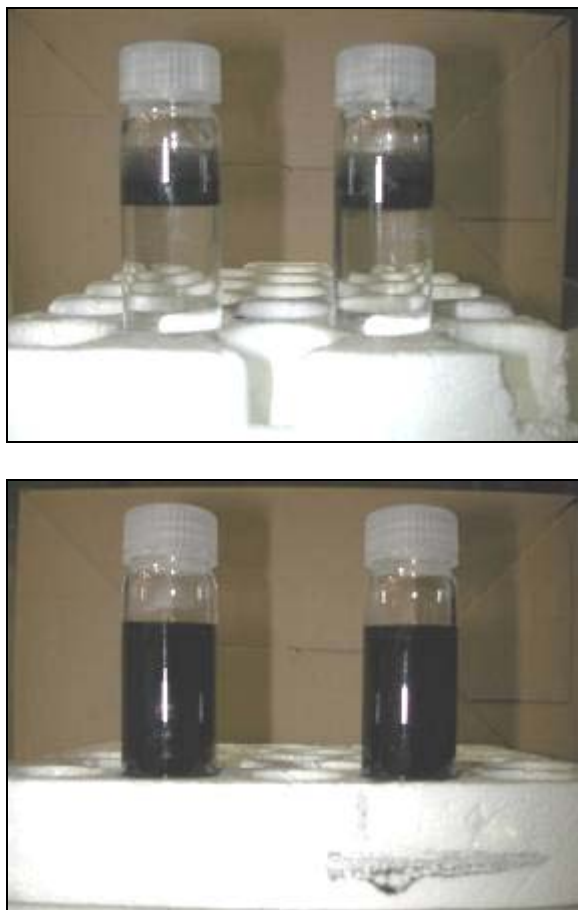


Figure 56 - Centrifuge Tubes Before (Top) and After (Bottom) Centrifugation

Four sections of solution from each centrifuge tube were collected and stored for analysis. The top 3 mL, or the injection layer, as well as three 9-mL sections from the “top,” “middle,” and “bottom” of the remaining solution were carefully pipetted off. Carbon sediment present at the bottom of the tubes was left undisturbed and not analyzed.

Samples were prepared for Raman spectroscopy analysis by drying a small drop of solution from each section on pieces of aluminum flashing. Scans of each sample were completed using both a 633nm and 785nm laser, and the results were analyzed for D band, G band, G' band, and RBM band location and intensity. To ascertain the effectiveness of this procedure for nanotube length fractionalization, the ratio of each peak compared to the D band were calculated for each section. A comparison of these values from the 633nm laser scans is shown in Table 31, and from the 785nm laser scans in Table 32.

Table 31- Raman Peak Ratios using 633nm Laser

| 633nm Laser (Metallic) | | | |
|-----------------------------------|------------------|-------------------|--------------------|
| Section | G/D Ratio | G'/D Ratio | RBM/D Ratio |
| <i>Injection Layer (Top 3 mL)</i> | 4.80 | 0.88 | 1.58 |
| <i>Section 1 (Top 9 mL)</i> | 3.33 | 0.58 | 1.44 |
| <i>Section 2 (Middle 9 mL)</i> | 3.46 | 0.53 | 1.71 |
| <i>Section 3 (Bottom 9 mL)</i> | 13.01 | 1.82 | 4.62 |

Table 32 - Raman Peak Ratios using 785nm Laser

| 785nm Laser (Semiconducting) | | | |
|-------------------------------------|------------------|-------------------|--------------------|
| Section | G/D Ratio | G'/D Ratio | RBM/D Ratio |
| <i>Injection Layer (Top 3 mL)</i> | 12.32 | 1.65 | 1.12 |
| <i>Section 1 (Top 9 mL)</i> | 9.86 | 1.01 | 8.05 |
| <i>Section 2 (Middle 9 mL)</i> | 15.55 | 2.40 | 4.20 |
| <i>Section 3 (Bottom 9 mL)</i> | 10.46 | 1.46 | 4.54 |

Overall, there was not a clearly-observable trend in the data. However, the 633nm scan of the “section 3” solution collected from the bottom 9 mL of the centrifuge tubes did produce some interesting and promising results. Despite relatively constant ratios in the sections above, the ratios for section 3 were all substantially higher than any of the other sections of solution tested. The reason for this is the intensity of the D band observed in the scan of section 3 is significantly smaller than any other section, and this may be an indication that the tubes present in section 3 contain fewer defects and/or are longer in length than the tubes present in the other sections.

5.4.3 Particle Reduction Via High-Speed Centrifugation

Eikos conducted evaluation of the effectiveness of high speed centrifugation (HSC) for reducing particles present in its CNT inks. The force applied by HSC causes dense graphitic particles to settle to the bottom of the ink, allowing “cleaner” ink to be collected at the top. Two materials, Nanoledge AIF I and Carbon Solutions Ex. 7, were chosen for testing. Each material was prepared and sonicated in accordance with standard Eikos operating procedures, transferred into 40 mL centrifuge tubes, and then centrifuged at 26,000 RCF for 2 hours. A Thermo Electron Corp. Sorvall RC6 plus Superspeed Centrifuge with an F13-12x50cy rotor was used. When centrifugation was complete, the top 5 mL of ink in each tube was carefully pipetted out, sonicated, and sprayed per standard Eikos procedure. The results of this experiment, along with the comparison particle counts of the same materials without HSC, are shown in Table 33.

Table 33: Effect of High Speed Centrifugation on Particle Count

| MATERIAL | PARTICLE COUNT | TOTAL AREA PARTICLES (um ²) | AVERAGE PARTICLE SIZE (um ²) | PARTICLE AREA FRACTION (%) | TOTAL AREA (um ²) | CALC #/ MM ² |
|---|----------------|---|--|----------------------------|-------------------------------|-------------------------|
| <u>Nanoledge</u> <u>#397 AIF</u> | 132 | 53.71 | 0.41 | 0.73% | 7313 | 18049 |
| (94.7 %T & 655 Ω/□) | 88 | 35.46 | 0.40 | 0.49% | 7190 | 12239 |
| (=93.5 %T @ 500 Ω/□) | 74 | 39.45 | 0.53 | 0.55% | 7227 | 10239 |
| | 81 | 23.83 | 0.29 | 0.32% | 7368 | 10993 |
| | 85 | 29.60 | 0.35 | 0.41% | 7285 | 11668 |
| REF#: 97-82-1 | 92 | 36.4 | 0.40 | 0.50% | 7277 | 12638 |
| <u>Nanoledge</u> <u>#397 AIF: 2h</u> <u>HSC</u> | 51 | 11.59 | 0.23 | 0.16% | 7353 | 6936 |
| (95.1 %T & 725 Ω/□) | 19 | 3.75 | 0.20 | 0.05% | 7238 | 2625 |
| (=93.5 %T @ 500 Ω/□) | 47 | 11.48 | 0.24 | 0.16% | 7268 | 6467 |
| | 36 | 6.80 | 0.19 | 0.09% | 7271 | 4951 |
| | 33 | 9.96 | 0.30 | 0.14% | 7193 | 4588 |
| REF#: 97-86-1 | 37 | 8.7 | 0.23 | 0.12% | 7265 | 5113 |
| <u>Carbon Soln.</u> <u>#420 Ex.7</u> | 35 | 9.75 | 0.28 | 0.14% | 7151 | 4895 |
| (94.8 %T & 1320 Ω/□) | 8 | 1.69 | 0.21 | 0.02% | 7332 | 1091 |
| (=89.1 %T @ 500 Ω/□) | 12 | 4.06 | 0.34 | 0.06% | 7299 | 1644 |
| | 34 | 7.43 | 0.22 | 0.10% | 7317 | 4647 |
| | 12 | 2.33 | 0.19 | 0.03% | 7343 | 1634 |
| REF#: 97-82-3 | 20 | 5.1 | 0.25 | 0.07% | 7288 | 2782 |
| <u>Carbon Soln.</u> <u>#420 Ex.7: 2h</u> <u>HSC</u> | 44 | 10.87 | 0.25 | 0.15% | 7376 | 5965 |
| (94.9 %T & 1790 Ω/□) | 36 | 7.05 | 0.20 | 0.09% | 7518 | 4788 |
| (=86.3 %T @ 500 Ω/□) | 34 | 8.18 | 0.24 | 0.11% | 7430 | 4575 |
| | 32 | 7.71 | 0.24 | 0.11% | 7321 | 4371 |
| | 20 | 4.41 | 0.22 | 0.06% | 7477 | 2675 |
| REF#: 97-86-2 | 33 | 7.6 | 0.23 | 0.10% | 7425 | 4475 |

HSC had a significant impact on the Nanoledge material, resulting in a 62% reduction from 92 particles per 7250 μm² to 37 particles per 7250 μm². The average size of particles also dropped dramatically, from 0.40 μm² to 0.23 μm².

In addition, the area fraction of coating covered by particles was lowered from 0.50% to 0.12%. The normalized RT performance of the material was unchanged. This data suggests the HSC experiment was effective at reducing particles present in Nanoledge ink, and was particularly effective at removing the largest particles from the material.

The experiment did not have a positive impact on the Carbon Solutions material. While particle size dropped slightly from 0.25 μm² to 0.23 μm², particle count rose from 20 to 33, and area fraction increased from 0.07% to 0.10%. Due to the variability present in



each sample, it is likely that the HSC did not actually increase particle count, but simply did not do anything to reduce it.

The HSC experiment shows promise, but it is a delicate procedure. Extreme care must be taken while handling centrifuge tubes to ensure settled particles are not re-introduced to the uppermost ink, and pipetting must be done at the center of the tube to avoid collecting particles that cling to the sides of the tube. The use of a swinging bucket rotor is recommended for future experiments to eliminate this possible source of error. In addition, longer centrifugation times may further enhance particle reduction.

5.4.4 Particle Reduction via Surfactant Centrifugation

Eikos investigated the use of surfactant, specifically sodium deoxycholate monohydrate (DOC), in conjunction with high speed centrifugation for the purpose of particle reduction. The use of surfactant should aid the transport of dense graphitic particles to the bottom of the tubes of ink during centrifugation, resulting in a greater reduction of particles in the uppermost ink than would be possible with HSC alone.

For this experiment, Eikos produced 90 mL of ink with a Nanoledge Ex. 7 CNT paste concentration of 1.4 wt-% and with a 0.25 wt-% additive of DOC. This ink was shear mixed at 8000 rpm for 3 minutes, and then sonicated for 180 seconds at 60% amplitude. An additional 150 mL of 0.25 wt-% DOC in filtered DI water was also prepared, and 25 mL was pipetted into six 40 mL centrifuge tubes. On top of this solution, 15 mL of the CNT/DOC ink was carefully pipetted in each tube. The six tubes were then loaded into a Thermo Electron Corp. Sorvall RC6 Plus Superspeed Centrifuge with an HB6 swing bucket rotor and centrifuged for 4 hours at 27,500 RCF.

Upon completion of centrifugation, each tube of ink was carefully removed and five 8 mL “sections” of each were pipetted off – the top 8 mL from each tube is referred to as “section 1,” the next 8 mL are referred to as “section 2,” and so on. Sections 1 and 3 of ink recovered from the centrifuge were then investigated for particle analysis.

Each section (48 mL) of ink investigated was flocculated with 10 drops of 37% reagent HCl and magnetically stirred for 3 minutes. Each section was then diluted to 250 mL with neat, filtered methanol and shear mixed for 5 minutes at 8000 RPM. These solutions were then filtered through 0.8 μm membrane filters with an aspirator and an overpressure of approximately 40 psi. Each filter was then rinsed with 300 addition mL of neat, filtered methanol, and then with 1000 mL of filtered DI water. Each filter was then scraped to recover the CNT material present. These materials were diluted to 10 mL with filtered 3:1 IPA:DI water, sonicated 40 seconds at 70% amplitude, and centrifuged 20 minutes at 16,000 RCF.

Finally, the top 6 mL of each of these prepared inks was recovered, sonicated for 10 seconds at 40%, and sprayed on clean borosilicate glass slides to between 94.0 – 95.0

%T. The resulting particles analyses of sections 1 and 3 are provided in Table 10, along with control samples of Nanoledge AIF and Ex. 7 materials.

Table 34: Effect of DOC Treatment on Particle Count

| MATERIAL | PARTICLE COUNT | TOTAL AREA OF PARTICLES (um ²) | AVERAGE PARTICLE SIZE (um ²) | PARTICLES AREA FRACTION (%) | TOTAL AREA MEASURED (um ²) |
|---|----------------|--|--|-----------------------------|--|
| AIF - STANDARD (94.7 %T & 655 Ω/□) (= 93.5 %T @ 500 Ω/□) REF#: 97-82-1 | 132 | 53.71 | 0.41 | 0.73% | 7313 |
| | 88 | 35.46 | 0.40 | 0.49% | 7190 |
| | 74 | 39.45 | 0.53 | 0.55% | 7227 |
| | 81 | 23.83 | 0.29 | 0.32% | 7368 |
| | 85 | 29.60 | 0.35 | 0.41% | 7285 |
| | 92 | 36.4 | 0.40 | 0.50% | 7277 |
| Ex. 7 - STANDARD (94.9 %T & 970 Ω/□) (= 91.5 %T @ 500 Ω/□) REF#: 97-99-1 | 29 | 4.87 | 0.17 | 0.07% | 7462 |
| | 35 | 8.37 | 0.24 | 0.11% | 7423 |
| | 44 | 10.10 | 0.23 | 0.14% | 7336 |
| | 43 | 6.66 | 0.16 | 0.09% | 7474 |
| | 16 | 6.89 | 0.43 | 0.09% | 7571 |
| | 33 | 7.4 | 0.24 | 0.10% | 7453 |
| Ex. 7 - DOC "Section 1" (Sprayed to 94.4 %T & 1015 Ω/□) (= 90.3 %T @ 500 Ω/□) REF#: 97-98-1 | 12 | 5.26 | 0.44 | 0.07% | 7492 |
| | 9 | 2.76 | 0.31 | 0.04% | 7445 |
| | 7 | 1.67 | 0.24 | 0.02% | 7523 |
| | 28 | 6.87 | 0.25 | 0.09% | 7445 |
| | 13 | 4.28 | 0.33 | 0.06% | 7456 |
| | 14 | 4.2 | 0.31 | 0.06% | 7472 |
| Ex. 7 - DOC "Section 3" (Sprayed to 94.8 %T & 970 Ω/□) (= 91.3 %T @ 500 Ω/□) REF#: 97-98-3 | 12 | 3.61 | 0.30 | 0.05% | 7449 |
| | 9 | 1.72 | 0.19 | 0.02% | 7462 |
| | 7 | 3.12 | 0.45 | 0.04% | 7486 |
| | 8 | 1.70 | 0.21 | 0.02% | 7485 |
| | 16 | 4.28 | 0.27 | 0.06% | 7357 |
| | 10 | 2.9 | 0.28 | 0.04% | 7448 |

The DOC/HSC treatment resulted in a large reduction of the particles present in the Nanoledge Ex. 7 ink. Although Ex.7 inks have fewer particles than AIF inks to begin with, sections 1 and 3 of the DOC experimental ink contained 58-70% fewer particles than the Ex. 7 control sample. In particular, section 3 (the middle 1/5th of ink from the centrifuge tubes) possesses some extremely favorable properties. It's normalized RT performance of 91.3 %T at 500 Ω/□ is only 0.2 %T less than the control spray of 91.5 %T at 500 Ω/□, and contains only 10 particles per approximately 7250 μm². Its area fraction of particles of 0.04% is also the lowest of any slide tested, and its average particle size of 0.28 μm² is comparable to the control slide.



5.4.5 Particle Analysis Method

Eikos developed and implemented a reliable and reproducible particle analysis procedure. The method utilizes a Nikon Eclipse ME600 microscope to obtain optical images of carbon nanotube coatings at 1000x magnification, and then uses Photoshop CS3 and ImageJ software for data analysis. The particle counts obtained with this procedure have been verified by AFM.

The coatings analyzed for particles are deposited to 94.0 – 95.0 %T on 1” x 3” borosilicate glass slides using Eikos’ spray coating technique. The coating surface is cleaned with compressed air prior to image acquisition to remove any loose airborne particulates that have accumulated. Coatings are visually focused at 1000x under the optical microscope, and then a fine adjustment of -7 is applied to account for the difference in camera optics. Images are illuminated with reflectance light at 70% intensity. No polarizing filters are used, the microscope A stop aperture is completely closed, and the F stop aperture is closed to a known diameter of 100 μm . Five images of each coated surface are taken with a 3.34 MP Nikon Coolpix 990 camera, one near each corner of the coated surface and one near the middle.

Images are then imported into Photoshop CS3 software. Each image is made binary using the stamp function (using a contrast setting of 40 and a smoothing setting of 5). Next, each image is opened using ImageJ software for actual particle analysis. The known aperture diameter is entered into the program, and then a binary threshold of 128 is applied. Using the polygonal area tool, the entire hexagonal-shaped aperture is selected for analysis. A slight edge around the aperture is left unselected to avoid measuring any edge artifacts present. The selected area is then analyzed using the “Analyze Particles” tool. The particle count, average particle size, total area measured, area of particles, and area fraction of particles of each picture is then obtained and recorded.

In order to validate this particle analysis technique, a small cross was drawn on the surface of a sample slide and the exact same area of its coating was measured using both the optical microscope and a Park Systems XE-70 AFM. The area of the coating analyzed was 50 μm x 50 μm . The AFM image was opened with XEI software included with the AFM and analyzed for grains with a minimum height threshold of 15 nm. The data obtained from this AFM scan, as well as the corresponding results obtained from the optical particle analysis procedure, are shown in Table 35.

Table 35: AFM Grain Count and Optical Particle Analysis Comparison

| Analytical Method | Grain Count | Total Area of Particles (um ²) | Average Area of Particles (um ²) | Area Fraction Covered by Particles |
|---|-------------|--|--|------------------------------------|
| AFM (15 nm Threshold) | 32 | 11.92 | 0.351 | 0.48% |
| Optical Microscope (1000X) | 36 | 5.796 | 0.161 | 0.23% |

The AFM and optical microscope particle analysis procedures arrived at nearly identical counts of 32 and 36 particles, respectively, when measuring the exact same area. The AFM method gives much higher values for particle areas, but this is most likely caused by an overestimation that results when the AFM tip takes time to return to the surface of the coating after traveling over a particle of large size. If spherical particles are assumed and particle volume is used for calculation, then the smallest particles detected by the AFM are approximately 175 nm in diameter. Since the AFM and optical particle counts closely agree, and this value is close to the detection limit of the microscope at 1000x, it is safe to assume that the optical particle analysis method is detecting particles that are 175-200 nm in diameter and larger. It is also reassuring to note that when made binary, the AFM and optical images appeared very similar to the naked eye. These pictures are compared in Figure 57: AFM and Optical Image Comparison.

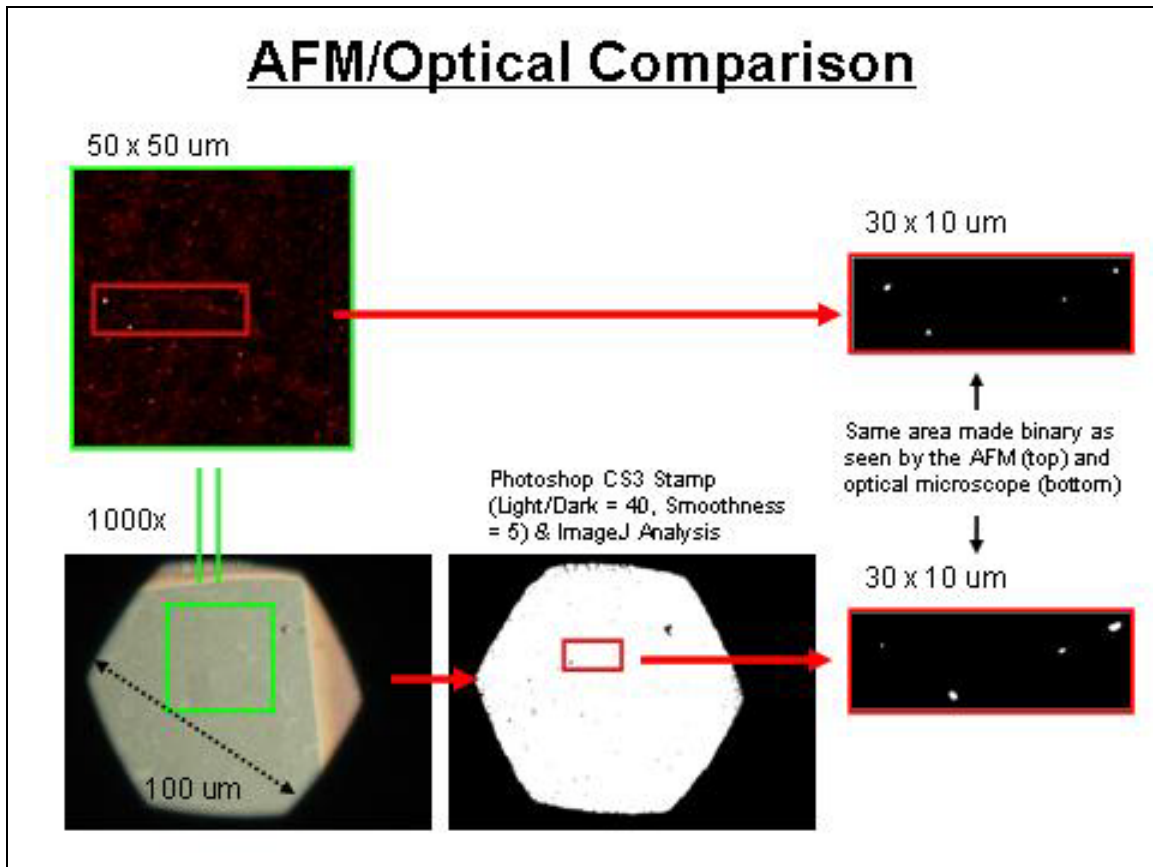


Figure 57: AFM and Optical Image Comparison

The optical particle analysis procedure is able to detect particles approximately 175-200 nm in diameter and up and is faster than running an AFM scan. The optical method also measures several different areas of a coating, as well as a much greater area of the surface in total, which improves the reliability of the results. Because of these advantages and because the method has been verified by AFM, the optical particle analysis procedure is used by Eikos to evaluate the effectiveness of particle reduction procedures.

5.5 Task 5: Binder Process Development/Formulation

To be useful in PV applications a TCC must meet the following requirements:

- 1) Optical transmission (%T) must be at least 90% in the middle of the visible region of light at a wavelength of 550nm.
- 2) Optical haze must be lower than 1%T.
- 3) Electrical resistivity (R) must be no higher than 500 Ohm/□.
- 4) The coating must pass through abrasion and adhesion testing according to MIL-C-675C standard.
- 5) The coating must stay within 30% of the original R/T performance after heat testing of 85°C for 500hr.
- 6) The coating must stay within 30% of the original R/T performance after humidity testing at 85°C and 85% humidity.

No single binder material combined with CNT was found capable of providing all of the technical criteria above. Building on prior work with sol-gel binder precursors Eikos has developed a method to deposit a triple coating of three separate binders that, in tandem, will meet PV specifications. Application of this triple binder system follows a specific process. Binder 1 was deposited via dip coating and cured at 130°C for 2 hours, binder 2 was then dip coated and cured at 130°C for 2 hours then washed with ethanol to remove surfactant. The third and final binder was then dip coated and cured at 140°C for 30min.

5.5.1 Binder Formulation and Deposition

Because nanotube coatings are wet-coated from dispersions at low temperature, it is most convenient to deposit binders using similar techniques. Fortunately, metal oxide coatings can be fabricated easily from solutions of metal alkoxides. This class of compounds has been used since the 1960s to make coatings, fibers, and monoliths.¹² Metal alkoxides have been especially successful as a liquid-based precursor for metal oxides because of their high purity, long shelf life, wide range of properties, and clean reaction products. Sol-gel chemistry has been successful in commercial applications, particularly for low emissivity window glazing¹³ and high purity optical fibers.¹⁴

Sol-gel chemistry¹⁵ is broadly defined as the preparation of ceramic materials by preparation of a *sol*, *gelation* of the sol, and removal of the solvent. A sol, distinguished from a solution, is defined as a suspension of fine particles of colloidal dimensions (1-1,000 nm) in a liquid. Metal alkoxides, $M(OR)_n$, where $R = Me, Et, Bu^t$, etc., are the most common precursors in sol-gel chemistry. Usually, one or more alkoxides in an organic solvent is used as a starting solution. Metal alkoxides react readily with water, leading to hydrolysis, condensation, and/or polymerization of the metal alkoxides in the form of linear or clustered M-O-M networks (i.e. a *sol*). In turn, alcohol and water are liberated. The condensation and polymerization process is dynamic, and eventually all alkoxides cross-link, leading to formation of a *gel*. The rate of the process and type of polymer can



be controlled in some cases (i.e. for silicon alkoxides) by the addition of a catalyst. In our case, the sol is used to create a coating because it is sufficiently fluid to create sub-100 nm coatings.

Once the solvent dries from the coating, a porous hydrated oxide film is formed. Mild heating can drive off some residual solvent and moderately densify the coating, but it retains significant organic and OH groups. Heating to several hundred degrees centigrade removes these residual groups and further densifies the coating. Heating also can crystallize the coating. Through the alkoxide pathway to metal oxides, there are a wide range of controllable variables that yield different coating properties. For example, the choice of alkoxide, catalyst, and even solvent can affect the resulting porosity and morphology of the coating. Additionally, the temperature, time, and environment of coating curing can alter density and crystalline structure. Functional properties, such as adhesion, hydrophobicity, and refractive index are also tunable using these basic variables.

Sol-gel synthesized coatings present many advantages over vacuum deposition in terms of processing. Because the precursors of the coatings are soluble in alcohols and other common solvents, the coatings can be formed using standard solution processing techniques. Without the need to control the atmosphere, arbitrarily large and curved substrates can be coated. At Eikos, Eikos are capable of dip, spray, draw-down, and spin coating of sol-gel precursors. In addition, Eikos have obtained an inkjet printer capable of directly patterned sol-gel coatings.

Coatings made from SiO_2 , Al_2O_3 , and VO_2 are useful for several applications. Silica is used as an anti-reflective or abrasion resistant coating. Alumina finds utility as a high temperature catalyst support, as well as a refractory protective coating. Vanadium dioxide coatings are touted for use in high speed optical switches and for active thermal control glazing. These coatings typically have one function, and the addition of other properties, like conductivity, is not possible without significantly changing the material composition. By making a composite with nanotubes, these coatings can maintain their original function while adding the function of the nanotubes.

SiO_2 coatings are useful in many applications, including abrasion resistant and anti-reflective coatings.¹⁶ Because of the sol-gel method allows us to tune the porosity of the coating, the effective refractive index of the air-silica composite can be decreased to the optimum region of 1.20-1.25 on typical optical glass.¹⁷ Nostell *et al.* demonstrated that a solution deposited silica AR coating on both sides of a piece of glass could increase transmission to as high as 99.5%, versus 90% for uncoated glass at 550 nm (Figure 58).¹⁶

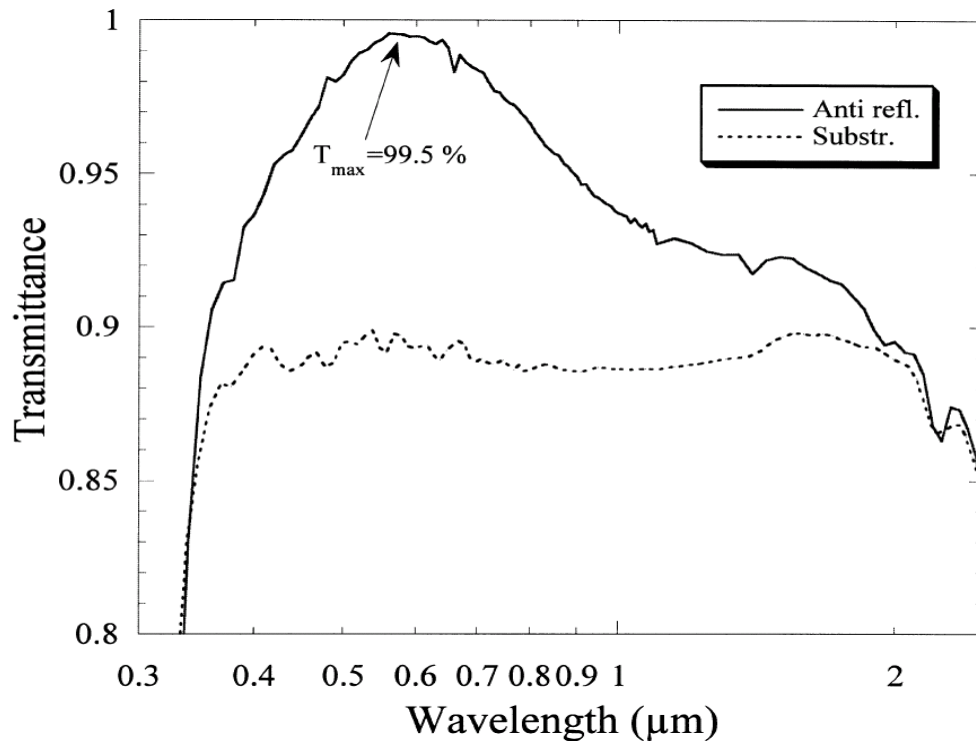


Figure 58: Transmission versus wavelength of glass and silica AR coating on glass. The glass was coated on both sides, reducing first and second surface reflectance.¹⁶

Eikos utilized the sol-gel technique to deposit a wide range of binders at atmospheric conditions to tune optical transparency and reflectivity of our coatings (Table 37). The focus was to produce transparent, conductive and robust coatings without the need for high temperature curing and expensive equipment such as a vacuum chamber. Highly porous silicon dioxide can have a refractive index as low as 1.2, while a dense titanium dioxide layer can have a refractive index of 2.46. Additionally, our porous binder allows the formation high-strength laminates because the adjacent polycarbonate layers can fuse *through the CNT and binder*.

Table 36: Materials Eikos can formulate and deposit via sol-gel method to form AR binder.

| Coating | Formula | Crystal Refractive Index | Amorphous Ref. Index |
|-----------------|--------------------------------|--------------------------|----------------------|
| Silicon dioxide | SiO ₂ | 1.46 | 1.20-1.46 |
| Aluminum oxide | Al ₂ O ₃ | 1.65 | 1.30-1.65 |
| Indium oxide | In ₂ O ₃ | 1.95 | 1.49-1.95 |
| Zinc oxide | ZnO | 1.97 | 1.49-1.97 |
| Cobalt oxide | COO | 2.00 | 1.50-2.00 |
| Vanadium oxide | V ₂ O ₃ | 2.00 | 1.50-2.00 |

| | | | |
|-------------------|--------------------------------|------|-----------|
| Tantalum oxide | Ta ₂ O ₅ | 2.03 | 1.52-2.03 |
| Zirconium dioxide | ZrO ₂ | 2.15 | 1.60-2.15 |
| Niobium oxide | Nb ₂ O ₅ | 2.20 | 1.65-2.20 |
| Chromium oxide | Cr ₂ O ₃ | 2.38 | 1.70-2.38 |
| Titanium dioxide | TiO ₂ | 2.46 | 1.74-2.46 |

Eikos formulated sol-gel liquids for titanium dioxide, niobium oxide, zinc oxide, silicon dioxide, aluminum oxide, zirconium oxide, and vanadium oxide. Eikos tested these formulations for wettability on glass, PET and polycarbonate and reformulate as necessary. This test were conducted by dip coating substrate into sol-gel solutions and pulling the substrate out at a controlled speed to give a uniform coating (Figure 59).

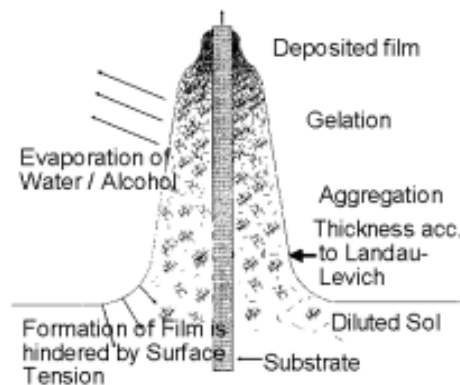


Figure 59: Schematic of dip coating for a sol-gel coating.

It is difficult to achieve uniform >100nm thick coatings. Once Eikos determine wettability of a sol on substrate and CNT, Eikos then developed methods to achieve reliable coating of even and thin films below 100nm. To accomplish this Eikos investigated use of sol formulations at variable concentrations. In addition dip coating speeds were adjusted to allow for a sol-gel bath to determine time needed for mass equilibrium to be met and the CNT and substrate surface to be evenly coated.

Eikos previously reported on the development of a CNT/triple binder coating capable of weathering environmental conditions. A new AR binder, called binder 3, was formulated to meet the PV criteria while reducing processing steps and cost. The first step after preparation of binder 3 was to determine optimal thickness of the binder layer in order to obtain the highest %T at 550nm on bare PET-453 substrate.

Binder 3 was then dip coated on PET substrate, previously spray coated with CNT to 600Ω/□. Interaction between binder 3 and CNT is good as demonstrated by an improvement in %T with its use. The average starting transparency of CNT coated PET samples was 82.8%T (+/- 0.5%) compared to 90.9%T (+/- 0.4%) after the addition of binder 3. Since the transparency specification for PV applications is 90%T this result allows binder 3 to not only replace the AR coating used in the triple binder system, but



reduces the processing time significantly. Good interaction between binder 3 and CNT also eliminates the need for a buffer layer, reducing the triple binder coating by (at least) one layer.

5.5.2 Binder Work Function and Roughness

Eikos continued working with NREL in fabrication and testing of OPV cells using CNT TCC as an electrode. For this effort a total of 34 glass slides were pattern coated with CNT according to NREL specifications. Samples were sent to NREL in two separate batches to be integrated into OPV cells and tested. At the request of NREL these CNT patterned samples were top coated with one of five antireflective (AR) binders. These binders are; A', Al, ACS, BCS, and Binder 3. By top coating the CNT PV electrode NREL and Eikos seek to gain three possible advantages:

1. To provide increased light transparency to the active layer
2. To 'level out' roughness from the CNT layer and in so doing remove the need for a PEDOT/PSS layer in the cell.
3. To take advantage of the work function of the binder material to facilitate hole/e⁻ movement in the cell.

The first batch of samples sent to NREL was comprised of 1" x 3" glass slides coated with each candidate binder, without an underlying CNT layer. Each sample was coated to match the binder thickness found previously to provide the best AR properties. Upon receipt of these samples NREL conducted tests to determine the Work-function of each binder coating, without the interference of a bottom CNT layer. Figure 60 indicates these binders have a good Work-function distribution, from 4.2eV for A1 to 4.9eV for Binder 3. This distribution should help Eikos and NREL tune the CNT/binder coating to determine effects on PV cell efficiencies.

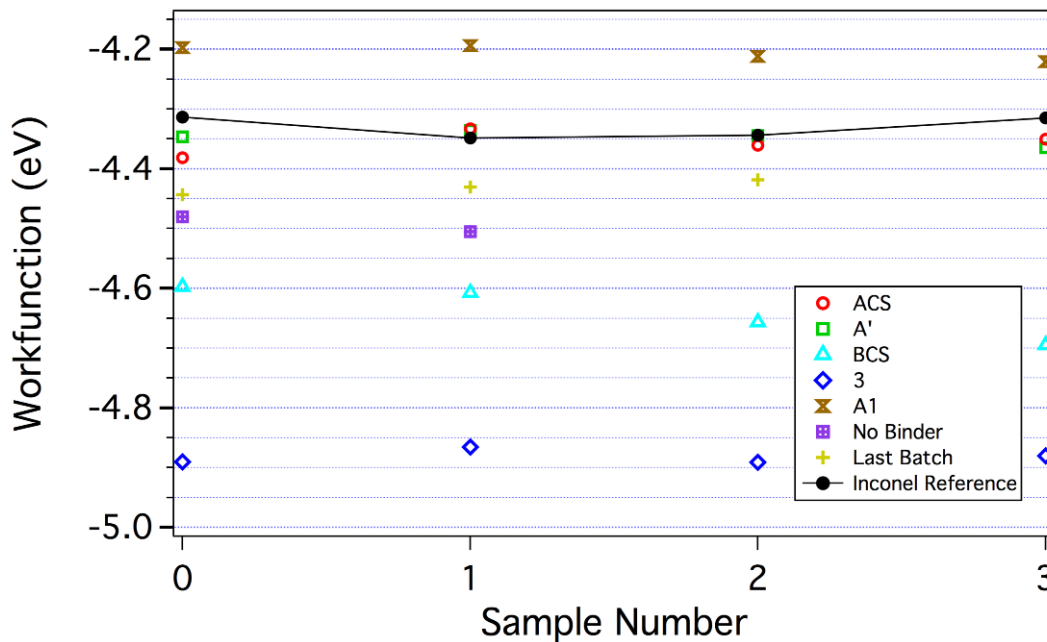


Figure 60: Work function for Eikos' AR binders.

For the second batch of samples Eikos integrated CNT with a top coat of each binder. Samples were coated by Eikos with CNT using our automated spray coater to $60 \Omega/\square$ (within 10% variability) using a pattern provided by NREL. Binder was deposited at two separate thicknesses. Each thickness was selected to provide optimum AR properties or match the thickness of the CNT electrode (50nm). The matrix of samples included thick and thin CNT coatings top coated with either a thick or thin coating of one of the five binders tested in this study. A total of 20 CNT-binder coated samples were tested along with two reference slides of thick or thin CNT coating without binder.

All coatings were deposited onto pre-cleaned 1" x 3" borosilicate glass slides. The cleaning procedure Eikos used was to 1) sonicate slides in a mild detergent solution for 20 minutes at 30°C, 2) sonicate slides in clean DI H₂O for 20 minutes at 30°C, 3) individually rinse each slide with high-pressure DI H₂O, 4) individually rinse each slide with filtered IPA, and 5) individually dry each tube with filtered, compressed air at 40 psi.

Unfortunately, none of these samples produced a working PV cell. Examination by optical profilometry indicates the surface roughness is too high for *all* samples (Table 37).

Table 37: Surface roughness for CNT/binder coatings

| Sample | Binder | Ra(nm) | Rq(nm) | Rz(nm) | Rt(nm) |
|------------|-----------|--------|--------|--------|--------|
| 103-131-1 | ACS | 5.3 | 6.64 | 49.21 | 61.28 |
| 103-131-2 | | 13.23 | 15.02 | 96.99 | 132.44 |
| 103-131-5 | | 9 | 10.93 | 74.48 | 81.42 |
| 103-131-6 | | 3.98 | 5.17 | 47.43 | 54.39 |
| 103-131-8 | A' | 3.73 | 4.51 | 35.58 | 56.94 |
| 103-131-9 | | 3.39 | 4.19 | 30.34 | 57.19 |
| 103-131-11 | | 3.02 | 4.12 | 30.41 | 42.54 |
| 103-131-12 | | 4.5 | 5.61 | 40.85 | 115.97 |
| 103-131-13 | BCS | 4.57 | 5.62 | 37.68 | 45.45 |
| 103-131-14 | | 4.24 | 6.11 | 86.4 | 101.76 |
| 103-131-17 | | 6.39 | 8.2 | 63.23 | 83.82 |
| 103-131-18 | | 5.7 | 7.46 | 63.62 | 74.06 |
| 103-131-19 | 3 | 10.99 | 13.97 | 114.81 | 275.81 |
| 103-131-21 | | 3.47 | 4.22 | 28.97 | 39.55 |
| 103-131-23 | | 3.99 | 5.13 | 69.5 | 94.55 |
| 103-131-24 | | 7.19 | 12.96 | 463.93 | 669.64 |
| 103-131-32 | A1 | 2.73 | 3.51 | 31.73 | 56.17 |
| 103-131-33 | | 4.69 | 5.68 | 30.29 | 33.49 |
| 103-131-35 | | 3.03 | 4.36 | 136.56 | 624.93 |
| 103-131-36 | | 4.08 | 5.17 | 49.61 | 87.01 |
| 103-131-37 | No Binder | 3.54 | 4.46 | 33.74 | 47.02 |
| 103-131-38 | | 3.16 | 3.99 | 28.88 | 34.19 |

Peaks of over 600nm were found for A1 and Binder 3 coated samples that can cause uneven facing with the PV active layer and result in shunting, which in turn, reduces the efficiency of the PV cell. In this case the cells did not work at all. Working PV cells were realized by the addition of a PEDOT/PSS over coat on the CNT/Binder layer. The PEDOT/PSS layer acts as a leveling agent, providing more even surface contact with the active layer. Samples over coated with PEDOT/PSS did produce working PV cells, but nothing that improves upon the 3.1% efficiency our samples.

While surface roughness is worse for binder coated samples the root cause seems to be from the underlying CNT coating (Figure 61). Several new methods and processing modifications are planned for smoothing the surface of these coatings after deposition, or to deposit an even coating directly on the end use substrate.

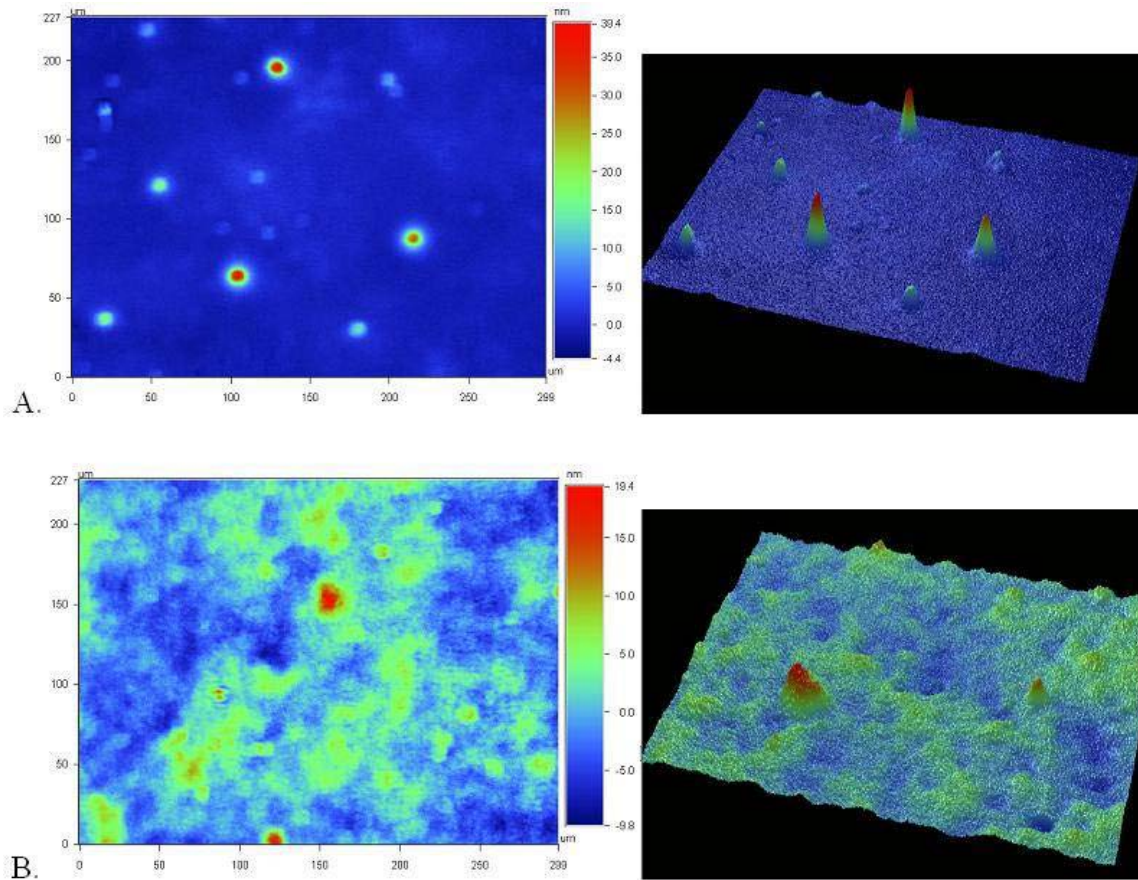


Figure 61: Optical profilometry image depicting surface roughness for A) A1 binder/CNT coating; and B) CNT coating without binder top coat

5.5.3 Binder as AR Coating

Eikos worked to optimize AR coatings for use as a top coat on conductive CNT networks. As reported Eikos has formulated a binder material, Eikos call Binder 3, which meets PV performance criteria while reducing processing steps and costs. Previous work involved formulating Binder 3 to meet RT performance requirements for PV applications and conducting durability tests of Binder 3 coatings on polymeric substrate including heat, heat/humidity, abrasion, and adhesion tests. During this period Eikos initiated further validation of Binder 3 including:

1. Determine the shelf life of current Binder 3 formulations and the affect on optical and electrical properties of the AR coating.
2. Study the influence of different substrate treatment on optical and electrical properties
3. Reformulate initial compositions of the solution for simplification of preparation.
4. Demonstrate the ability to provide AR properties on multiple substrates.



While this work is ongoing, Eikos has formulated this binder to be stable for 6 months. In addition, Eikos has successfully demonstrated deposition of this binder on multiple substrate materials. The increase of transparency as a result of deposition of Binder 3 on glass was 3.5% for a single coat. This is lower than previously reported for Binder 3 coated on polymeric substrates. The 5-15% resistivity decrease resulting from deposition of Binder 3 on to glass is in line with previously reported values for polymeric substrate.

5.5.4 Binder Replacement of PEDOT/PSS

NREL expressed great interest in using Eikos' sol-gel based oxide binders as a substitute for PEDOT:PSS within OPV cells. PEDOT:PSS has two functions within a OPV cell: 1) To facilitate charge transfer between the active layer and the conductive layer; and 2) to help cushion the surface roughness of the conductive layer from the active layer.

Previously Eikos investigated five of Eikos binder formulations, coated on glass, and were tested for work function by NREL. This work was pursued in more depth for the remainder of this program. Several action items will be pursued, these are:

- Re-evaluate two promising binders tested previously in this program.
- Formulate binders with favorable work functions capable of good charge transfer and in so doing replace PEDOT:PSS.
- Integrate new binders into OPV cells based on literature search and internal R&D.
- Evaluate work function of new sol-gel based binders alone and imbedded within a CNT network to determine if Eikos can tune the work function of the conductive layer.
- Fabricate and test OPV cells with newly developed binder-CNT conductive layers.

All action items were accomplished in a three part experimental procedure:

Step 1: Evaluate Binder Coating

Based on a literature search of oxides used to supplant PEDOT:PSS and our own internal knowledge of binder chemistry a total of four sol-gel based oxide binders were down selected for trials. Step 1 trials were done by coating pre-cleaned glass slides then cured. The effect of sol concentration, coating thickness and number of binder layers were evaluated. Characterization of each coating includes transparency, tint and haze, surface roughness, and work function evaluation.

Step 2: Evaluate Binder-CNT Coating

Binders tested to have good optical properties (low haze, no tint and high transparency) during Step 1 were evaluated in Step 2. Glass slides will be spray coated to 50 Ohm/sq., scraped to remove asperities, dipped with candidate binder coatings down selected from Step 1, then cured. Characterization of Step 2 samples included resistivity, transparency, surface roughness, and work function evaluation.

Step 3: Integrate New Binders in OPV Cells

Binder coatings down selected in Steps 1-2 was then integrated into OPV cells for testing and efficiency evaluation. Glass slides were spray coated with CNT to 50 Ohm/sq. using the “Racetrack” pattern used by NREL (Figure 62). Samples were then be dip coated with candidate binders, cured, and then sent to NREL for integration into OPV cells. NREL provided performance characterization of all cells in the form of current vs. voltage curves and power conversion efficiencies.

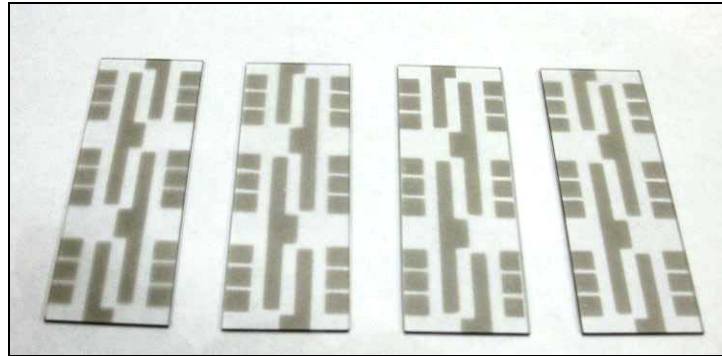


Figure 62: Glass Slides ‘Racetrack’ patterned with CNT to 50 Ohm/sq.

Task 6: Durability Testing

The current optimal formulation for Eikos’ triple binder/CNT coating meets all but one PV specifications as follows:

- 1) Optical transmission is 87%T at 550nm, showing a max transparency of 92.5% at 830nm.
- 2) Optical haze is within experimental error (0.5%T), as caused by coating thickness variations.
- 3) Electrical resistivity is maintained ~500 Ohm/ (usually below 600 Ohm/□, depending on starting resistivity).
- 4) RT performance is unchanged as a result of adhesion and abrasion testing.
- 5) All samples easily pass heat testing.
- 6) Humidity tests were passed with much less than the required 30% gain in resistivity (usually around 10%). %T is reduced by 0.5-1.0% as a result of this test.

One side effect of this formulation is the resulting binder shifts the maximum %T out of the visible spectrum into the infrared (830nm). These effects, along with continued investigation of mechanical properties, are being studied.

Binder 3 coatings pass adhesion tests, but did not pass the heat and humidity tests. To protect binder 3 from environmental conditions a proprietary top coat was used. Optimum deposition of the top coat was found to be a dip coat followed by a cure at



125°C for 30minutes. Four total top coated samples were prepared, see Table 39. Samples 21 and 22 were coated with binder 3 dried at room temp for 1 minute then top coated before curing. Samples 23 and 24 were coated with binder 3, cured at 125°C for 30minutes, then top coated and cured again. Sample 22 and 24 were then humidity tested according to the specification above. The benefits of binder addition to CNT coatings can be seen in Table 38. The addition of binder 3 lowers resistivity by an average of 100 Ω/\square and increases transparency 7-8%. Curing binder 3 before the addition of the top coat enables the formation of a protective barrier by the top coat that passes the humidity test specified for PV applications (sample 24).

Table 38: RT performance and environmental stability of CNT/binder 3 coatings on PET using a protective top coat

| Sample | Resistivity (Ω/\square) | | Transparency (%T) | | Humidity Testing (% change) |
|--------|----------------------------------|-----------------------|-------------------|-----------------------|-----------------------------|
| | CNT | w/binder 3 + Top Coat | CNT | w/binder 3 + Top Coat | |
| 21 | 719 | 600 | 82.5 | 90.7 | |
| 22 | 592 | 565 | 82.2 | 90.0 | 32% |
| 23 | 759 | 618 | 82.2 | 90.8 | |
| 24 | 620 | 527 | 82.8 | 90.0 | 21% |



6 Publications/Presentations/Travel/Meetings

Herein is a list of key events that occurred during this Grant. These include papers published, presentations, and trips and meetings:

1. Power Point presentation titled *Transparent Coatings for Solar Cell Research* was given by Eikos during the kick off meeting for this project on October 6th, 2008. Eikos employees in this meeting included VP of Engineering Paul Glatkowski, Senior Engineer David Britz and Staff Engineer Robert Braden. Other attendees included Project Monitor Leon Fabick of NREL, Andrea Barnes of NREL and Jim Payne of the DOE.
2. David A. Britz, Evgeniya P. Turevskaya, Paul J. Glatkowski, “Highly Transparent Carbon Nanotube Films for ESD Protection,” *Proceedings of SPRAT XX, Sept. 25-27, Cleveland, OH, 2007*.
3. MA Contreras, TM Barnes, J van de Lagemaat, G Rumbles, TJ Coutts, C Weeks, P Glatkowski, I Levitsky, J Peltola, DA Britz, “Replacement of transparent conductive oxides by single-wall carbon nanotubes in Cu(In,Ga)Se-2-based solar cells,” *Journal of Physical Chemistry C*, **111**, 14045-14048 (2007).
4. 34th IEEE Photovoltaic Specialist Conference (June 7-12, 2009): Paul Glatkowski and Patrick Mack attended the 34th IEEE Photovoltaic Specialist Conference as a presenter of a poster covering important aspects of Invisicon[®] Technology in respect to PV energy. Several hundred people viewed the poster, took handouts and some left business cards. Eikos also surveyed the conferences exhibit hall and attended numerous oral presentations while in attendance from Monday afternoon to Thursday noon. Reason for Visit:
 - a. Present current work on capabilities of Invisicon[®] in PV to the academic community, government agencies, and industry.
 - b. Make contact with new people at prime contractors, companies, and within funding agencies.
 - c. Meet with current collaborators specifically at AFRL, NREL, and DOE.
 - d. Paul Eikos staff submitted a technical paper based on work information presented at the 34th IEEE Photovoltaic Specialist Conference. This work is titled “Carbon Nanotube Transparent Electrodes: a Case for Photovoltaics”.
5. Eikos visited the FujiFilm Dimatix facility in Lebanon, NH on January 30th. The purpose of that visit was to get firsthand knowledge of the DMP-2831 ink jet printer.



6. Paul Glatkowski, the project PI, traveled Denver to give the Annual Review project presentation March 9-10 at the 2009 DOE Program Review Conference. A coating evaluation was performed by Dave Landis at Euclid Lab Coaters in Bay City, Michigan, on March 26 at one of the company's facilities.
7. Site Visit to NREL (August 12, 2009); Eikos Research Director Mike O'Connell traveled to Golden Co, to meet with Teresa Barnes and other NREL staff. Topics of discussion included future collaboration between NREL and Eikos in CdTe and OPV devices.
8. Leslie (Jim) Payne, the Project Officer of this program, traveled from Golden, CA to Franklin, MA for a site visit and met with Paul Glatkowski and Mike O'Connell. Paul and Mike gave the above presentation and lead a tour of Eikos to inform Jim of our capabilities.
9. Eikos attended the fall Materials Research Society (MRS) meeting in Boston, MA from November 30-December 4th 2009.
10. Eikos (Paul J Glatkowski, PI) presented at the 2010 Solar Energy Technologies Program Peer Review on Tuesday, May 25th from 9:15 to 9:45. This meeting took place at the Omni Shoreham Hotel, Washington, DC on May 24-27.
11. Eikos presented at the 28th annual Space Power Workshop in El Segundo, CA on April 8th, 2010. This work was funded by USAF and has resulted in coating technology complementary to the work being undertaken in this DOE grant since the same work could benefit terrestrial application in the PV markets:
12. Presentation entitled: "Radiation Resistant Carbon Nanotube ESD and AR Coatings for PV Power Generation in Space"
13. Eikos presented at the Energy Solar Energy Technologies Program Annual Review on Tuesday, May 25th from 9:15 to 9:45, in Washington DC. That presentation was uploaded to the DOE submission site with this report.



7 References Cited

8

-
- ¹ C.J. Brabec, N.S. Sariciftci, and J.C. Hummelen, *Adv. Funct. Mater.* **11**, 15 (2001).
- ² Barnes, T et. al., *SWCNT Networks as Transparent Electrical Contacts in Photovoltaics*, National Renewable Energy Lab, Golden, CO, 2007.
- ³“Indium price soars as demand for displays continues to grow,” <http://www.compoundsemiconductor.net/articles/magazine/11/5/5/>, March, 16, 2006; and J. F. Carlin, Jr., “Indium 2006,” *U.S. Geological Survey*, January, 2006.
- ⁴ D. Arthur, P. Glatkowski, P. Wallis and M.Trottier, “Flexible Transparent Circuits from Carbon Nanotubes”, *SID '04 Digest of Technical Papers*. p 582 (2004).
- ⁵ Z. Huo, C..Tsung, W.Huang, X. Zhang, P. Yang. *Nano-letters*. **2008**, No7, 2041-2044
- ⁶ N. Pazos-Perez, D.Baranov, S.Irsen, M. Hilgendorff, at al. *Langmuir*, **2008**, 24, 9855-9860
- ⁷ Wang, Y. Hu, C. Lieber, S. Sun. *J. of Amer. Chem. Soc.*(communic.), **2008**,130, 8902-8903
- ⁸ <http://www.cimananotech.com/sante.aspx>; Product Description, Cima Nanotech, 2009.
- ⁹ “ Advanced Curing for printed Electronics”, http://www.novacentrix.com/images/downloads/PF_Brochure_4pg.pdf, Stan Farnsworth, NovaCentrix, January, 2009.
- ¹⁰ “ Advanced Curing for printed Electronics”, http://www.novacentrix.com/images/downloads/PF_Brochure_4pg.pdf, Stan Farnsworth, NovaCentrix, January, 2009.
- ¹¹ <http://www.scsolutions.com/public/product/cmp-controllers.html>
- ¹²E. Wainer, German Patent 1,249,832, April 11, 1968. and B.E. Yoldas *J.Mater.Sci.*, **10**, 1856, 1975.
- ¹³H. Dlisch, *Sol-Gel Technology for Thin Films, Fibers, Preforms, Electronics, and Specialty Shapes*, ed. L.C. Klein, Noyes, Park Ridge, NJ, 1988.
- ¹⁴ H.G. Sowman, European Patent Application 87301350.2, February 17, 1987.
- ¹⁵ *Sol-Gel Science: The Physics and Chemistry of Sol-Gel Processing*, C.J. Brinker, G.W. Scherer, Academic Press, Boston, 1990.
- ¹⁶ “Optical and mechanical properties of sol-gel AR films for solar energy applications,” P. Nostell *et al.*, *Thin Solid Films*, **351**, 170, 1999.
- ¹⁷ C.J. Brinker in *Transformation of Organometallics into Common and Exotic Materials: Design and Activation*, NATO ISI series E, no. 141, ed. R.M. Laine (Martinus Nijhoff, Dordrecht, 1988).